APPENDIX A2

Local 3D Hydrodynamic Model Validation - Time Series Plots

Autumn 2005

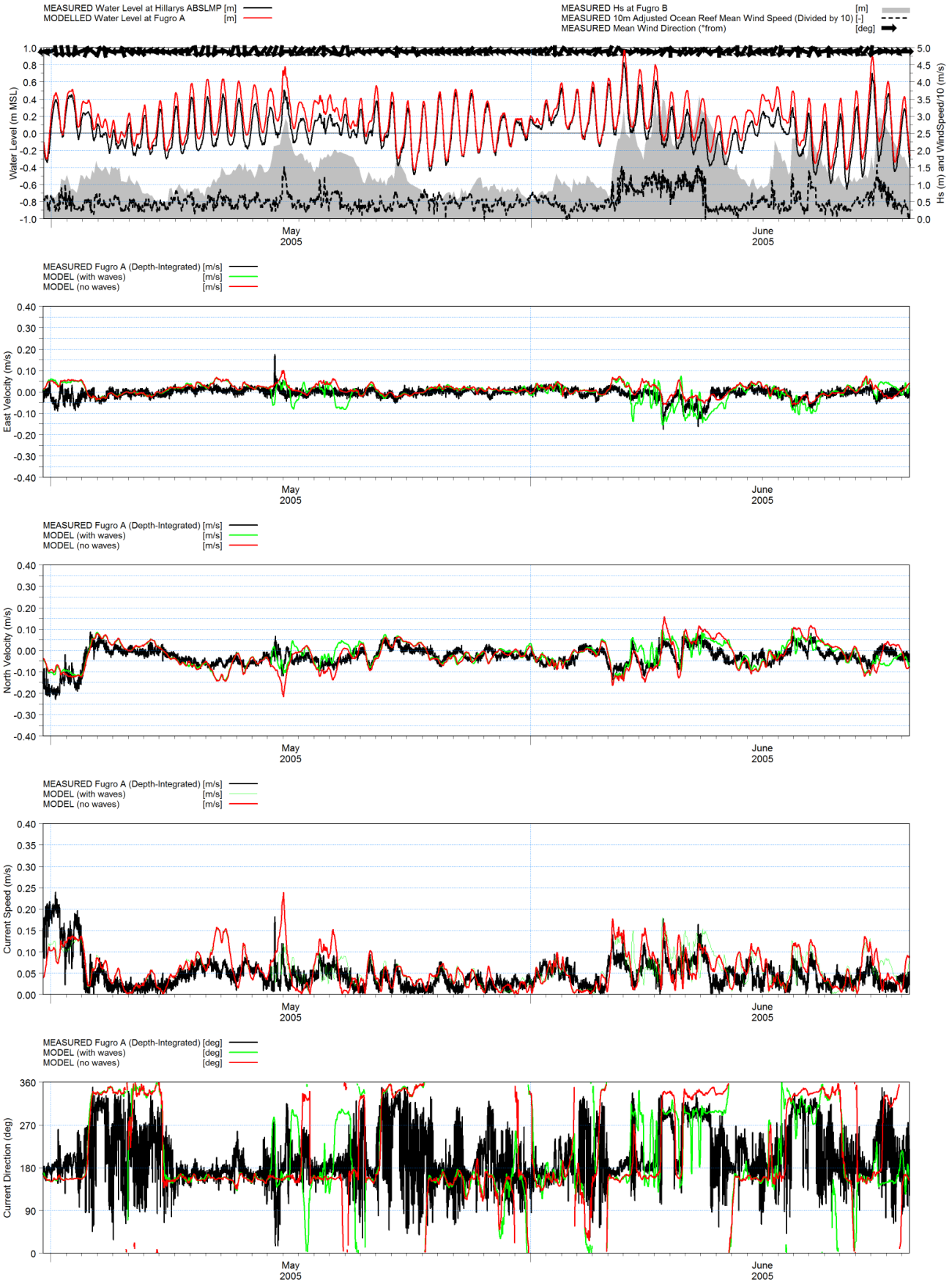

Figure A2-1a: Local 3D Hydrodynamic Model vs. Fugro A. Depth-integrated, Autumn 2005.

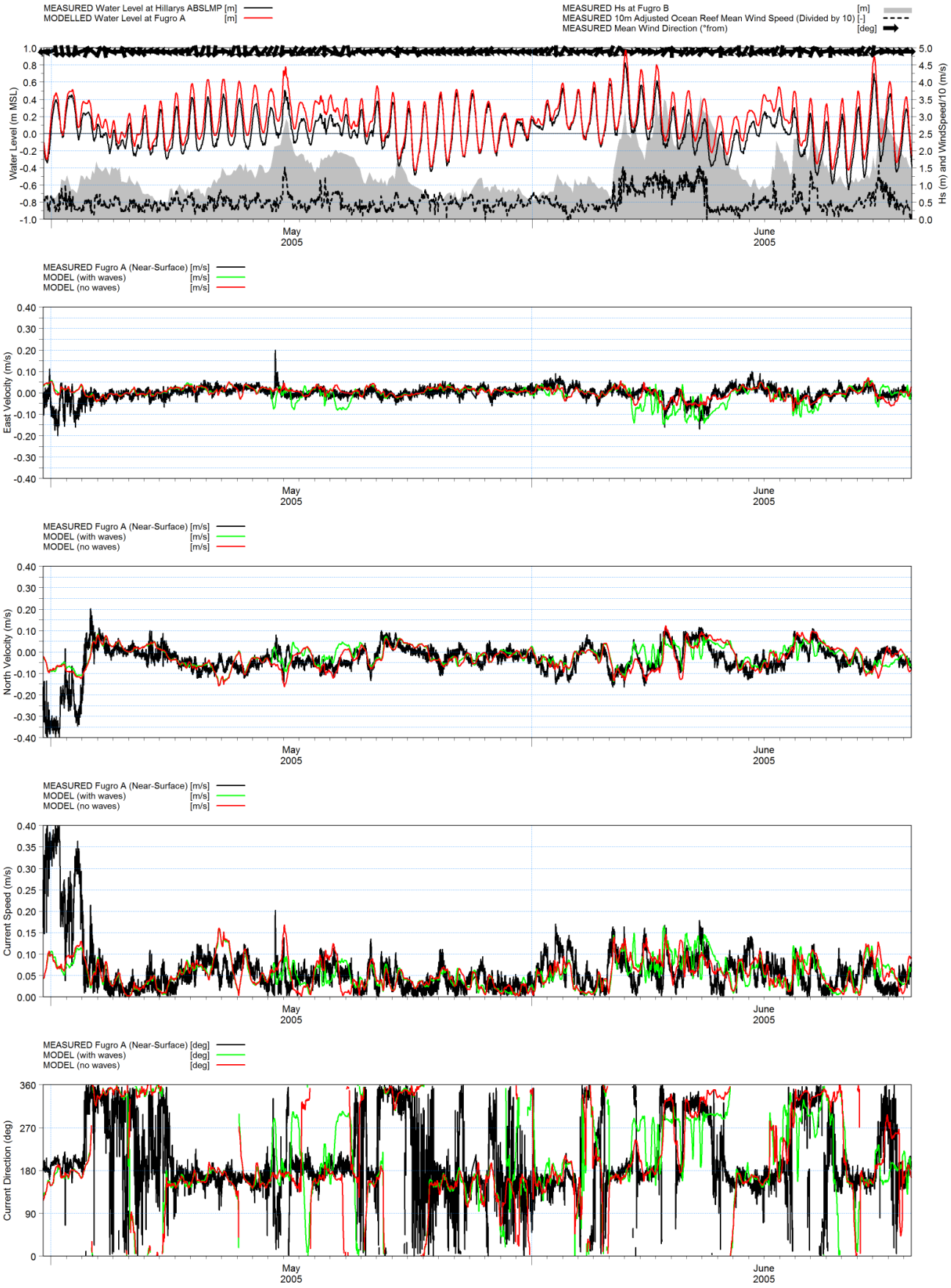

Figure A2-1b: Local 3D Hydrodynamic Model vs. Fugro A. Surface, Autumn 2005.

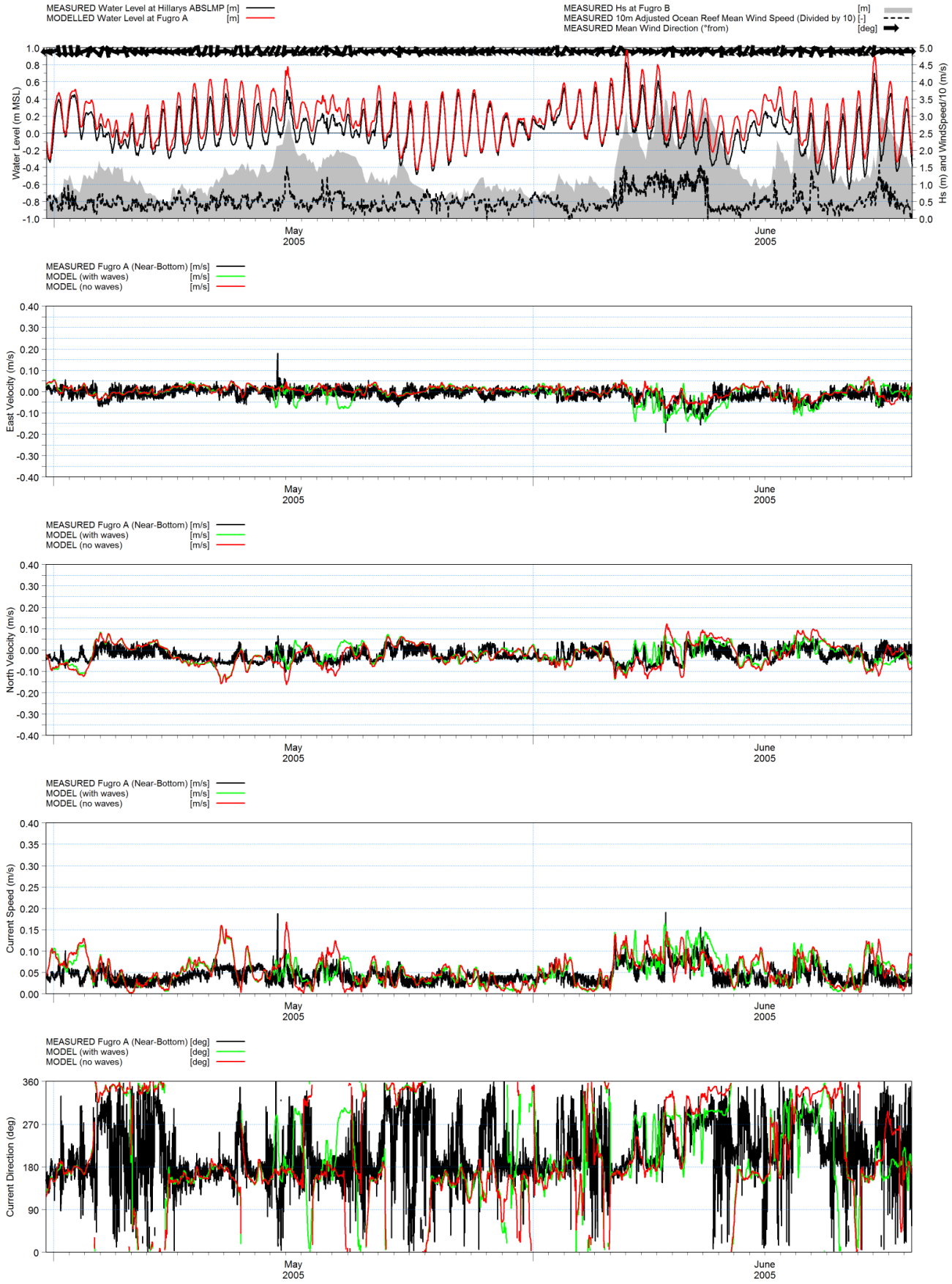

Figure A2-1c: Local 3D Hydrodynamic Model vs. Fugro A. Bottom, Autumn 2005.

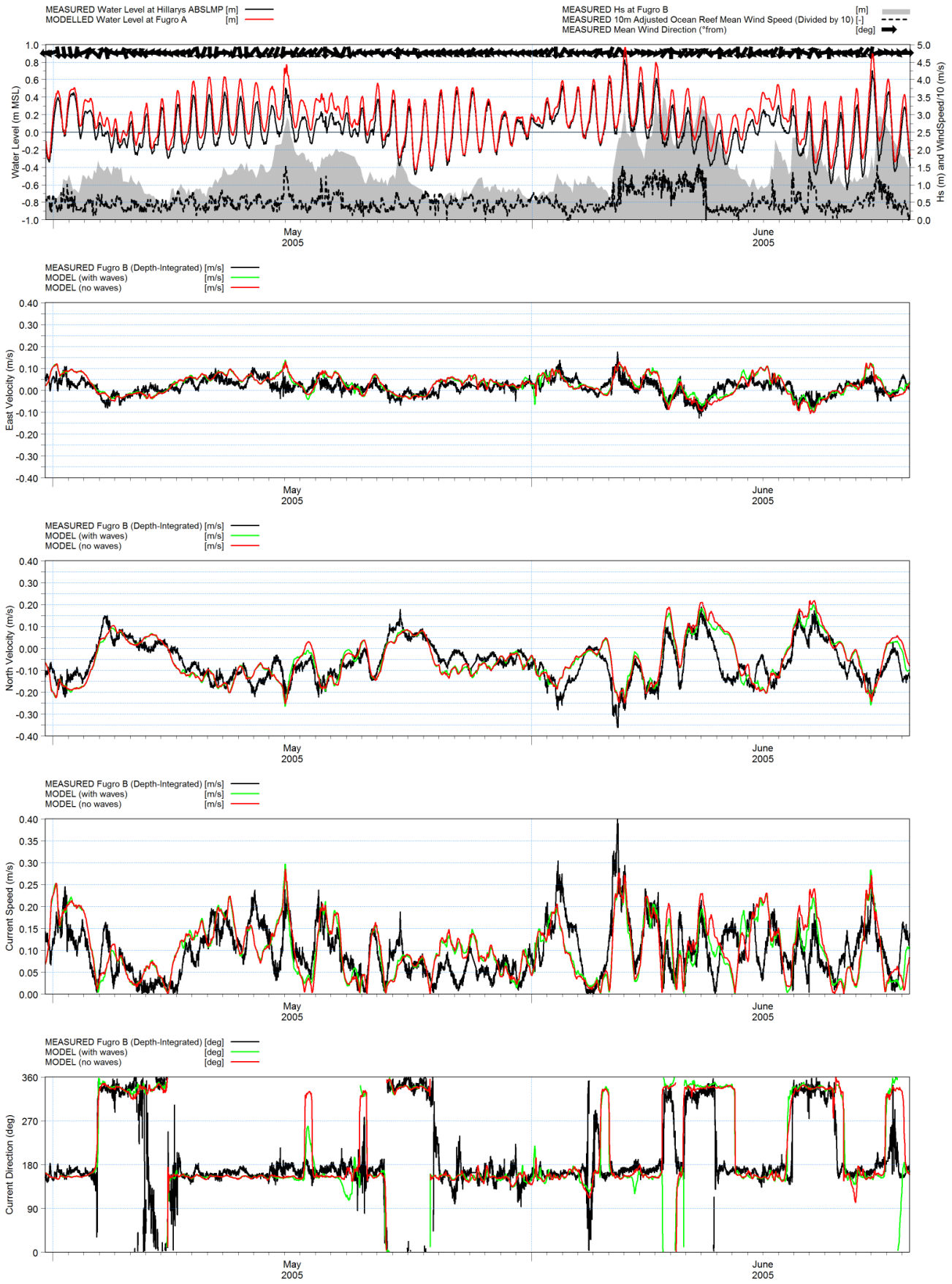

Figure A2-2a: Local 3D Hydrodynamic Model vs. Fugro B. Depth-integrated, Autumn 2005.

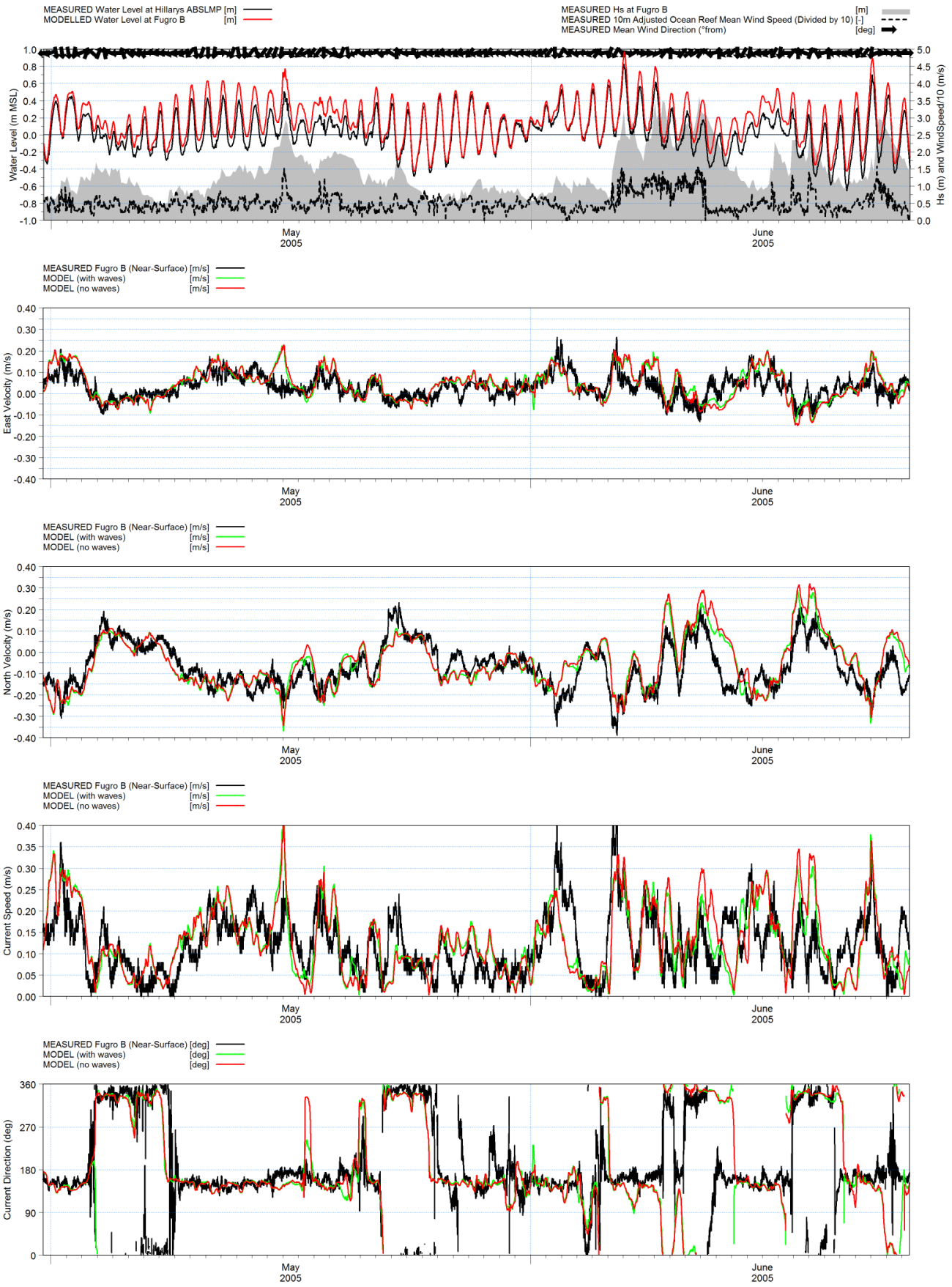

Figure A2-2b: Local 3D Hydrodynamic Model vs. Fugro B. Surface, Autumn 2005.

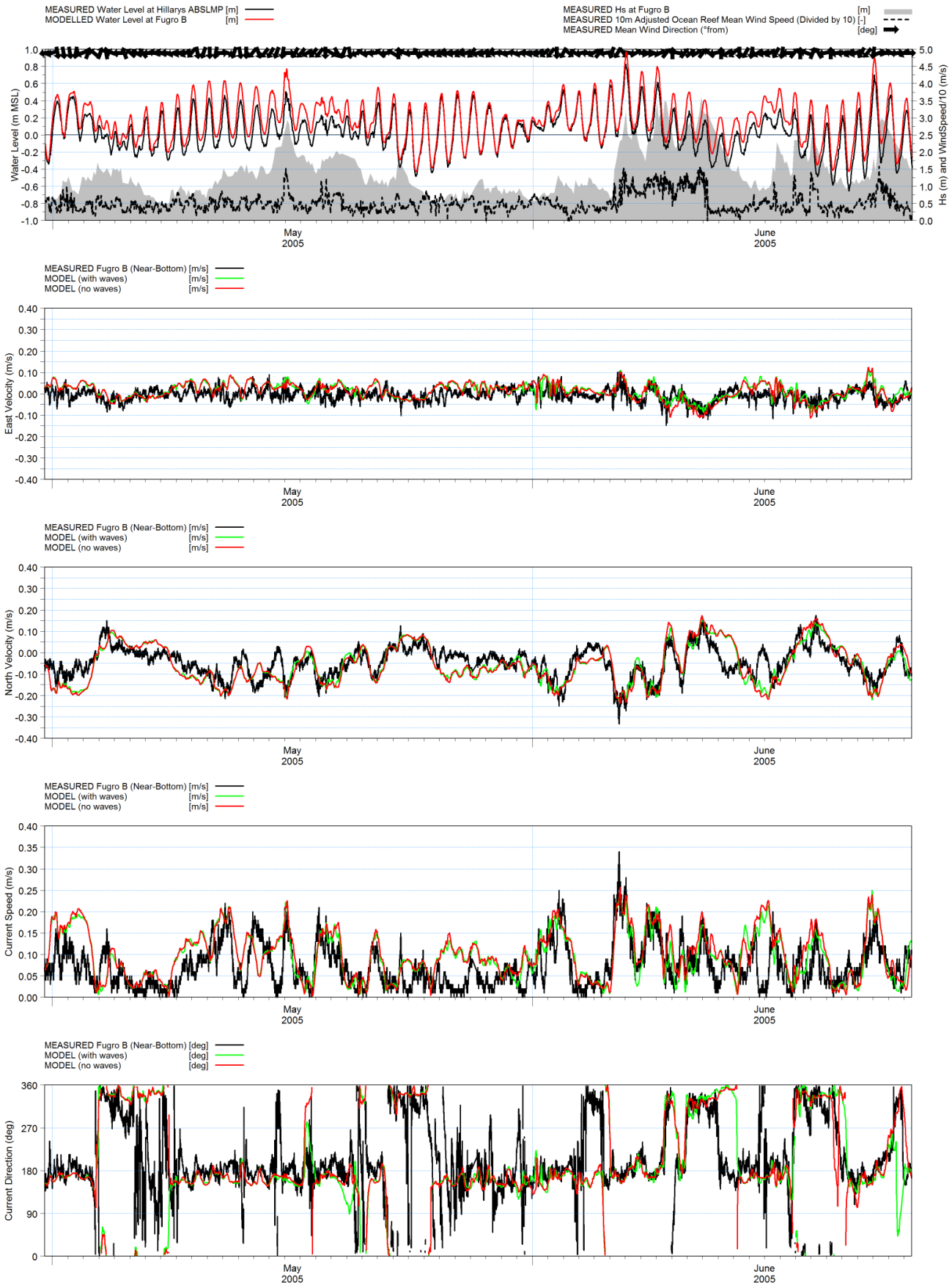

Figure A2-2c: Local 3D Hydrodynamic Model vs. Fugro B. Bottom, Autumn 2005.

APPENDIX A3

Local 3D Hydrodynamic Model Validation - Time Series Plots

Winter 2017

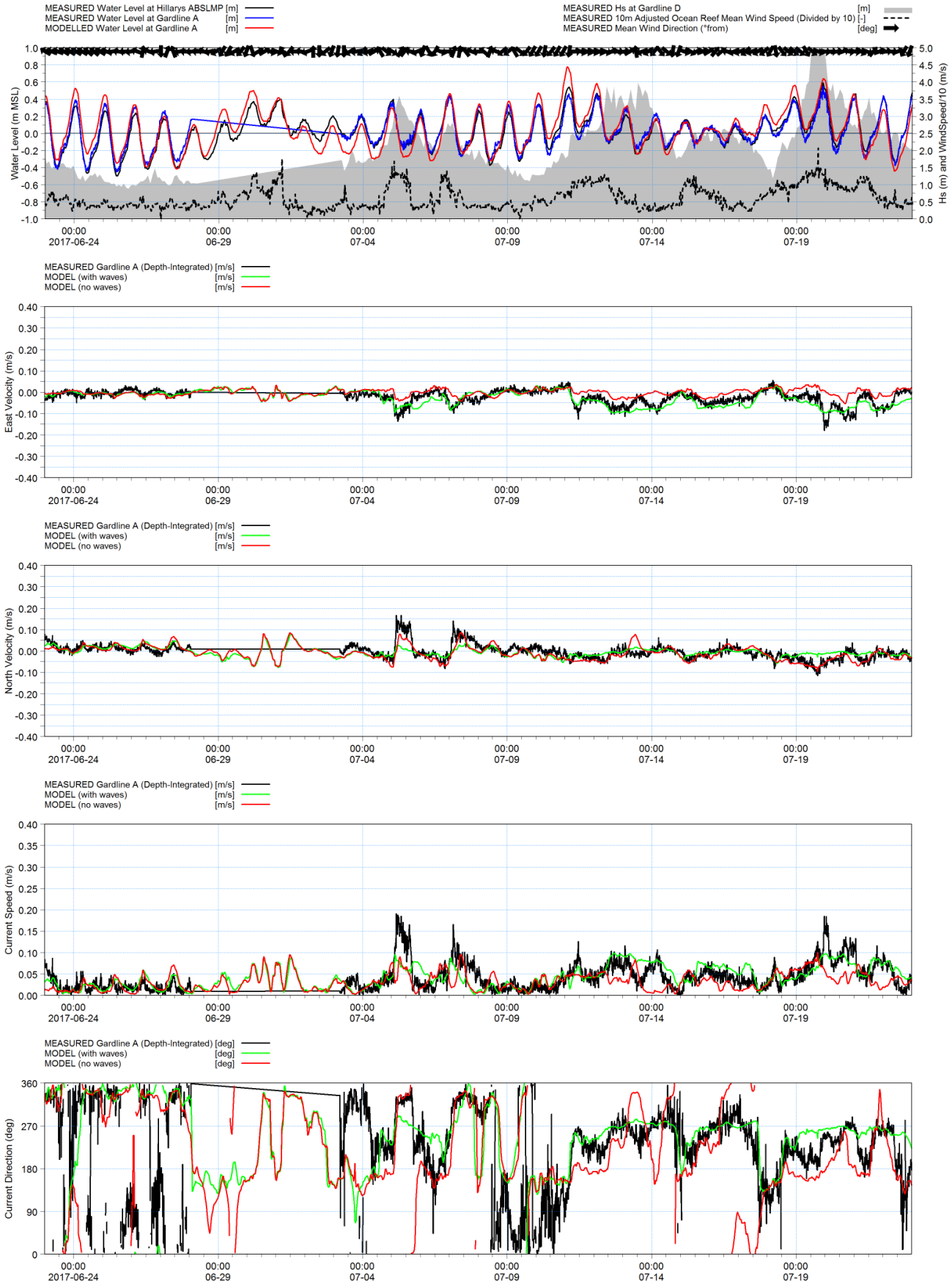

Figure A3-1a: Local 3D Hydrodynamic Model vs. Gardline A. Depth-integrated, Winter 2017.

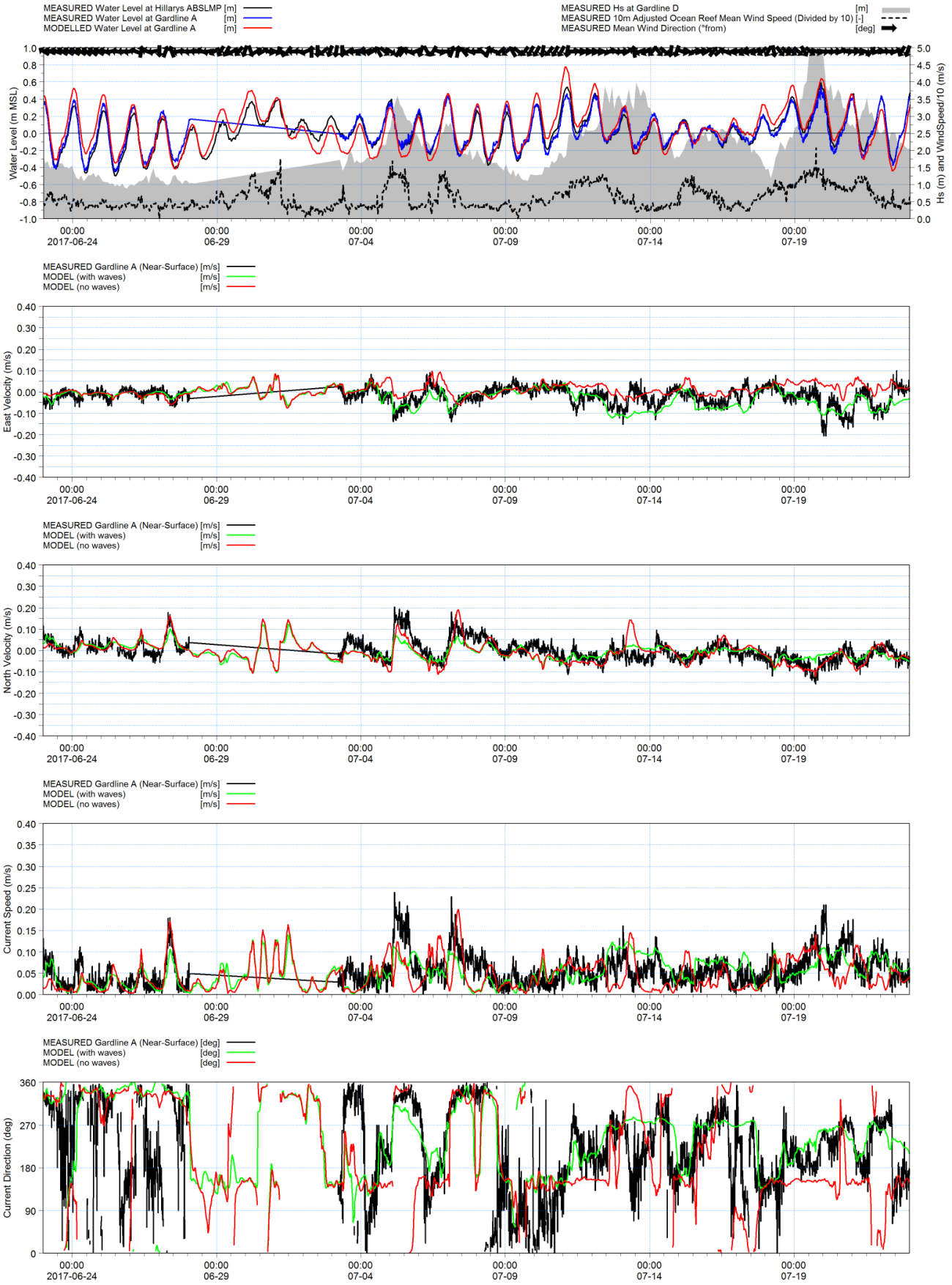

Figure A3-1b: Local 3D Hydrodynamic Model vs. Gardline A. Surface, Winter 2017.

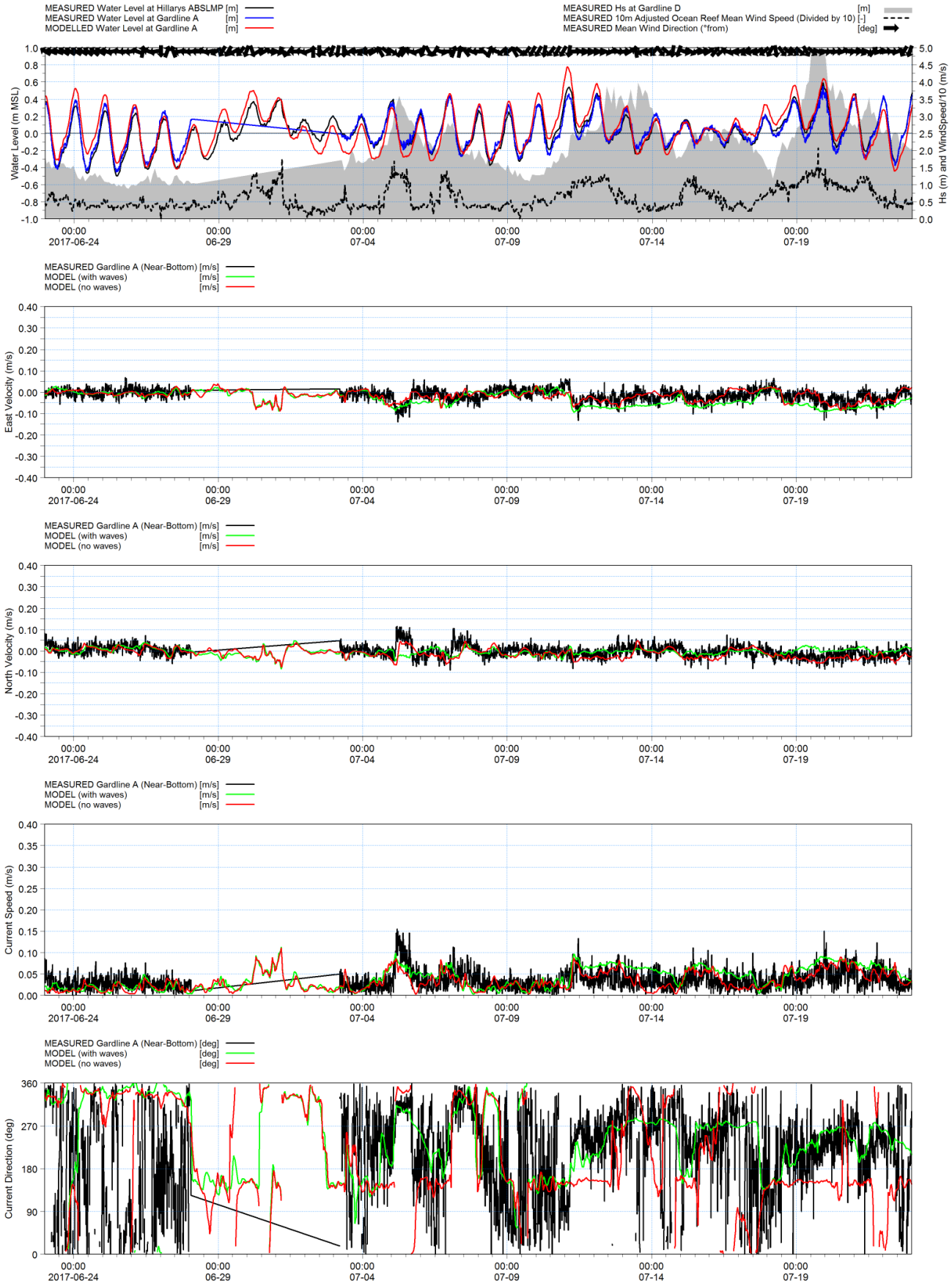

Figure A3-1c: Local 3D Hydrodynamic Model vs. Gardline A. Bottom, Winter 2017.

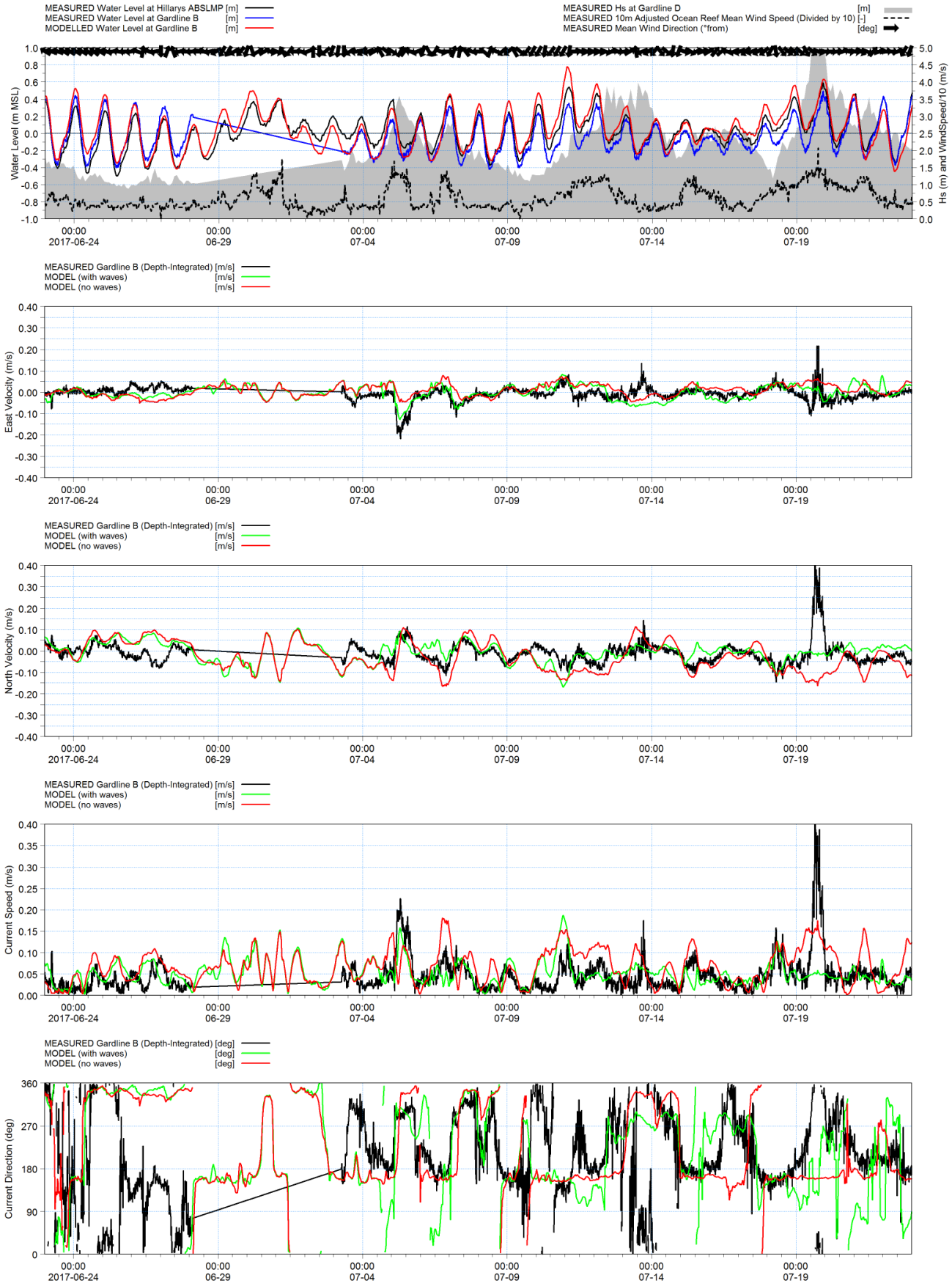

Figure A3-2a: Local 3D Hydrodynamic Model vs. Gardline B. Depth-integrated, Winter 2017.

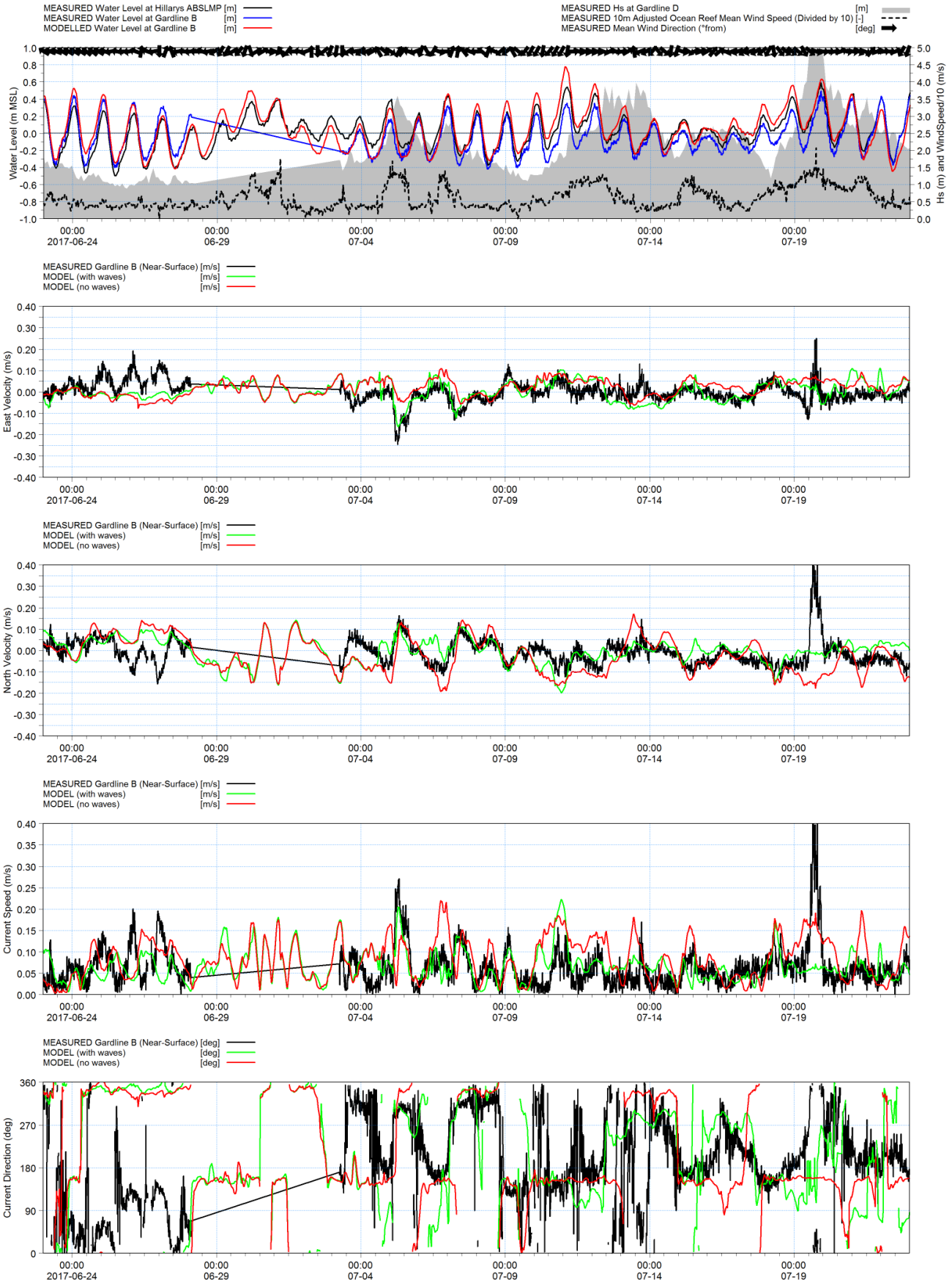

Figure A3-2b: Local 3D Hydrodynamic Model vs. Gardline B. Surface, Winter 2017.

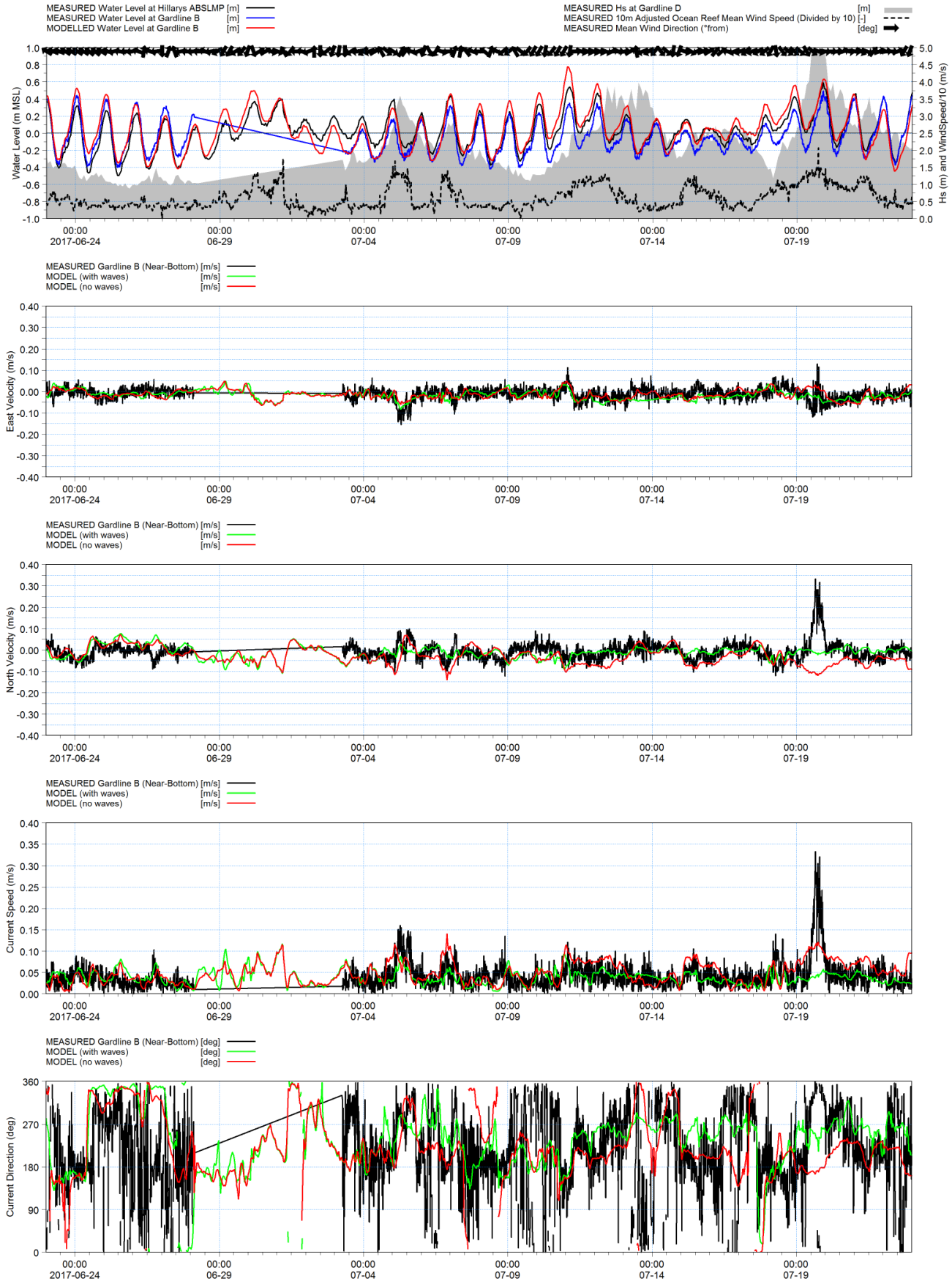

Figure A3-2c: Local 3D Hydrodynamic Model vs. Gardline B. Bottom, Winter 2017.

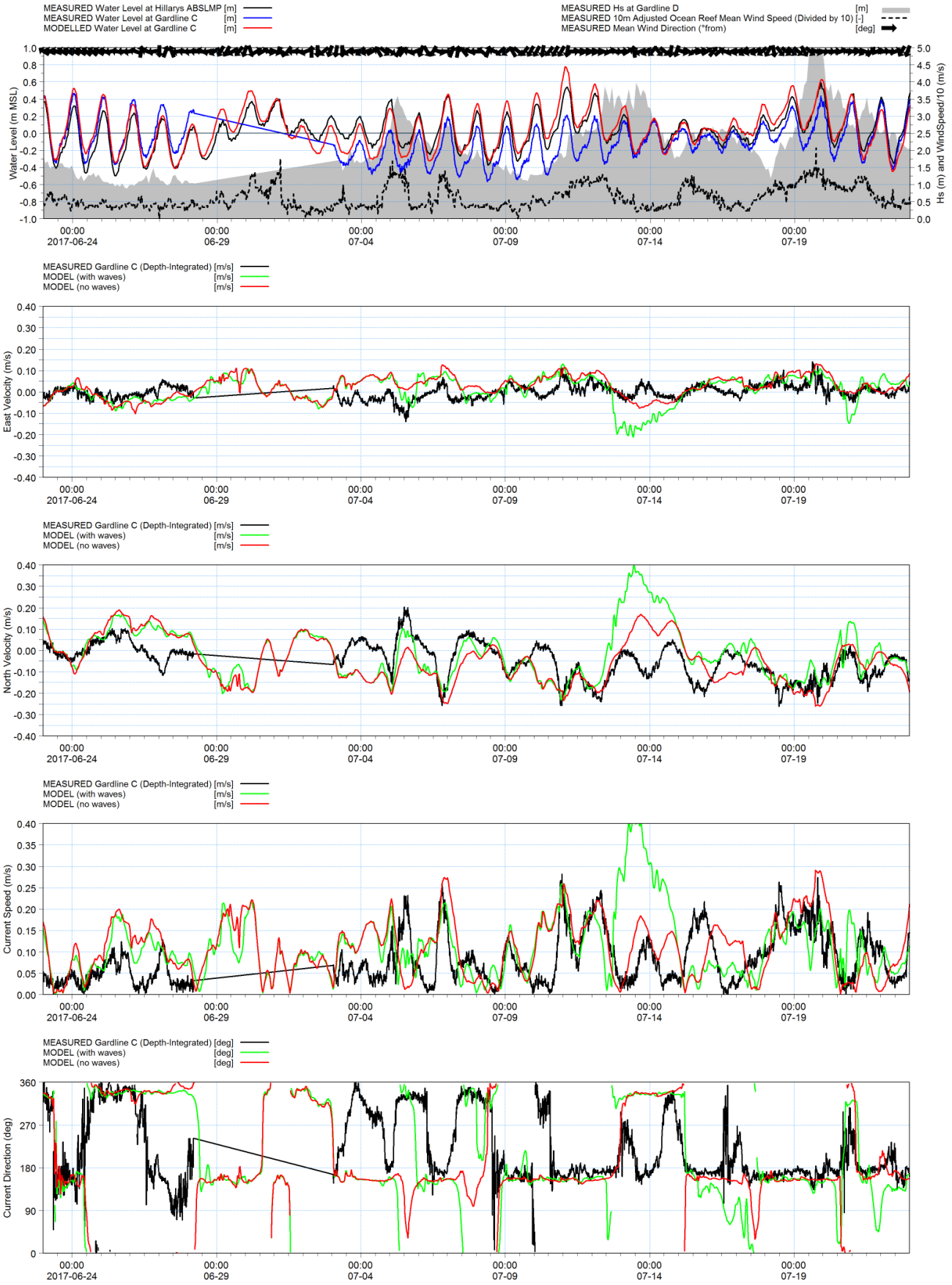

Figure A3-3a: Local 3D Hydrodynamic Model vs. Gardline C. Depth-integrated, Winter 2017.

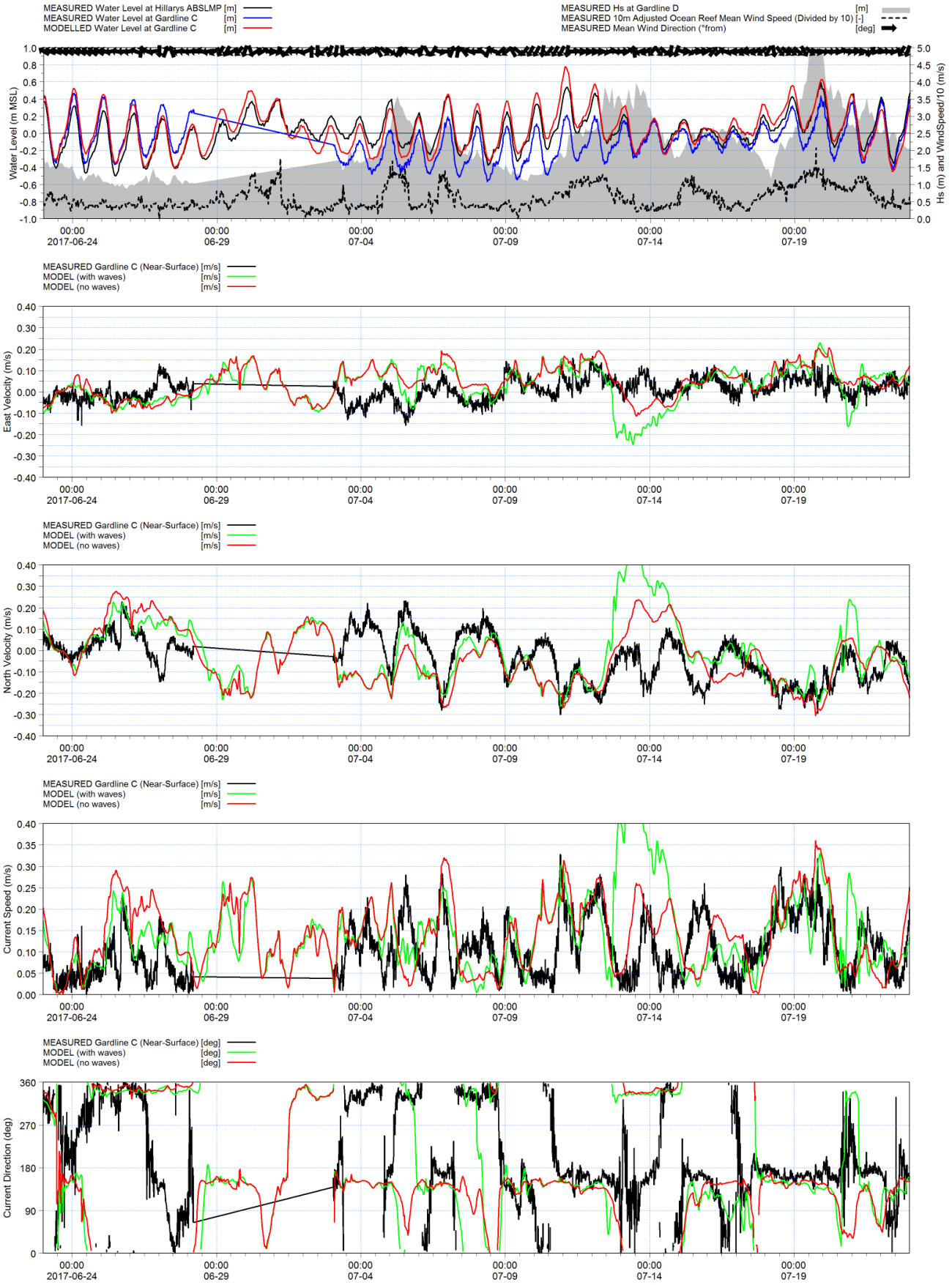

Figure A3-3b: Local 3D Hydrodynamic Model vs. Gardline C. Surface, Winter 2017.

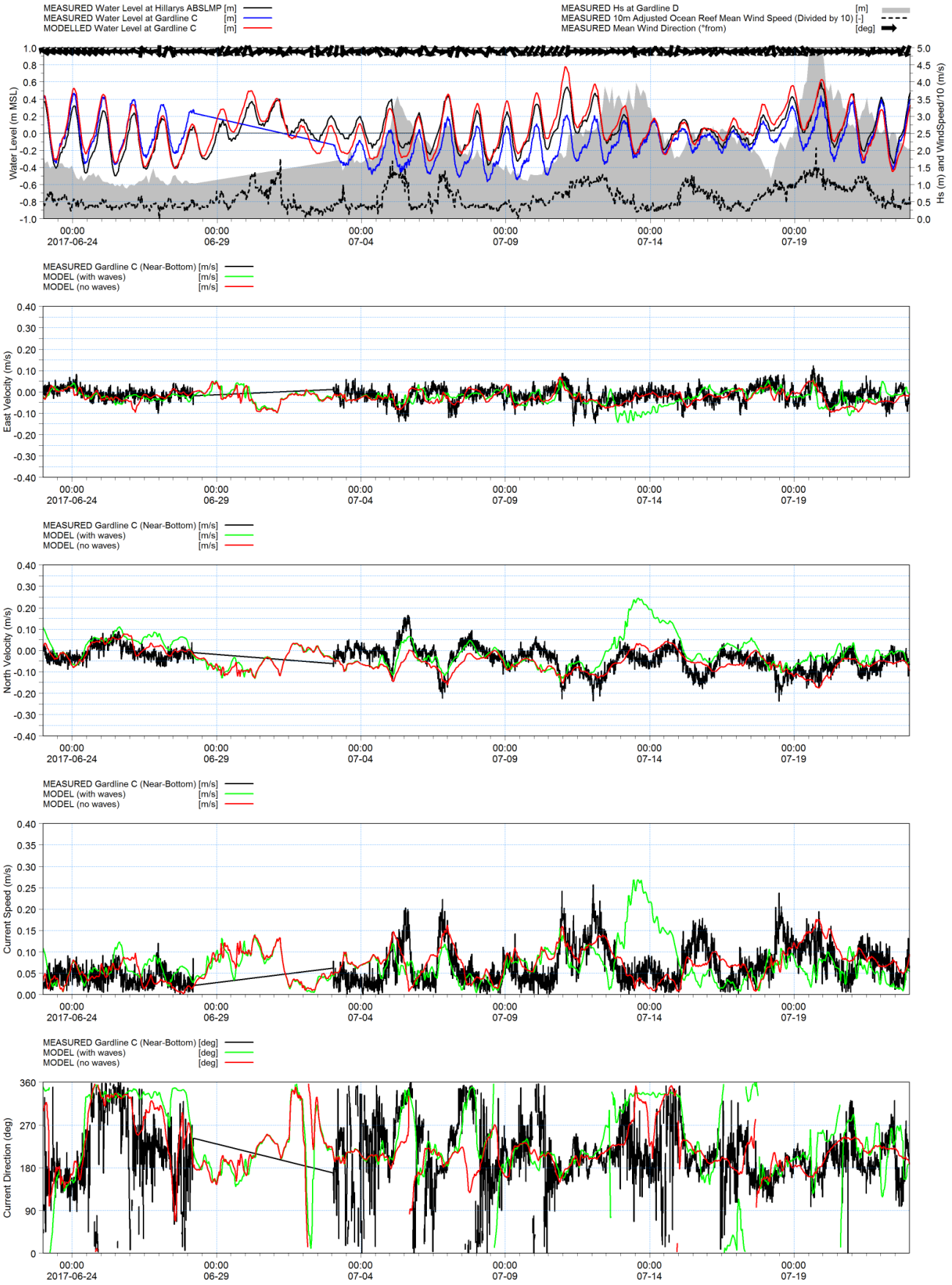

Figure A3-3c: Local 3D Hydrodynamic Model vs. Gardline C. Bottom, Winter 2017.

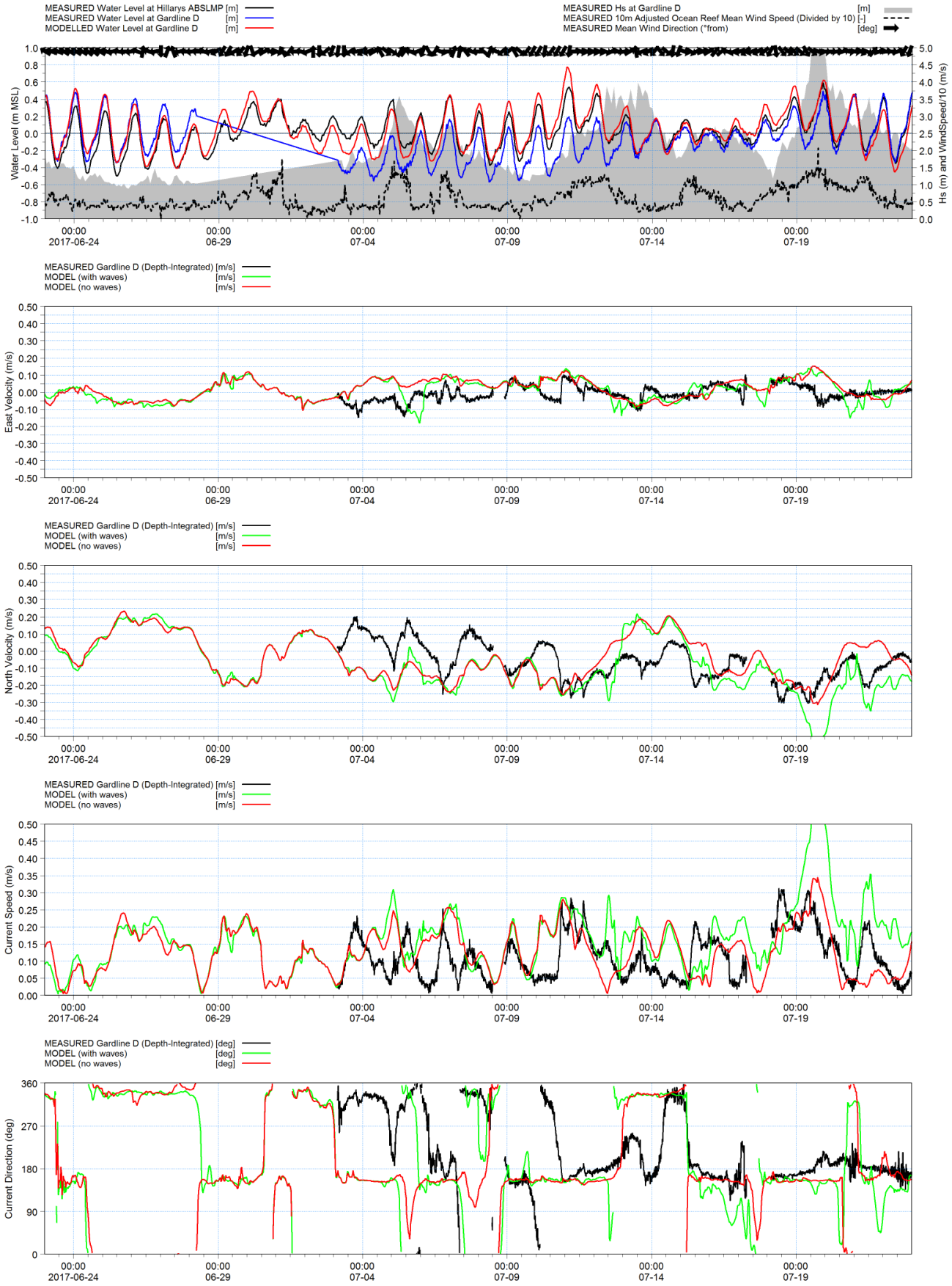

Figure A3-4a: Local 3D Hydrodynamic Model vs. Gardline D. Depth-integrated, Winter 2017.

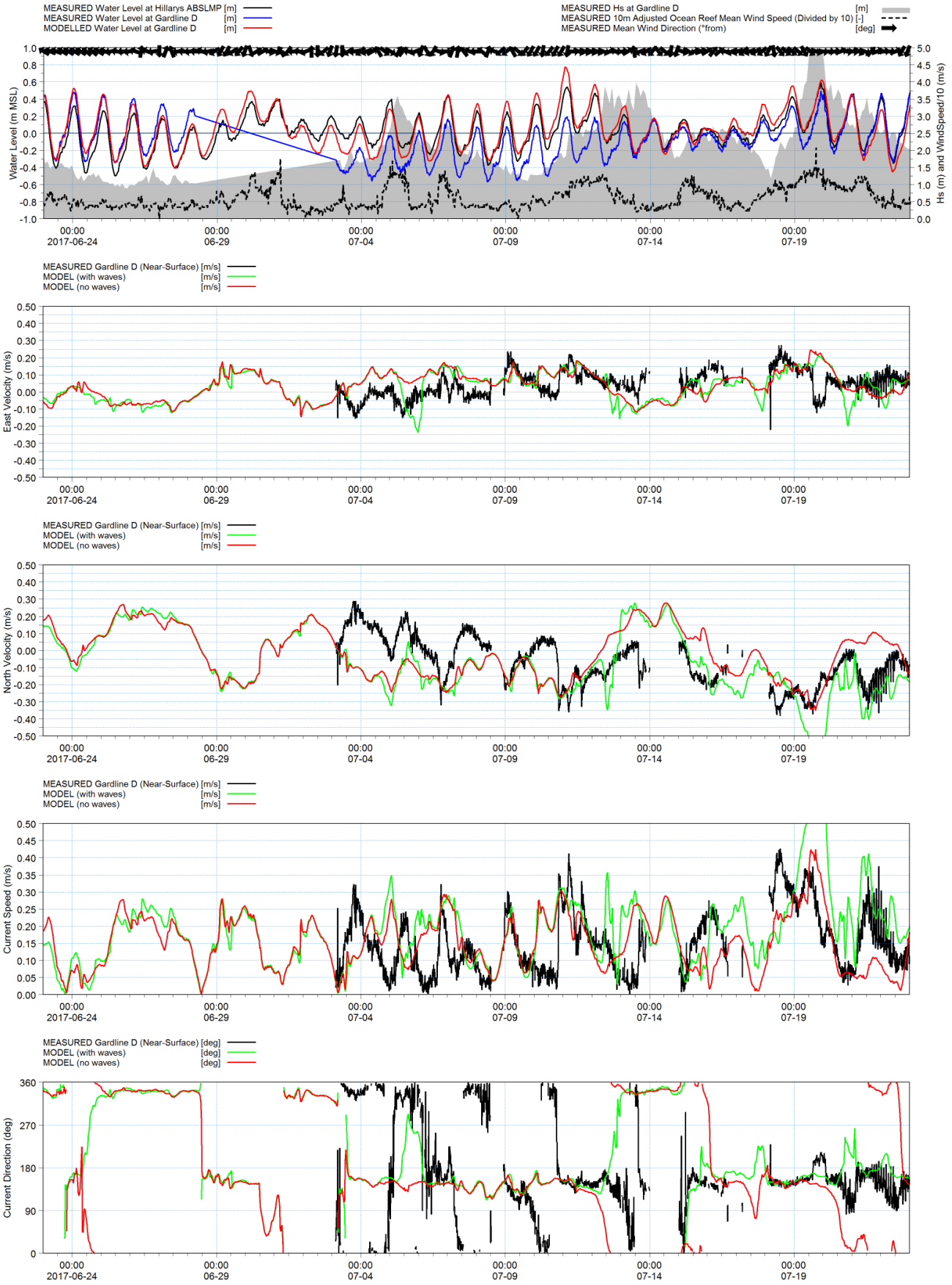

Figure A3-4b: Local 3D Hydrodynamic Model vs. Gardline D. Surface, Winter 2017.

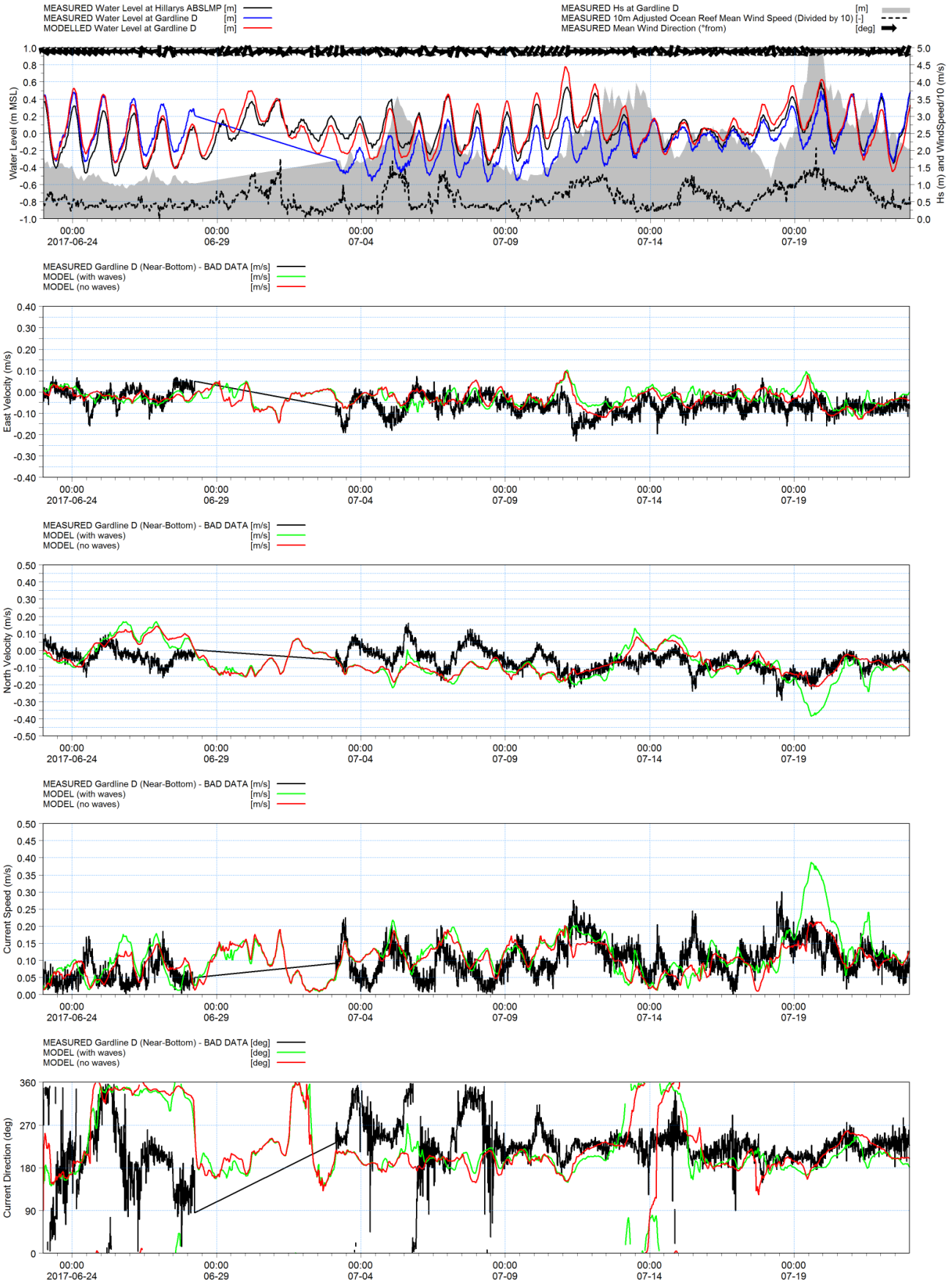

Figure A3-4c: Local 3D Hydrodynamic Model vs. Gardline D. Bottom, Winter 2017.

APPENDIX A4

Local 3D Hydrodynamic Model Calibration - Time Series Plots

Summer 2017

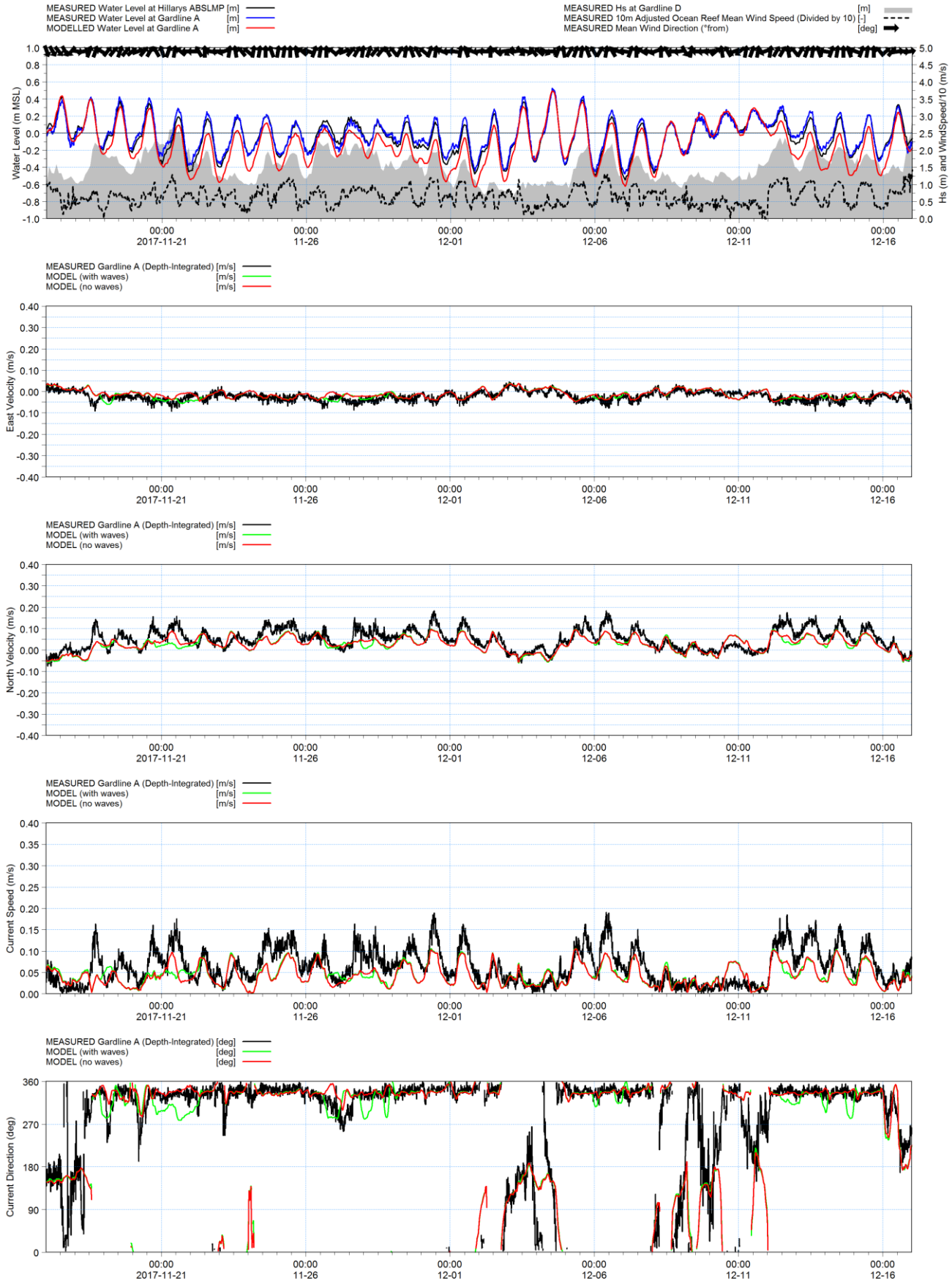

Figure A4-1a: Local 3D Hydrodynamic Model vs. Gardline A. Depth-integrated, Summer 2017.

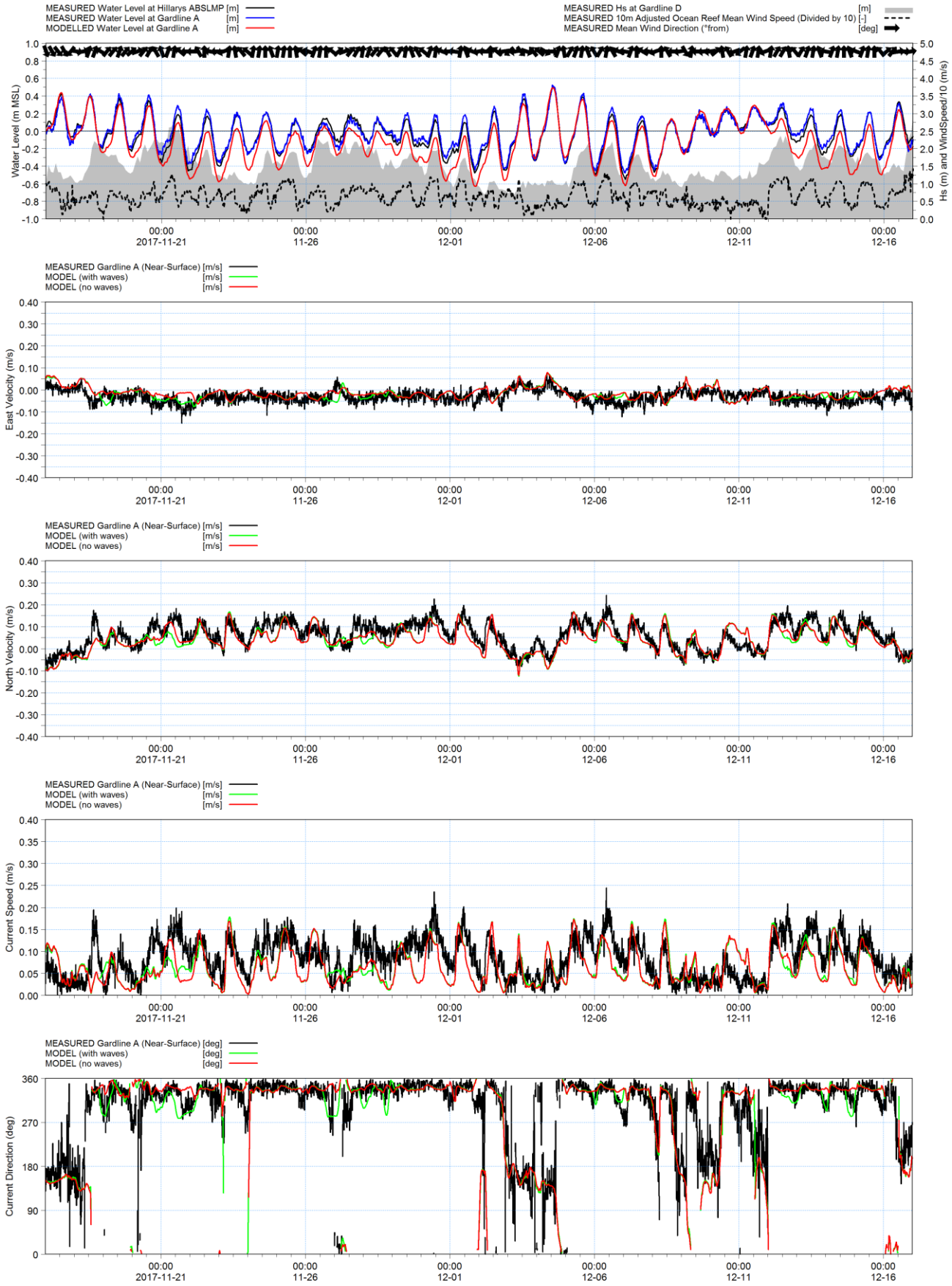

Figure A4-1b: Local 3D Hydrodynamic Model vs. Gardline A. Surface, Summer 2017.

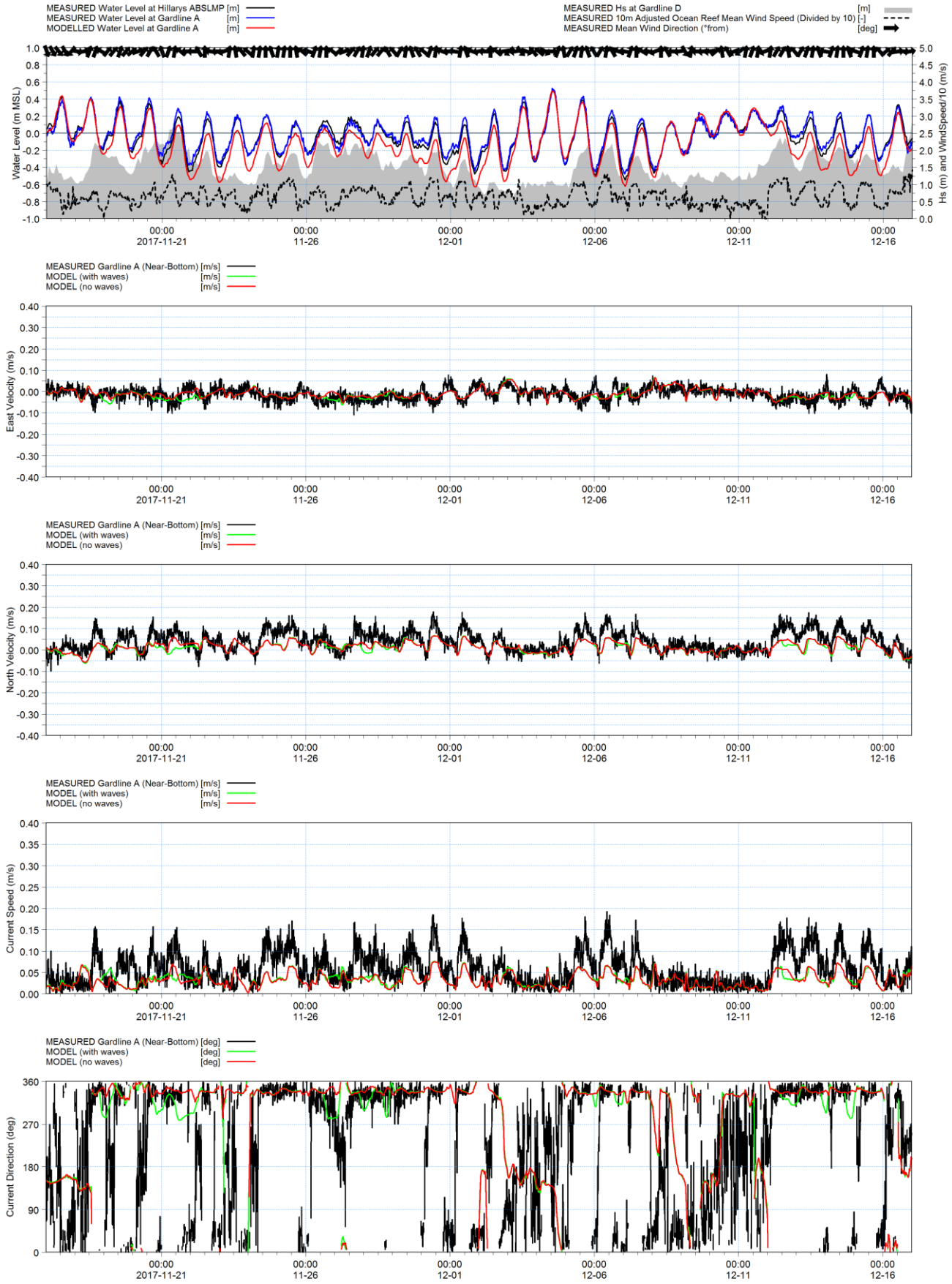

Figure A4-1c: Local 3D Hydrodynamic Model vs. Gardline A. Bottom, Summer 2017.

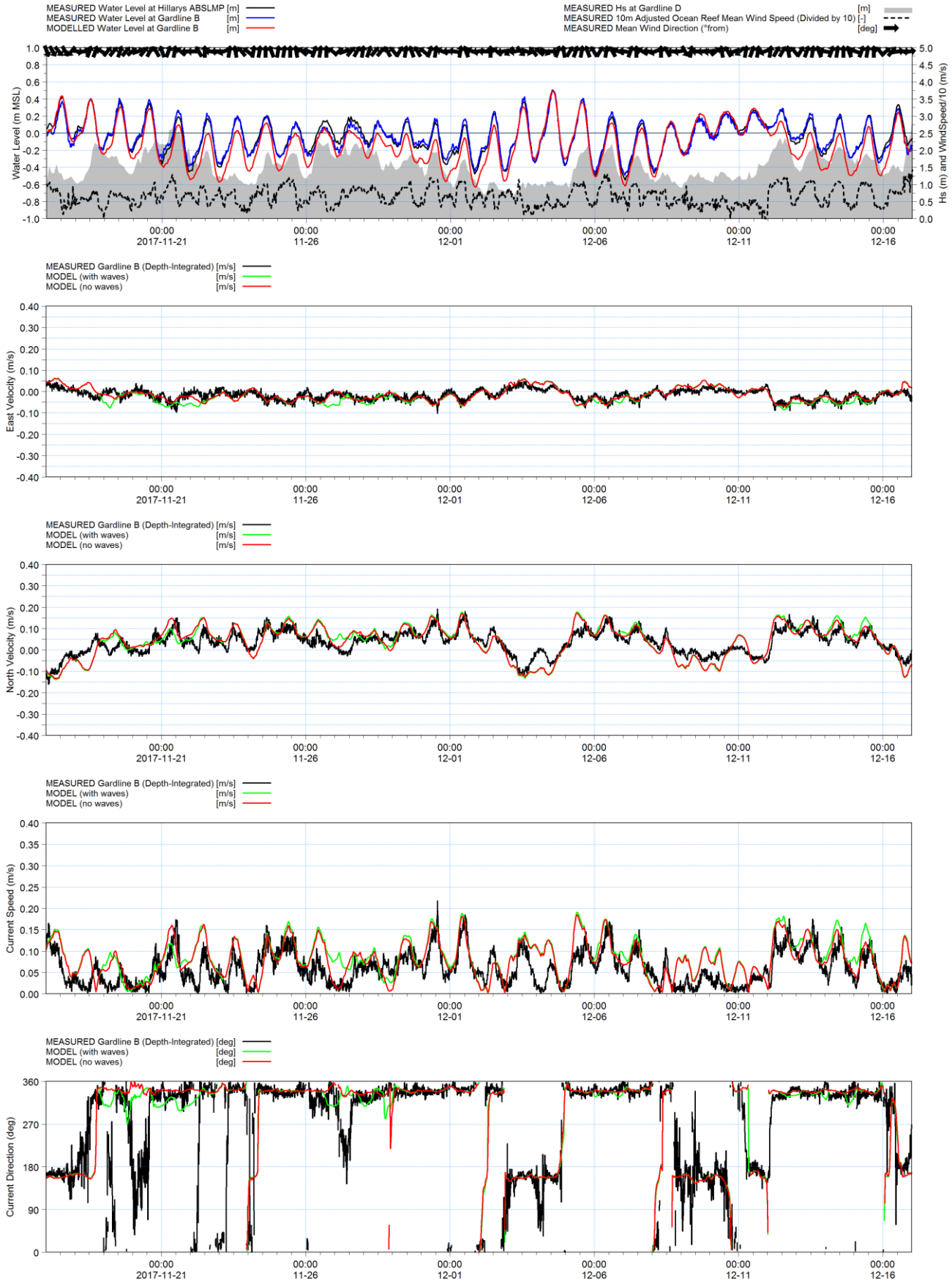

Figure A4-2a: Local 3D Hydrodynamic Model vs. Gardline B. Depth-integrated, Summer 2017.

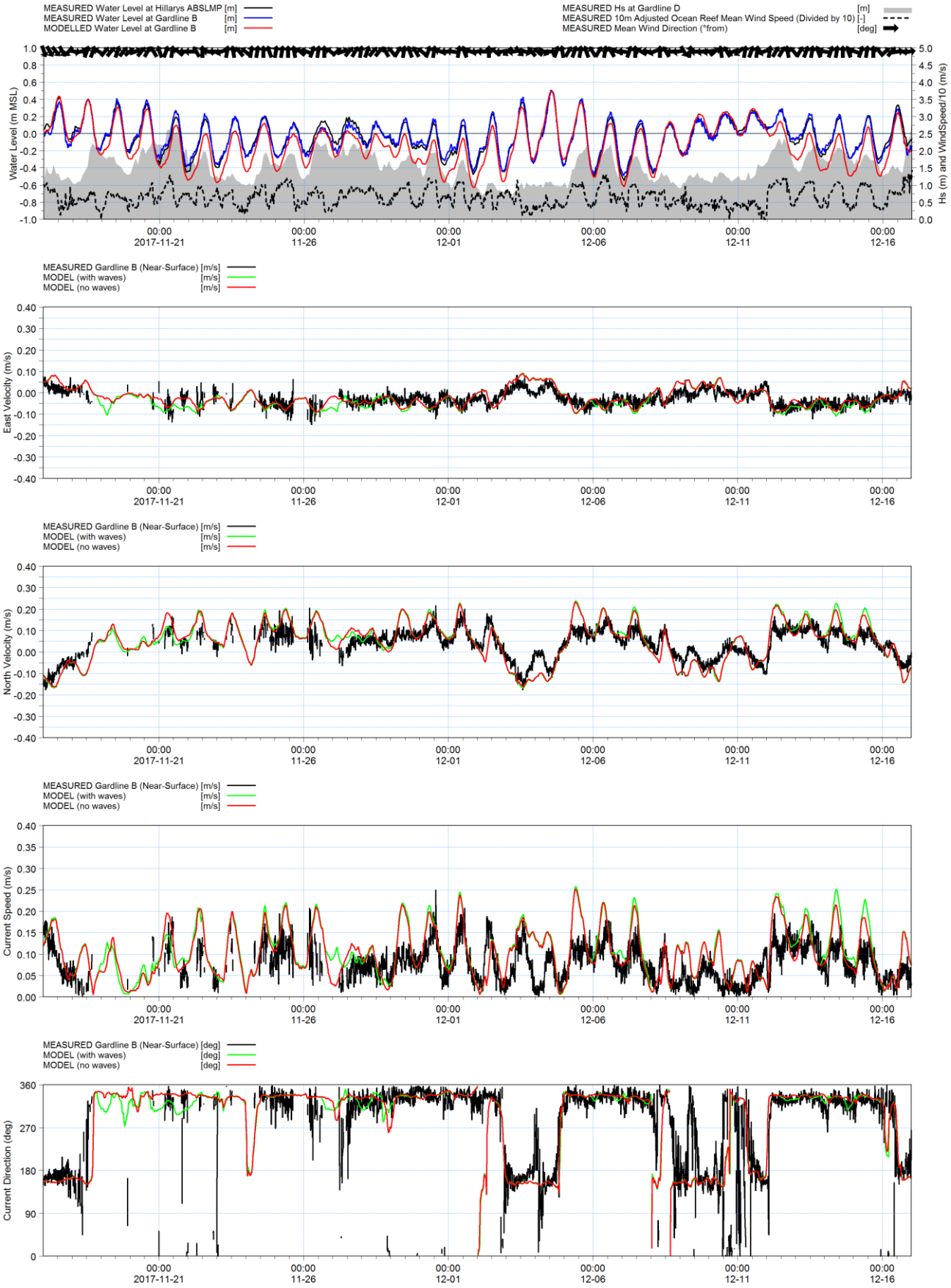

Figure A4-2b: Local 3D Hydrodynamic Model vs. Gardline B. Surface, Summer 2017.

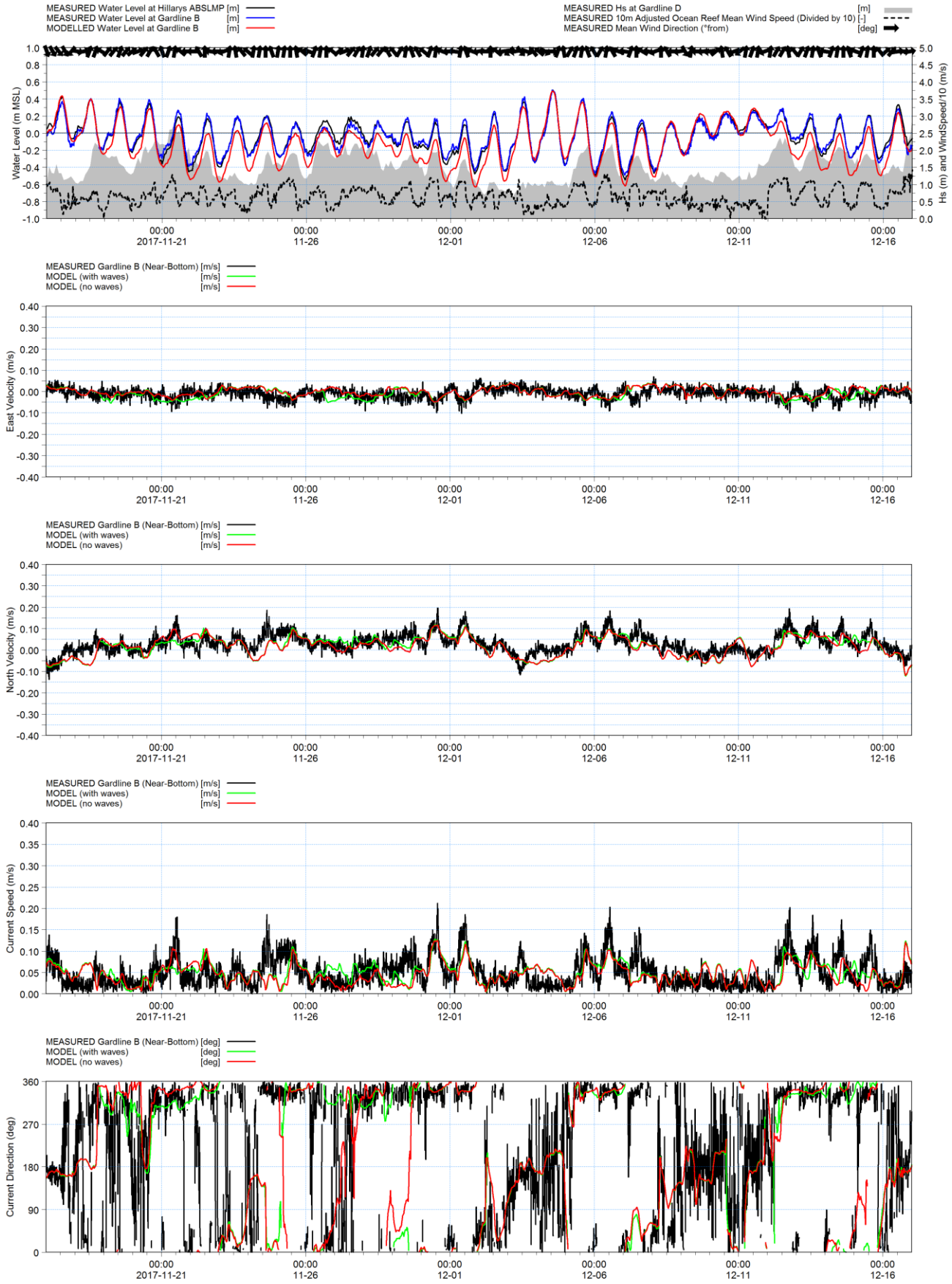

Figure A4-2c: Local 3D Hydrodynamic Model vs. Gardline B. Bottom, Summer 2017.

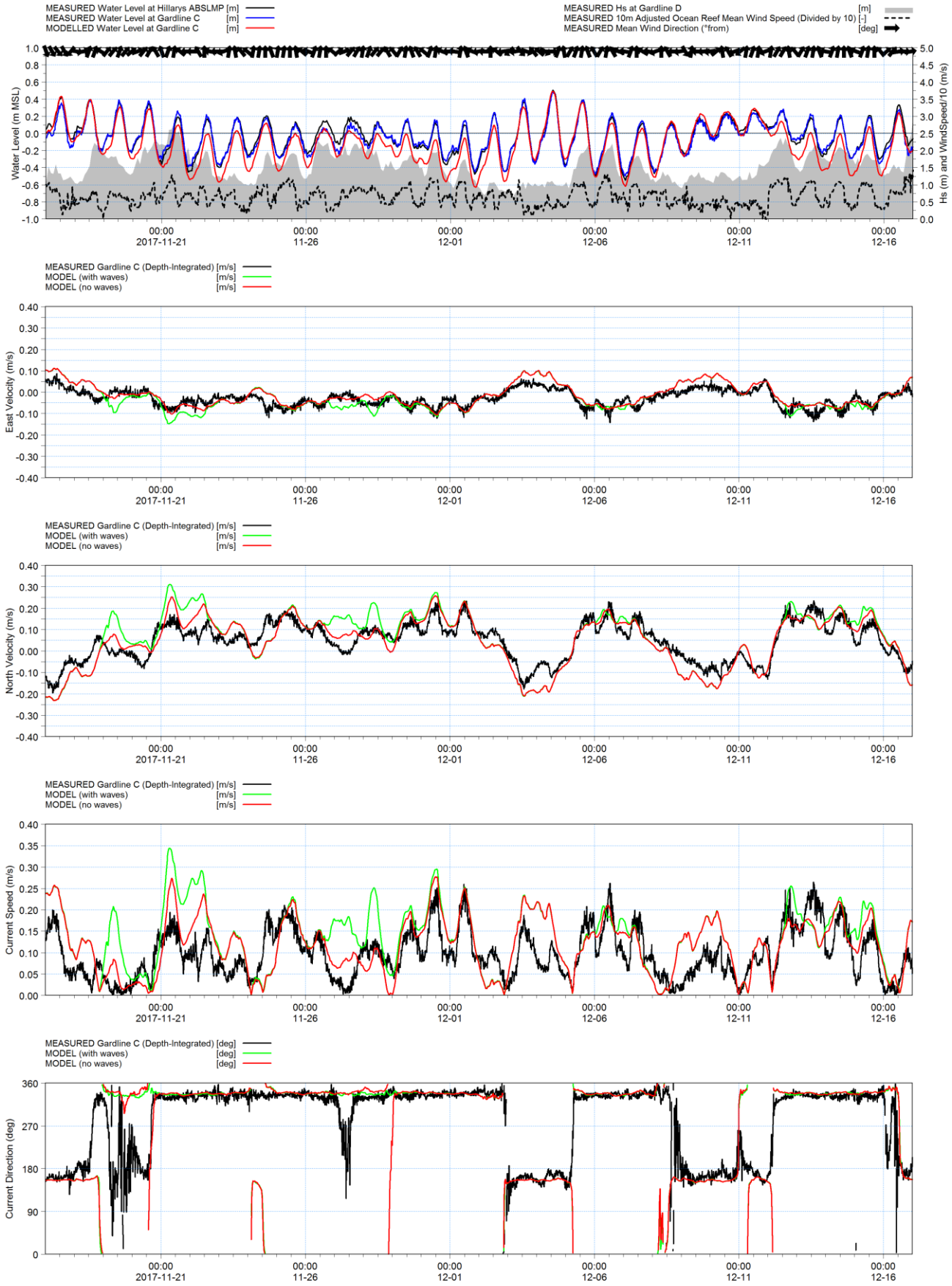

Figure A4-3a: Local 3D Hydrodynamic Model vs. Gardline C. Depth-integrated, Summer 2017.

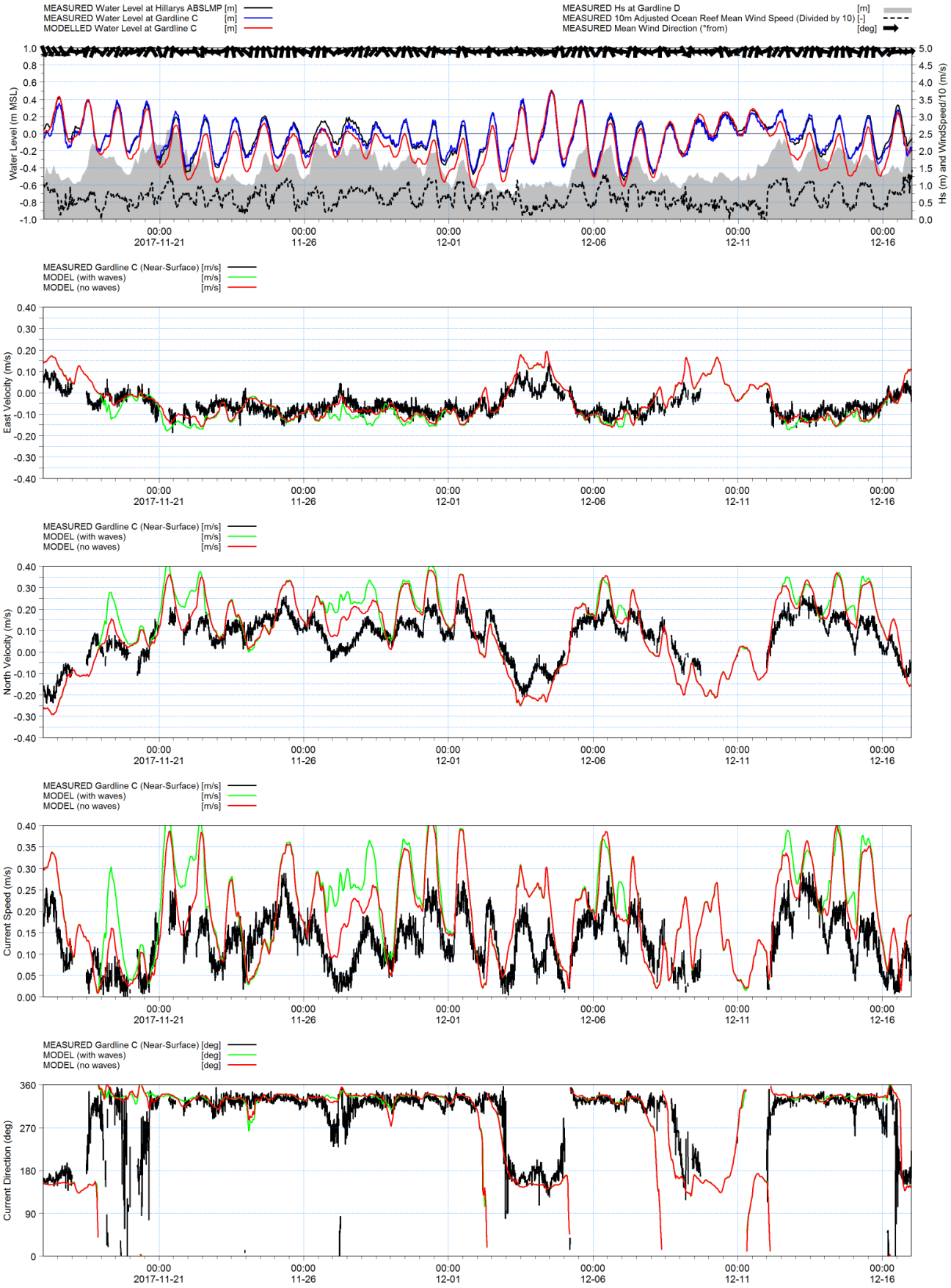

Figure A4-3b: Local 3D Hydrodynamic Model vs. Gardline C. Surface, Summer 2017.

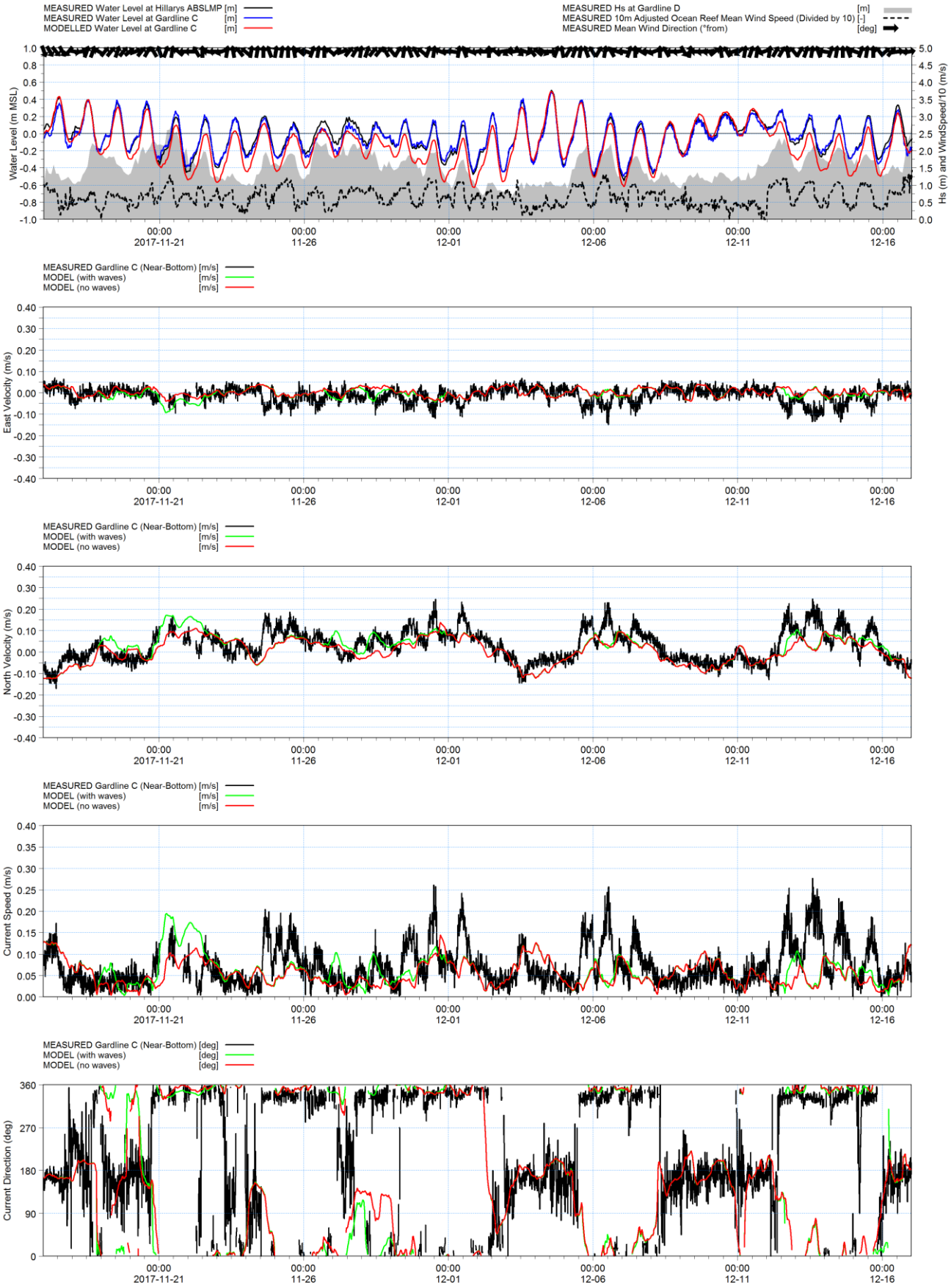

Figure A4-3c: Local 3D Hydrodynamic Model vs. Gardline C. Bottom, Summer 2017.

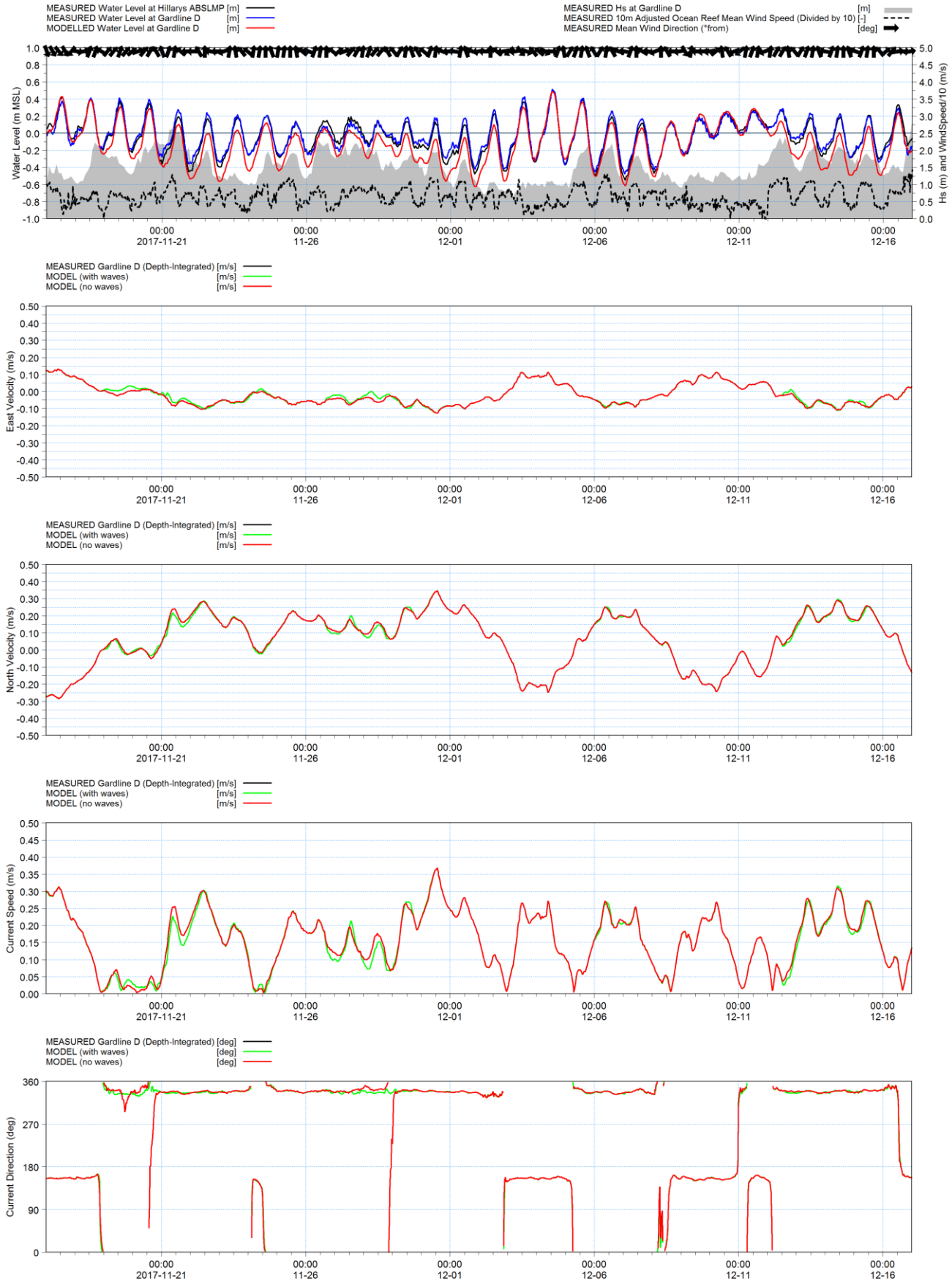

Figure A4-4a: Local 3D Hydrodynamic Model vs. Gardline D. Depth-integrated, Summer 2017.

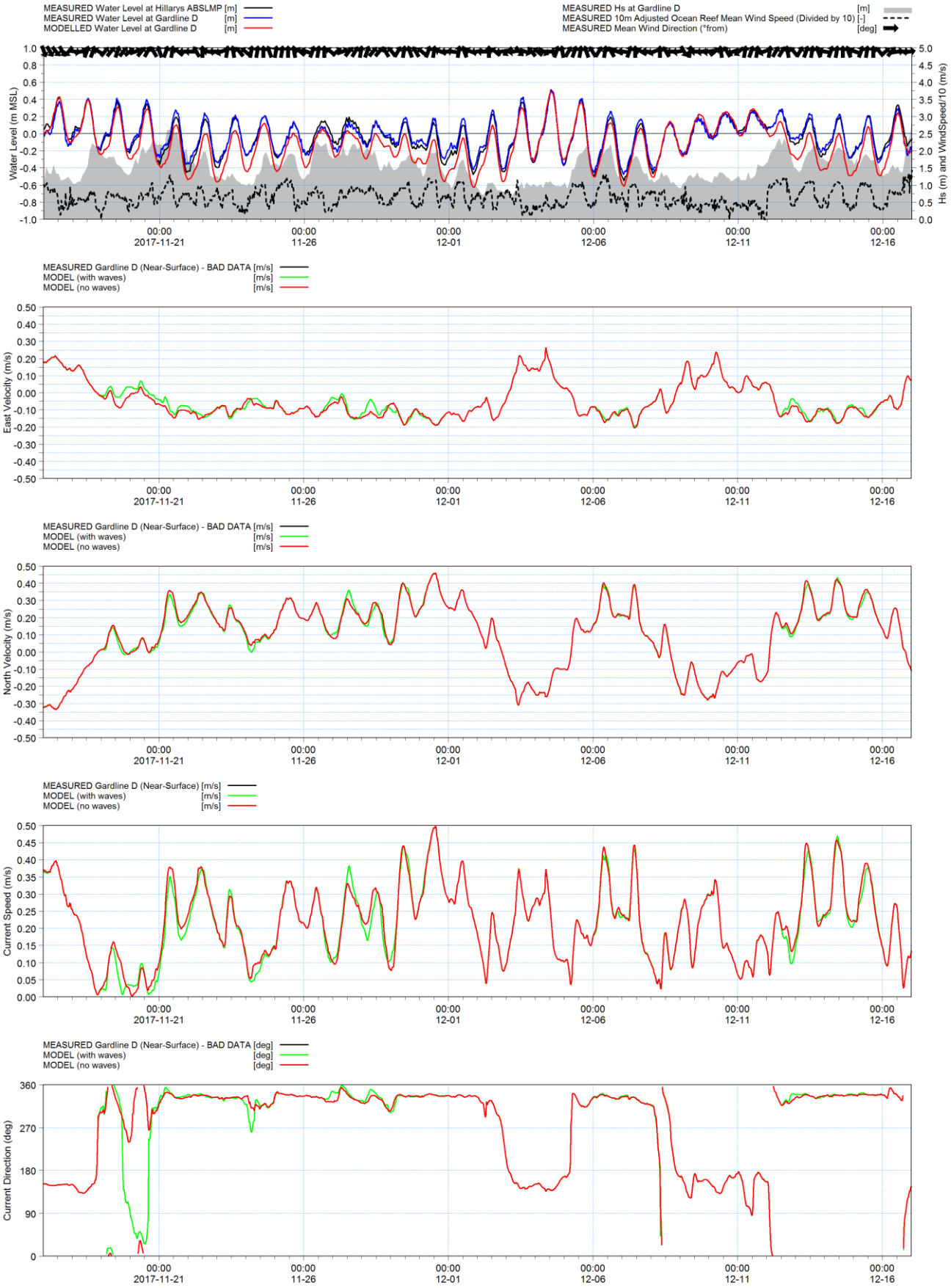

Figure A4-4b: Local 3D Hydrodynamic Model vs. Gardline D. Surface, Summer 2017.

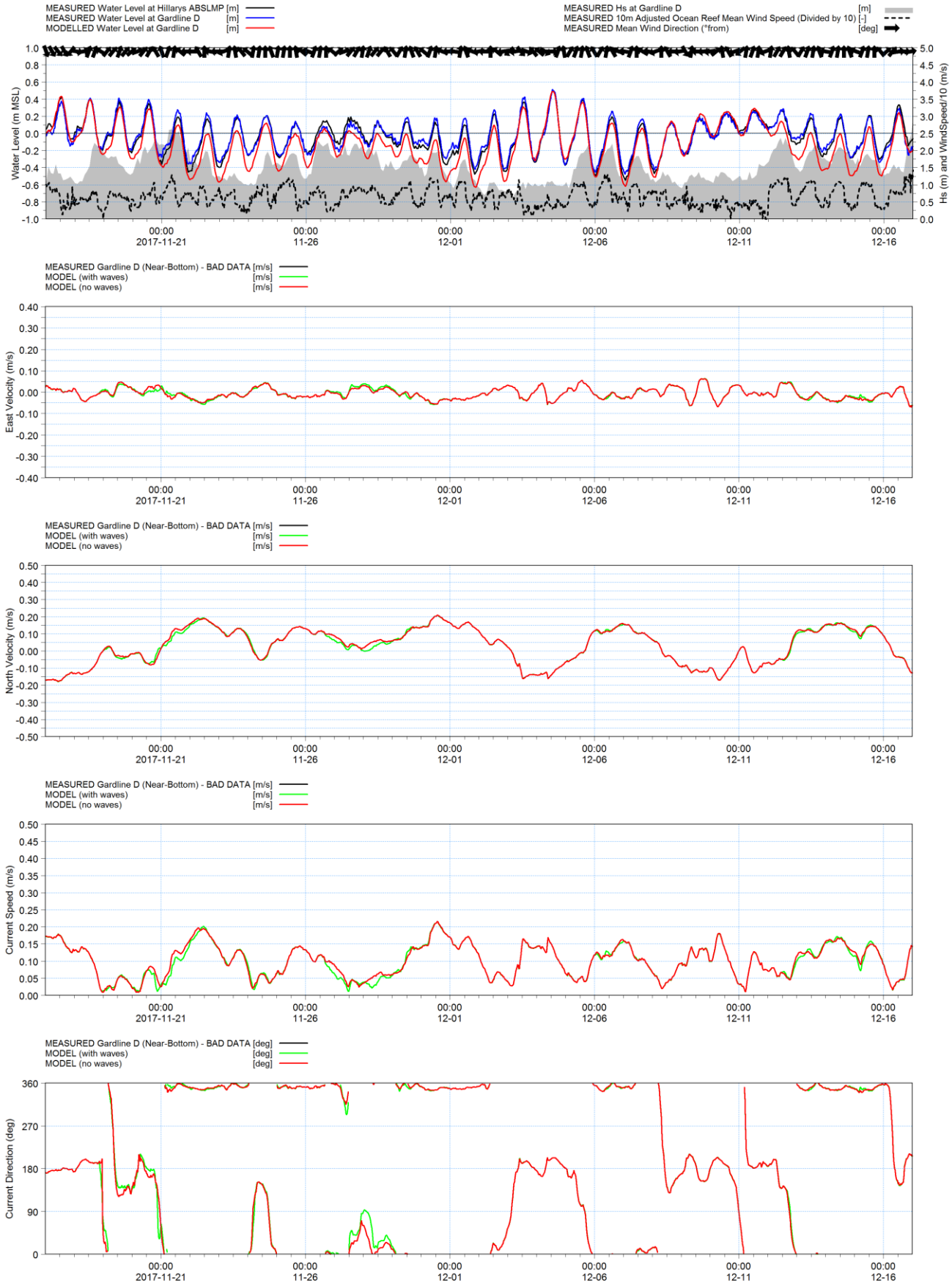

Figure A4-4c: Local 3D Hydrodynamic Model vs. Gardline D. Bottom, Summer 2017.

APPENDIX B1

Local 3D Model Autumn 2017 Calibration

Current Speed Scatter Plots

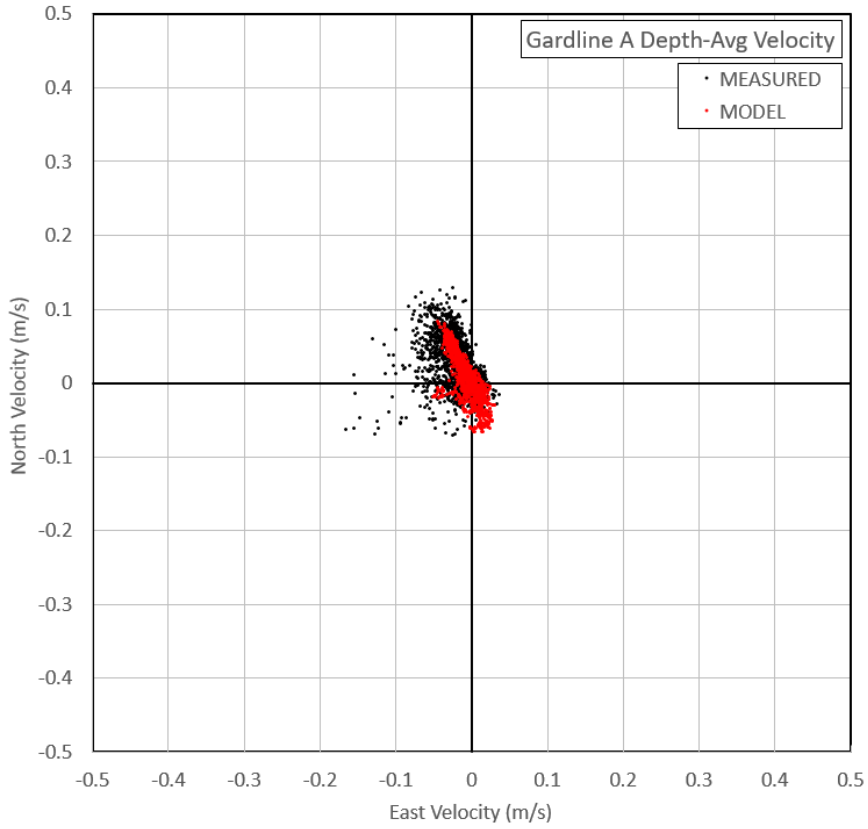

Figure B1-1a Scatter plot of modelled vs. measured current speeds at Gardline A. Depth-integrated, Autumn 2017.

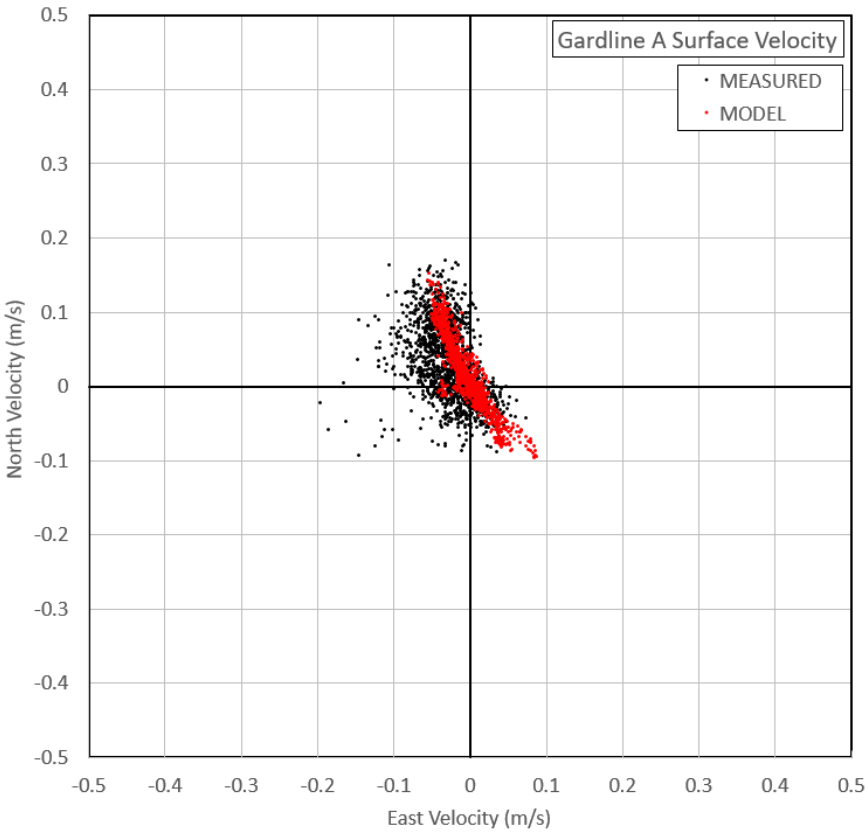

Figure B1-1b Scatter plot of modelled vs. measured current speeds at Gardline A. Surface, Autumn 2017.

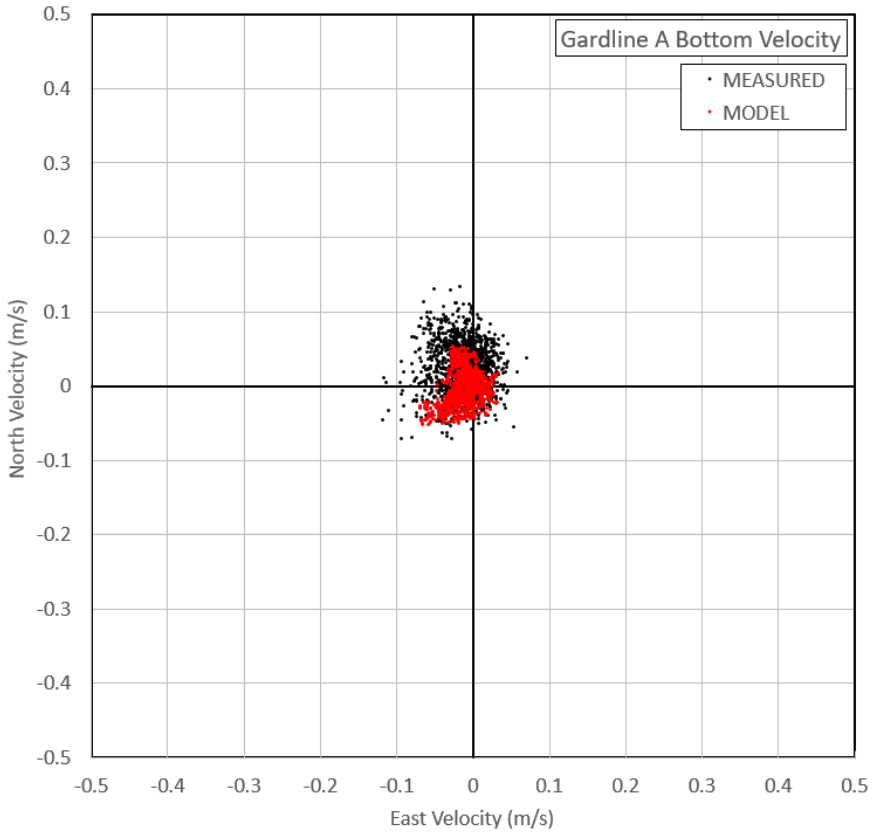

Figure B1-1c Scatter plot of modelled vs. measured current speeds at Gardline A. Bottom, Autumn 2017.

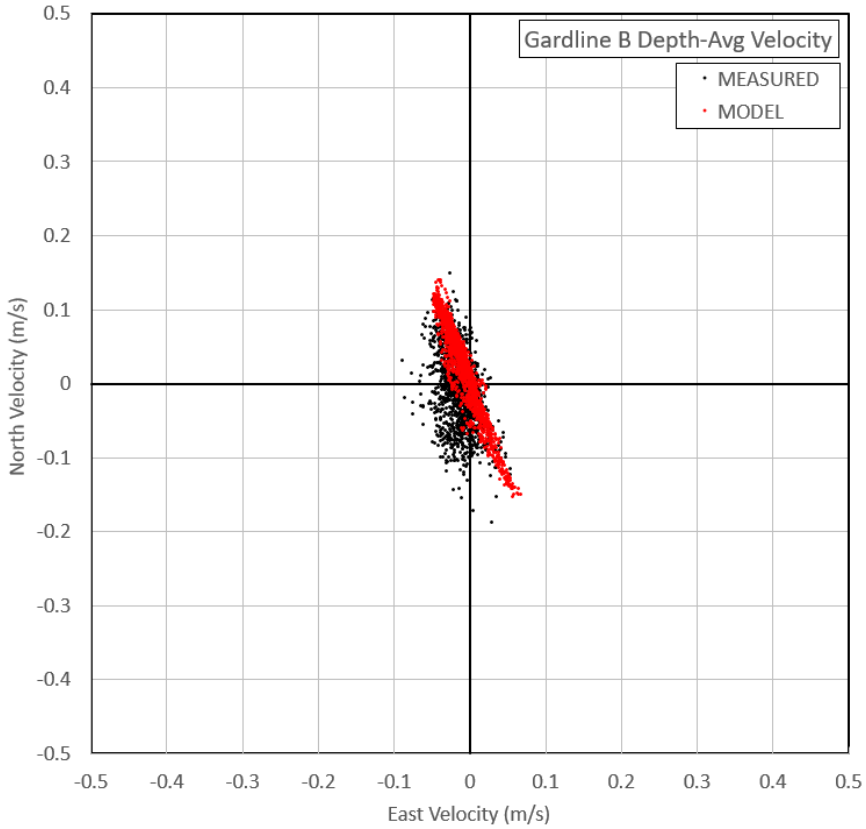

Figure B1-2a Scatter plot of modelled vs. measured current speeds at Gardline B. Depth-integrated, Autumn 2017.

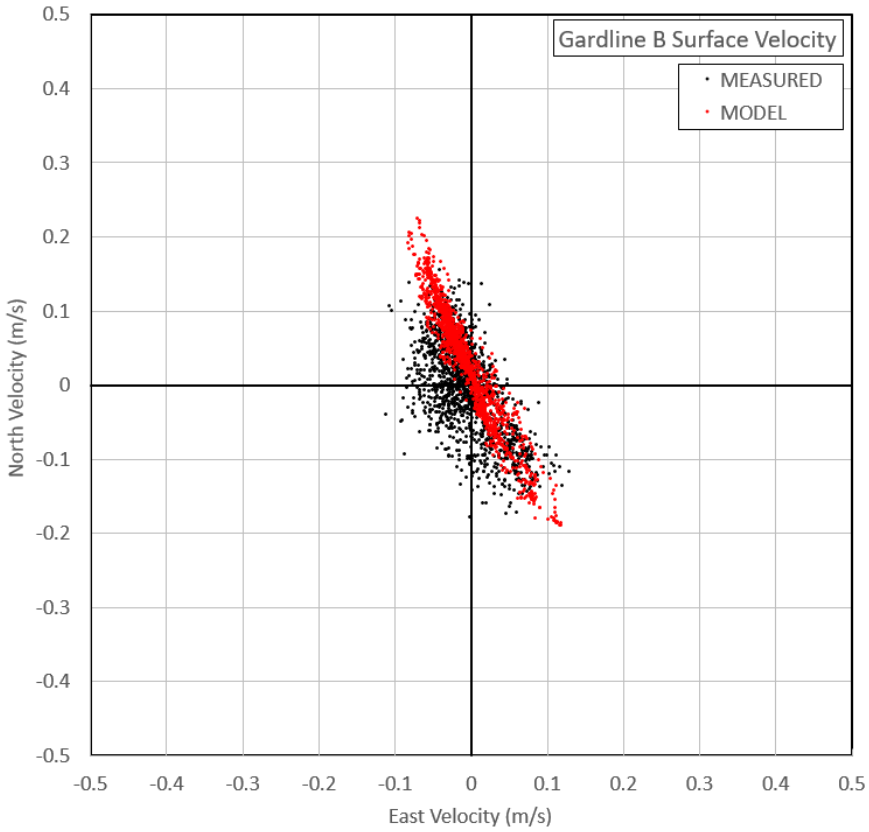

Figure B1-2b Scatter plot of modelled vs. measured current speeds at Gardline B. Surface, Autumn 2017.

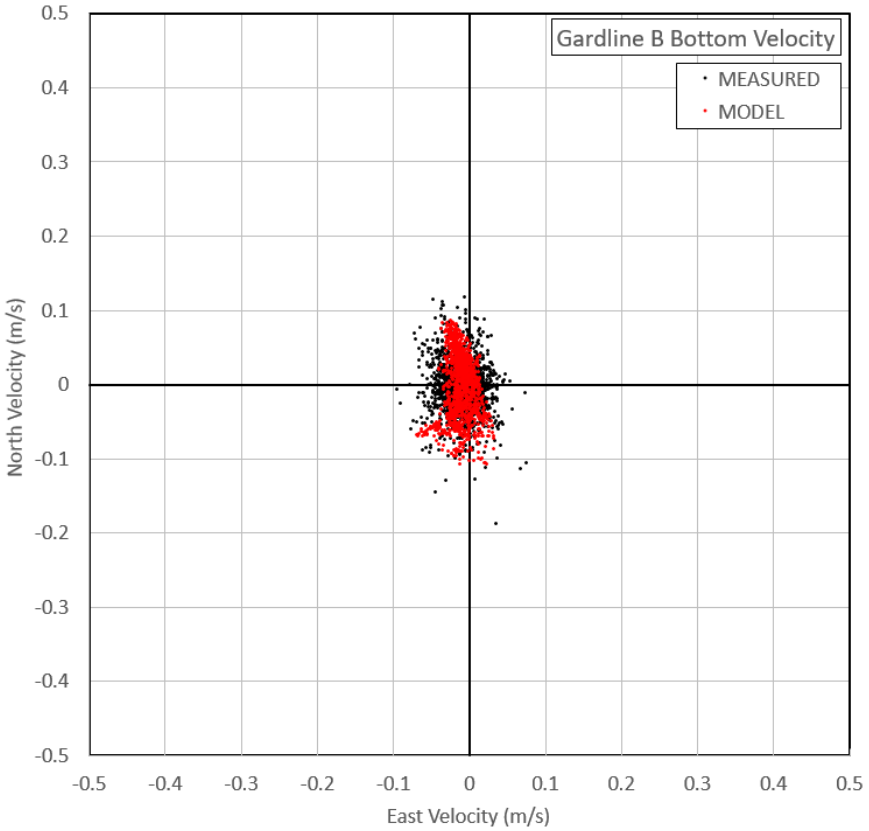

Figure B1-2c Scatter plot of modelled vs. measured current speeds at Gardline B. Bottom, Autumn 2017.

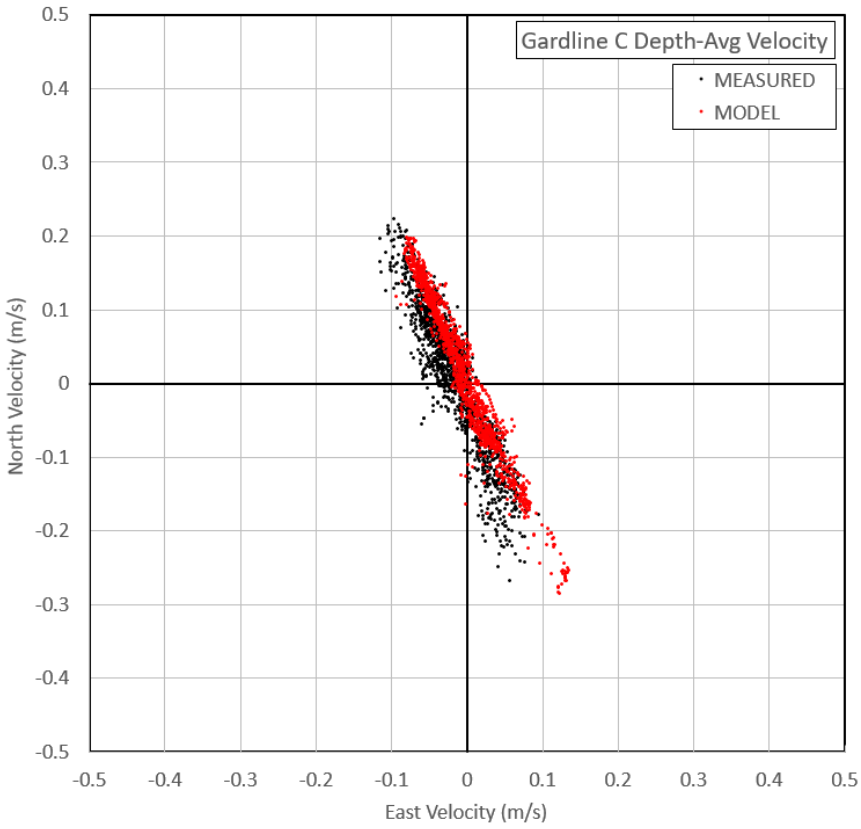

Figure B1-3a Scatter plot of modelled vs. measured current speeds at Gardline C. Depth-integrated, Autumn 2017.

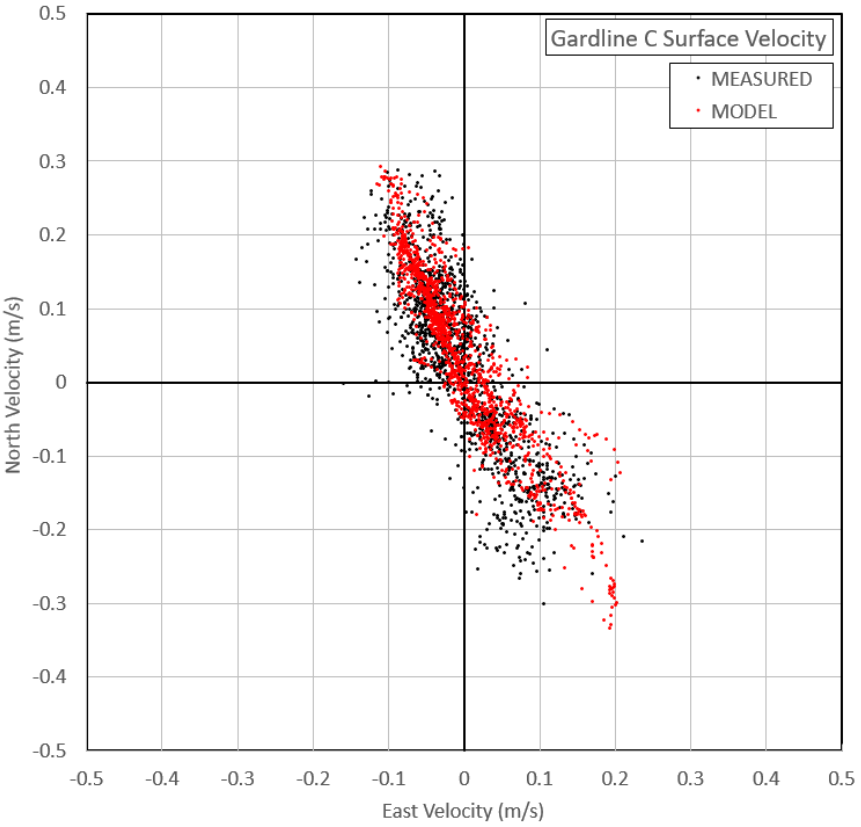

Figure B1-3b Scatter plot of modelled vs. measured current speeds at Gardline C. Surface, Autumn 2017.

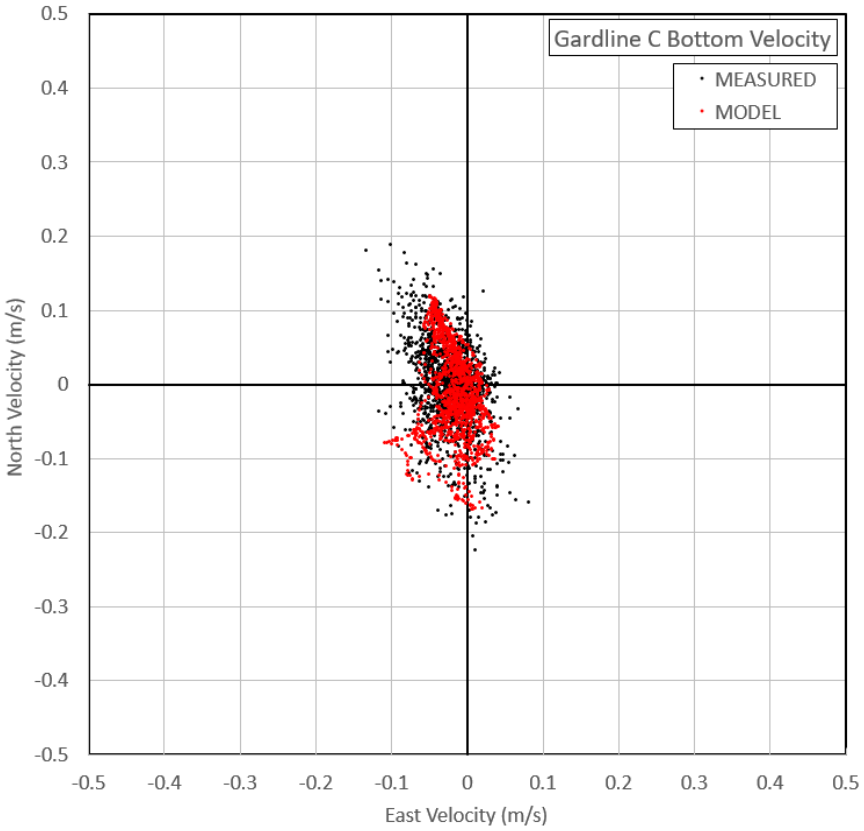

Figure B1-3c Scatter plot of modelled vs. measured current speeds at Gardline C. Bottom, Autumn 2017.

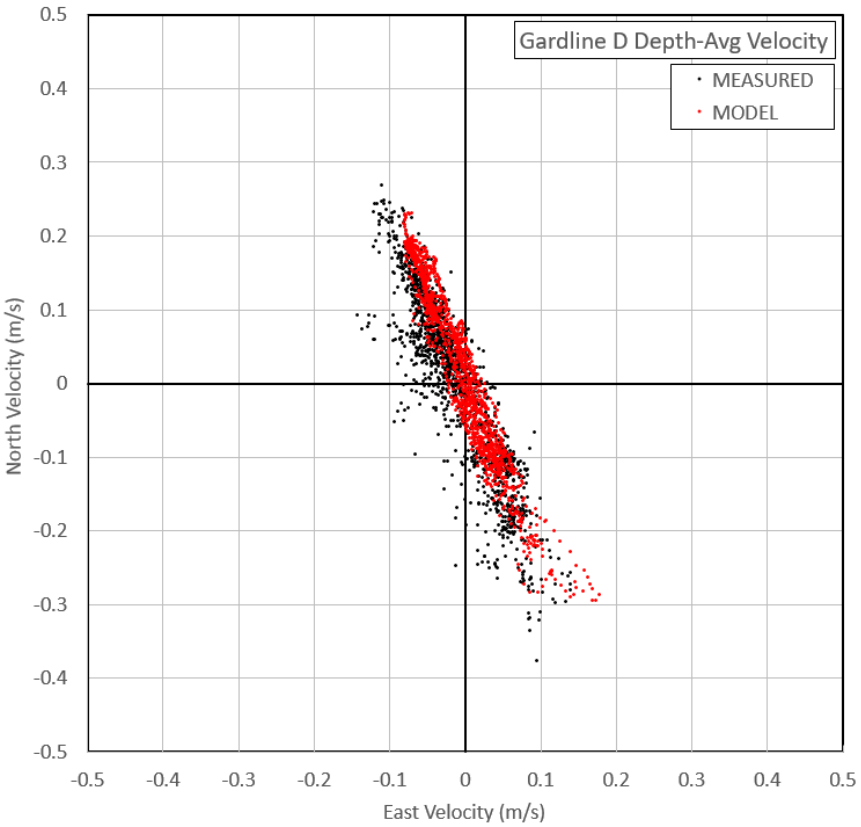

Figure B1-4a Scatter plot of modelled vs. measured current speeds at Gardline D. Depth-integrated, Autumn 2017.

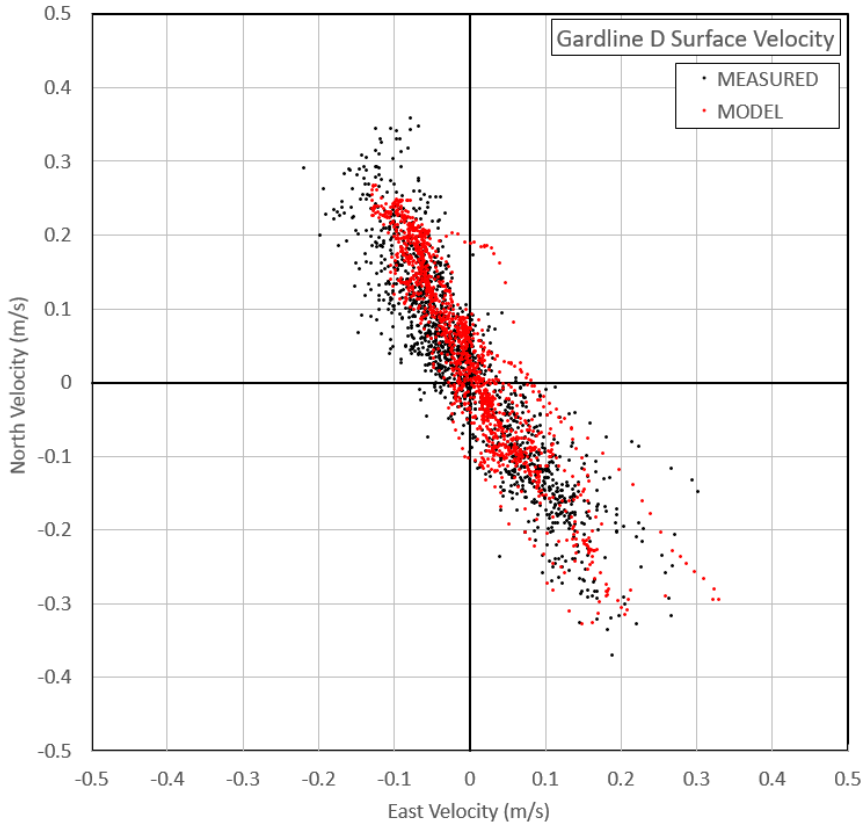

Figure B1-4b Scatter plot of modelled vs. measured current speeds at Gardline D. Surface, Autumn 2017.

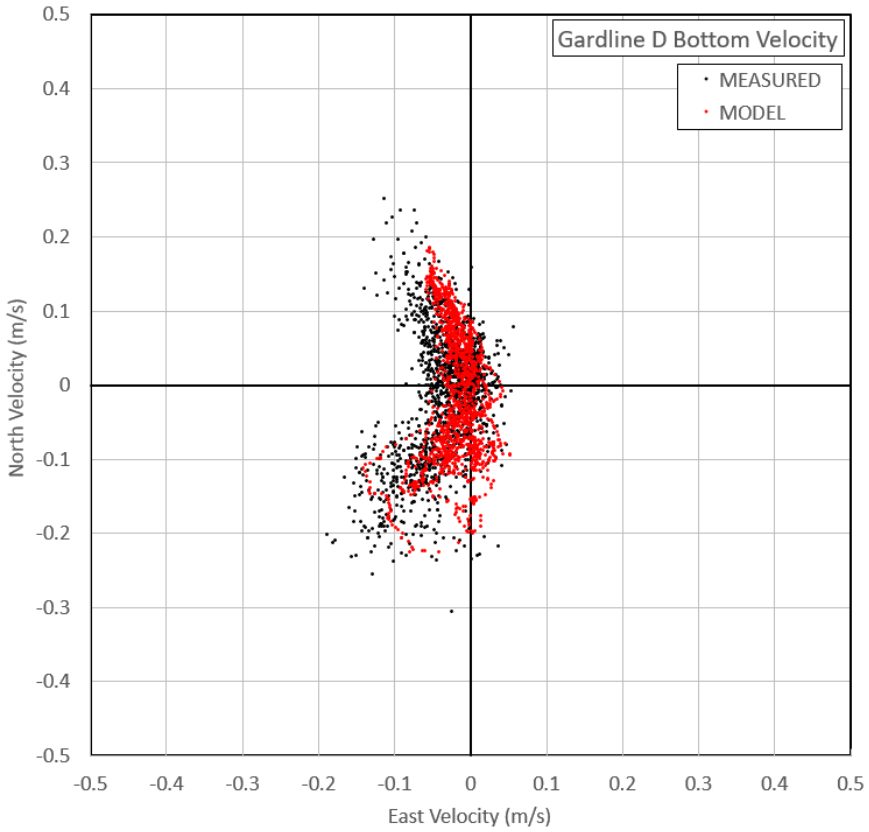

Figure B1-4c Scatter plot of modelled vs. measured current speeds at Gardline D. Bottom, Autumn 2017.

APPENDIX B2

Local 3D Model Autumn 2005 Validation

Current Speed Scatter Plots

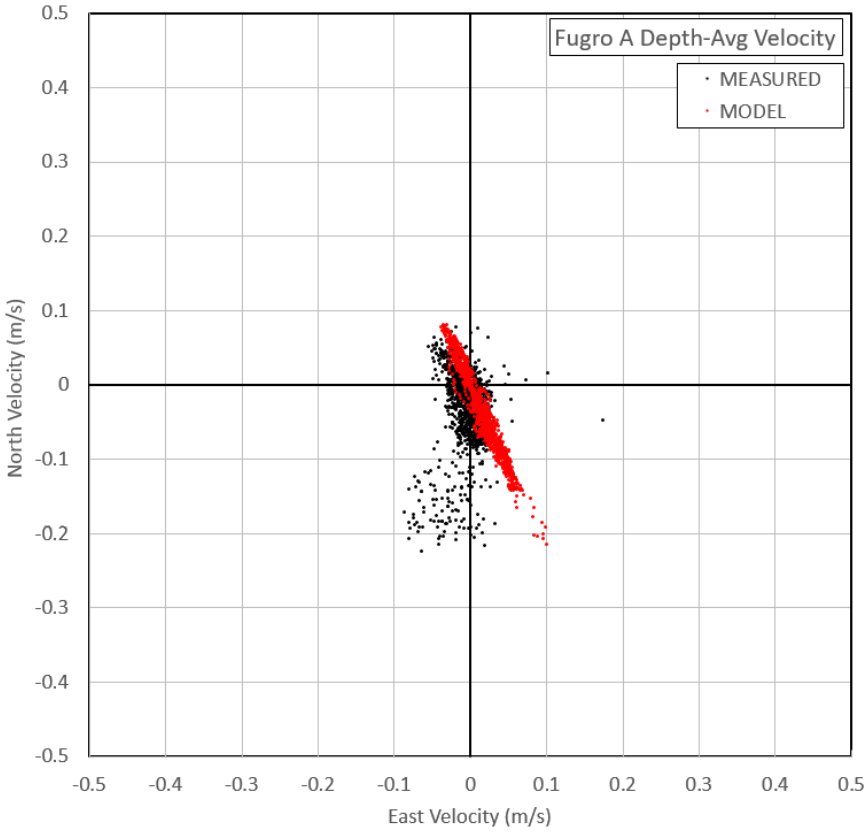

Figure B2-1a Scatter plot of modelled vs. measured current speeds at Fugro A. Depth-integrated, Autumn 2005.

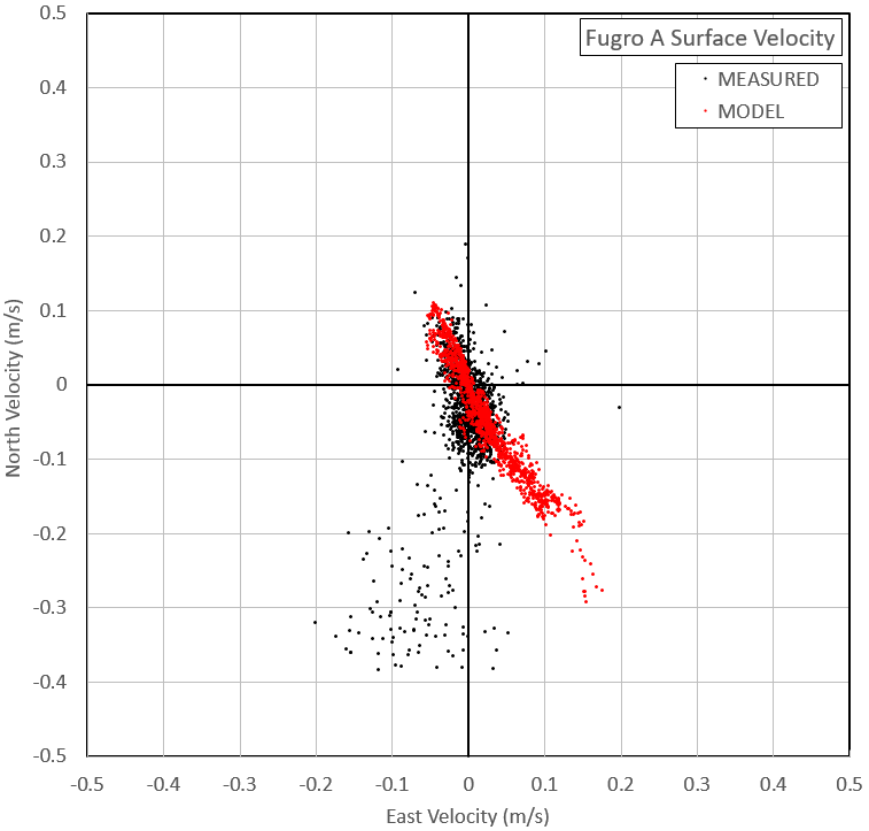

Figure B2-1b Scatter plot of modelled vs. measured current speeds at Fugro A. Surface, Autumn 2005.

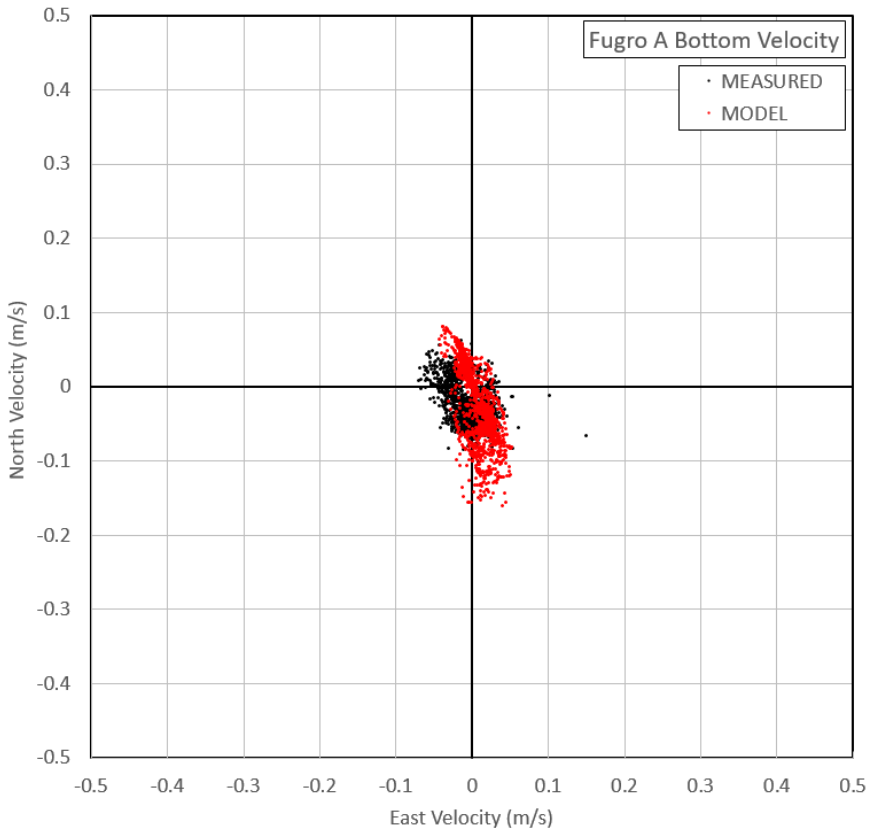

Figure B2-1c Scatter plot of modelled vs. measured current speeds at Fugro A. Bottom, Autumn 2005.

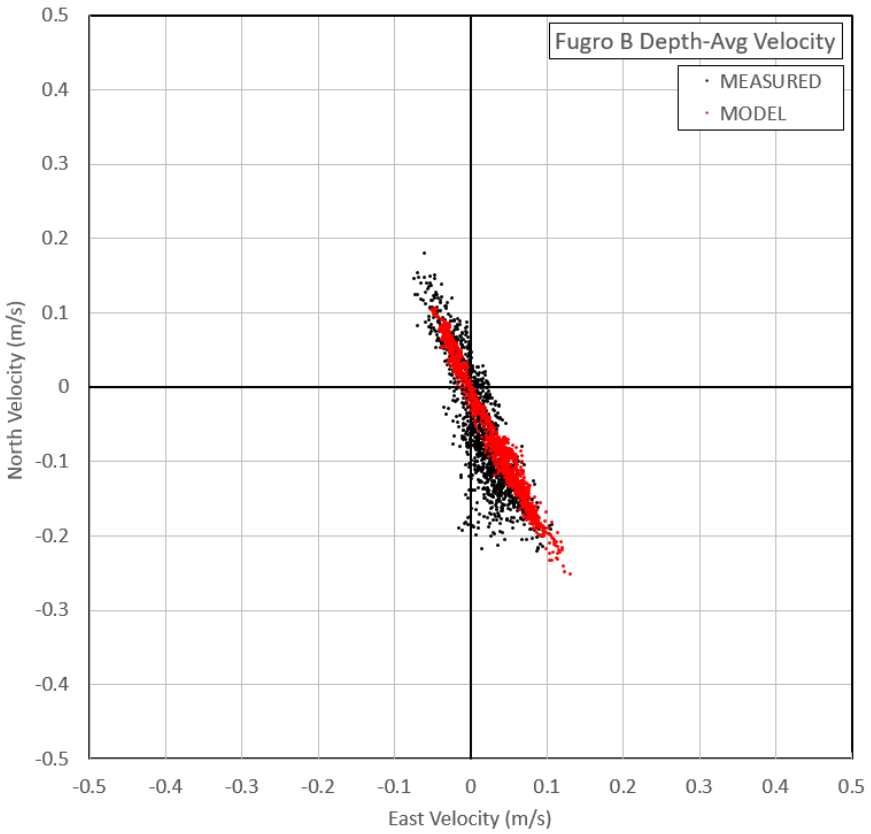

Figure B2-2a Scatter plot of modelled vs. measured current speeds at Fugro B. Depth-integrated, Autumn 2005.

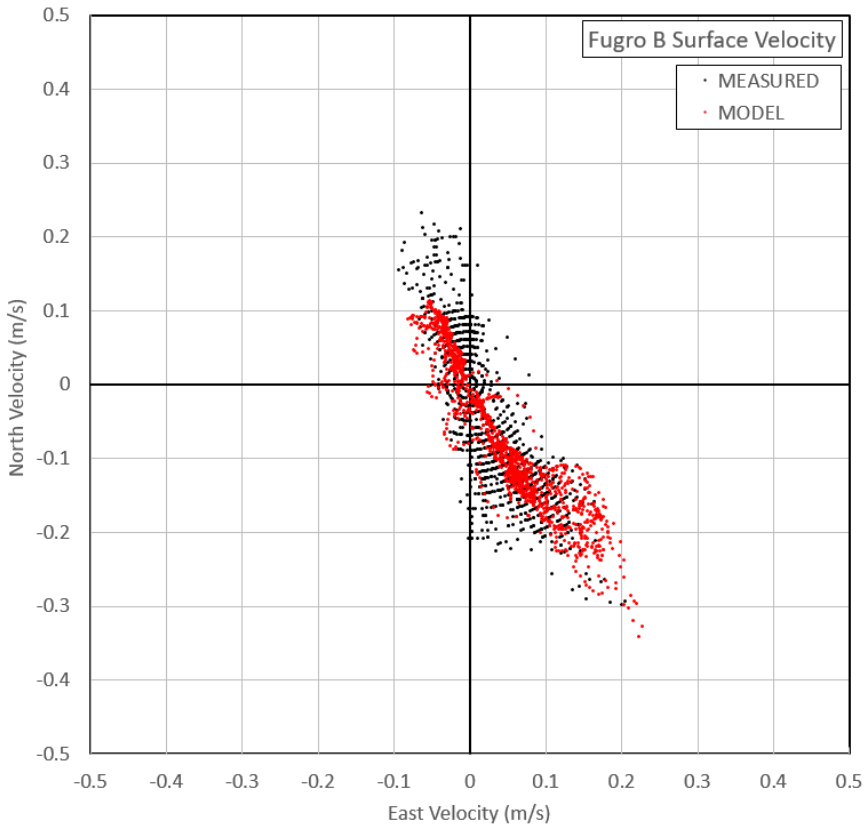

Figure B2-2b Scatter plot of modelled vs. measured current speeds at Fugro B. Surface, Autumn 2005.

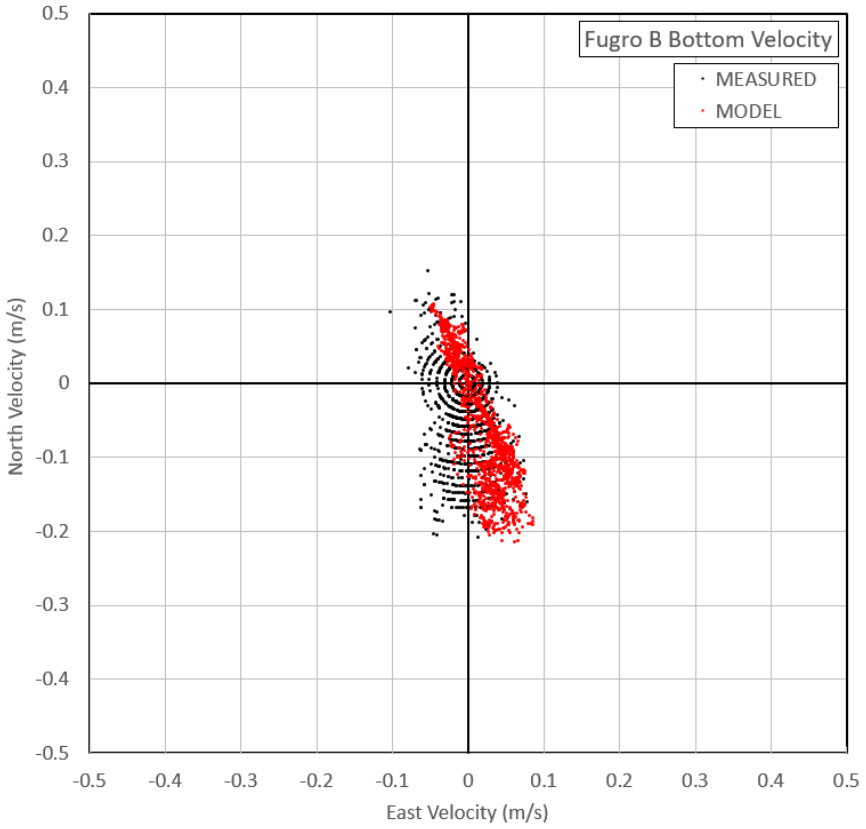

Figure B2-2c Scatter plot of modelled vs. measured current speeds at Fugro B. Bottom, Autumn 2005.

APPENDIX B3

Local 3D Model Winter 2017 Validation

Current Speed Scatter Plots

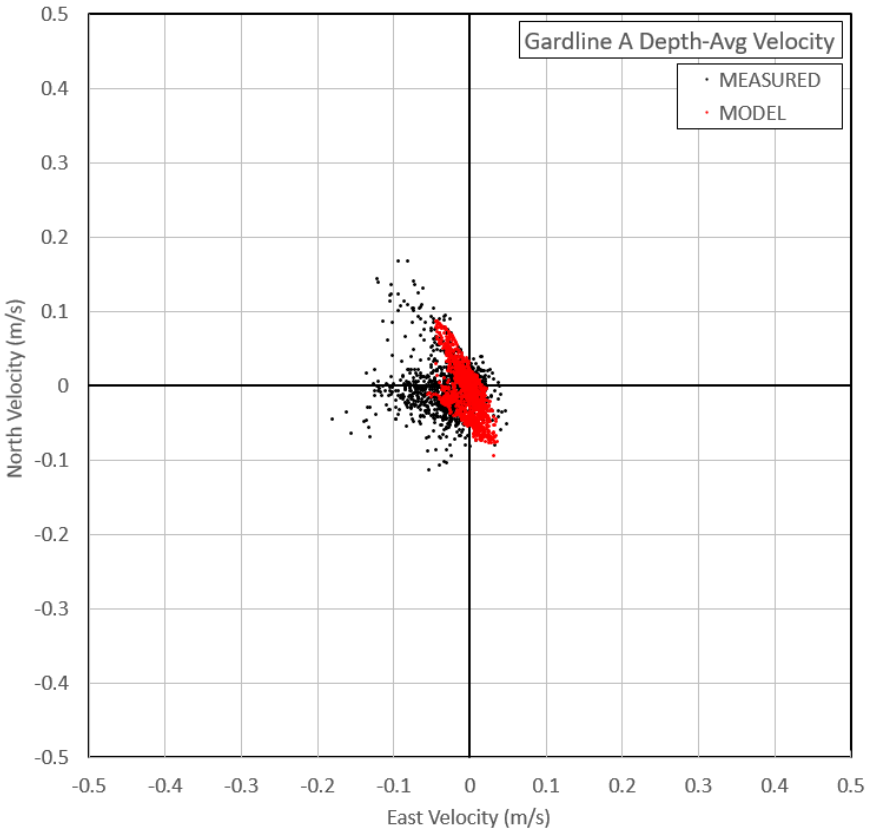

Figure B3-1a Scatter plot of modelled vs. measured current speeds at Gardline A. Depth-integrated, Winter 2017.

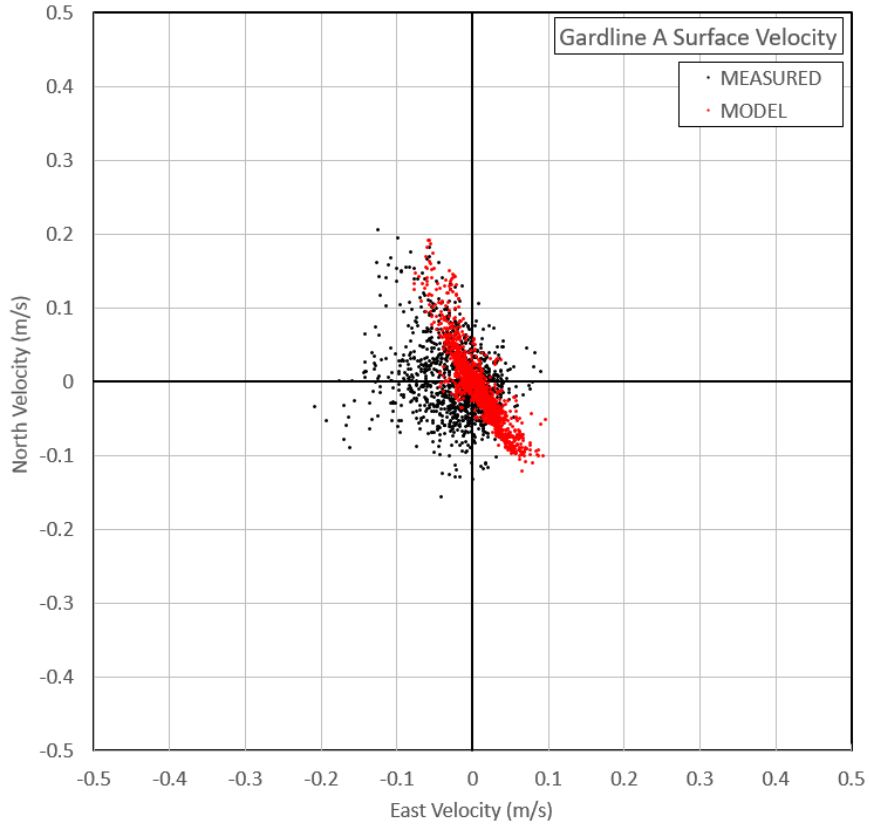

Figure B3-1b Scatter plot of modelled vs. measured current speeds at Gardline A. Surface, Winter 2017.

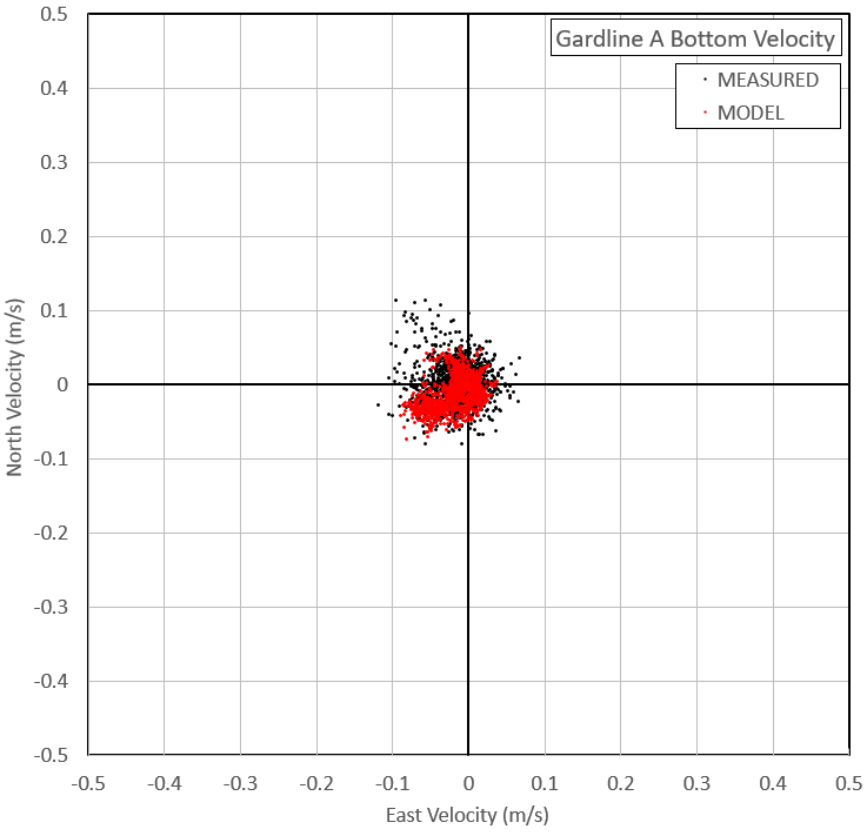

Figure B3-1c Scatter plot of modelled vs. measured current speeds at Gardline A. Bottom, Winter 2017.

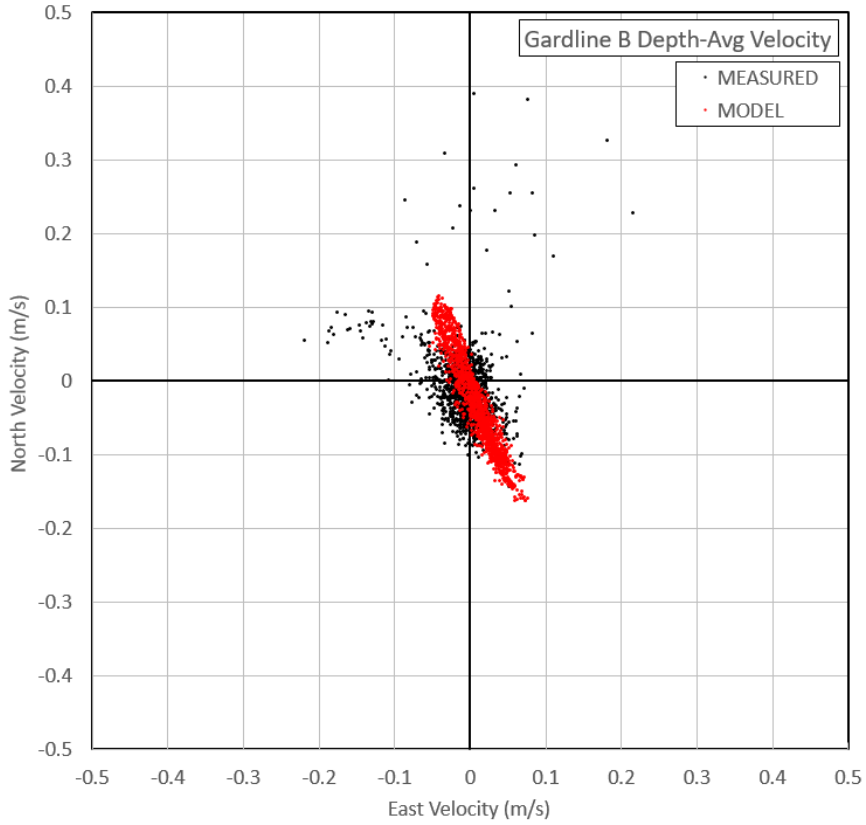

Figure B3-2a Scatter plot of modelled vs. measured current speeds at Gardline B. Depth-integrated, Winter 2017.

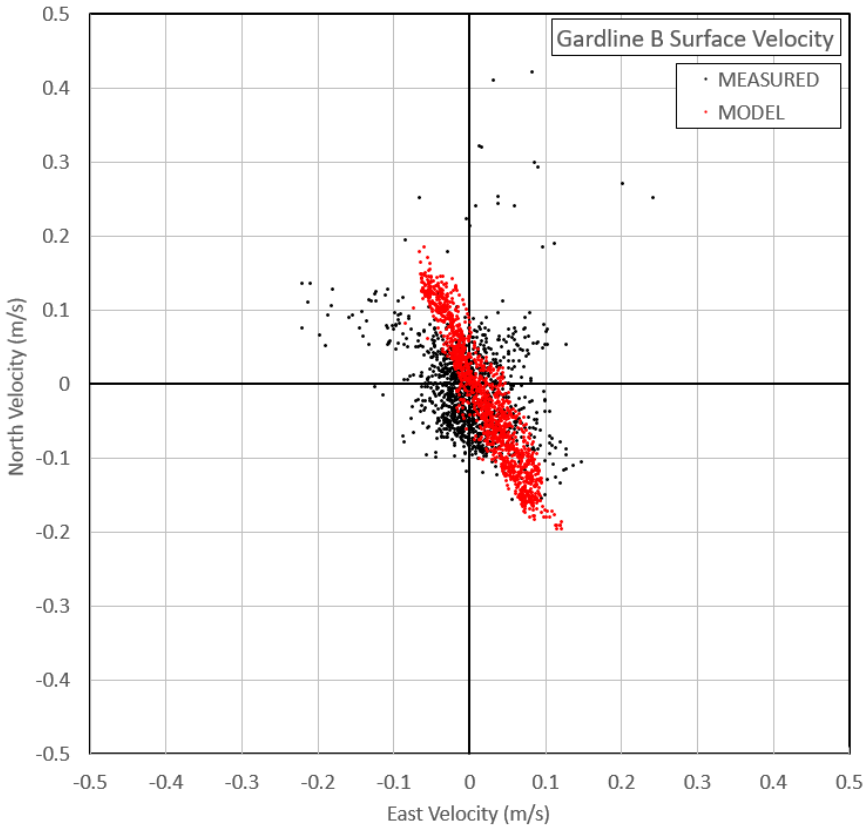

Figure B3-2b Scatter plot of modelled vs. measured current speeds at Gardline B. Surface, Winter 2017.

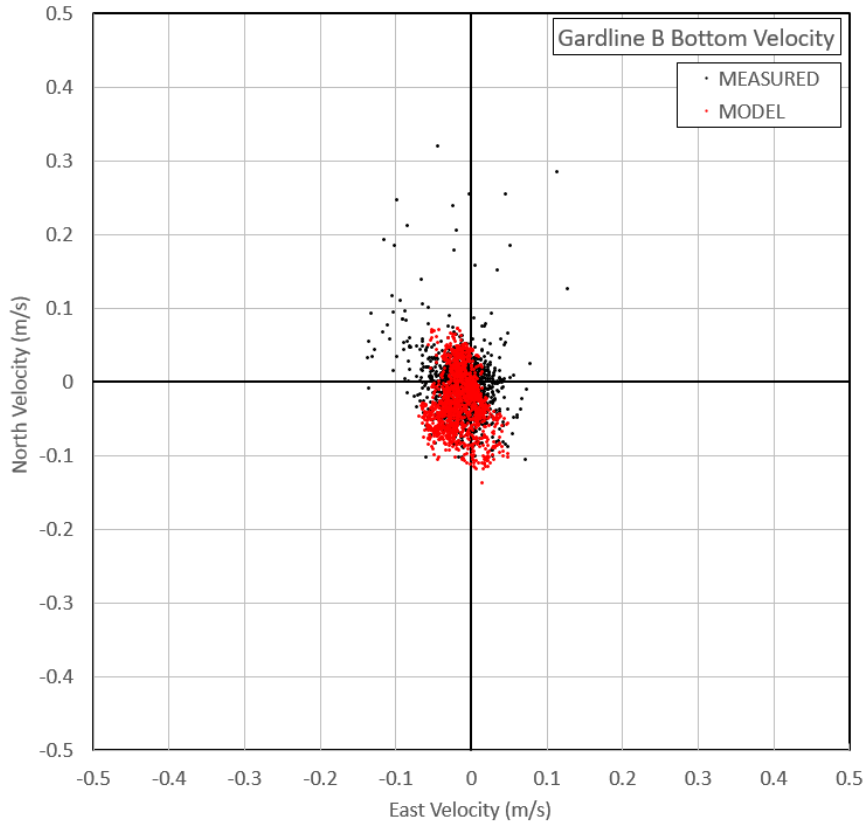

Figure B3-2c Scatter plot of modelled vs. measured current speeds at Gardline B. Bottom, Winter 2017.

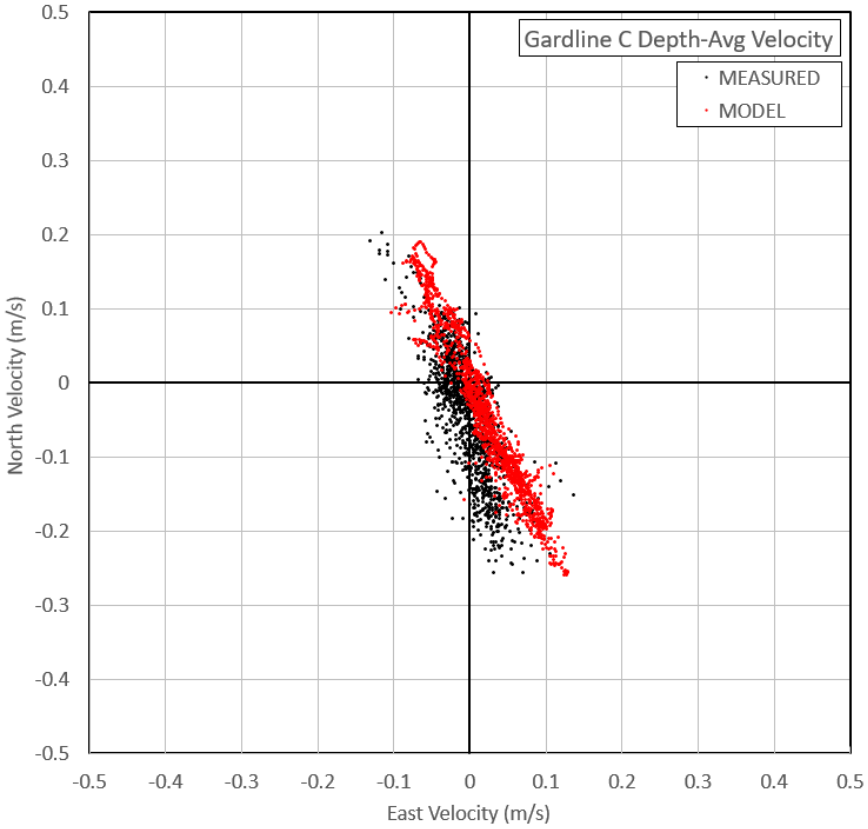

Figure B3-3a Scatter plot of modelled vs. measured current speeds at Gardline C. Depth-integrated, Winter 2017.

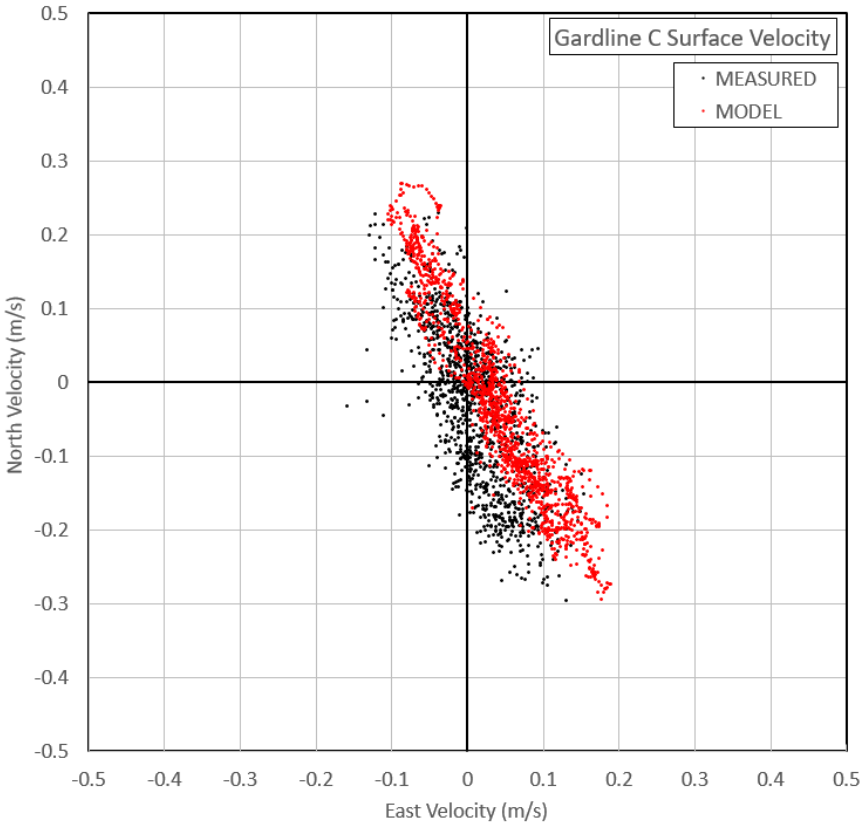

Figure B3-3b Scatter plot of modelled vs. measured current speeds at Gardline C. Surface, Winter 2017.

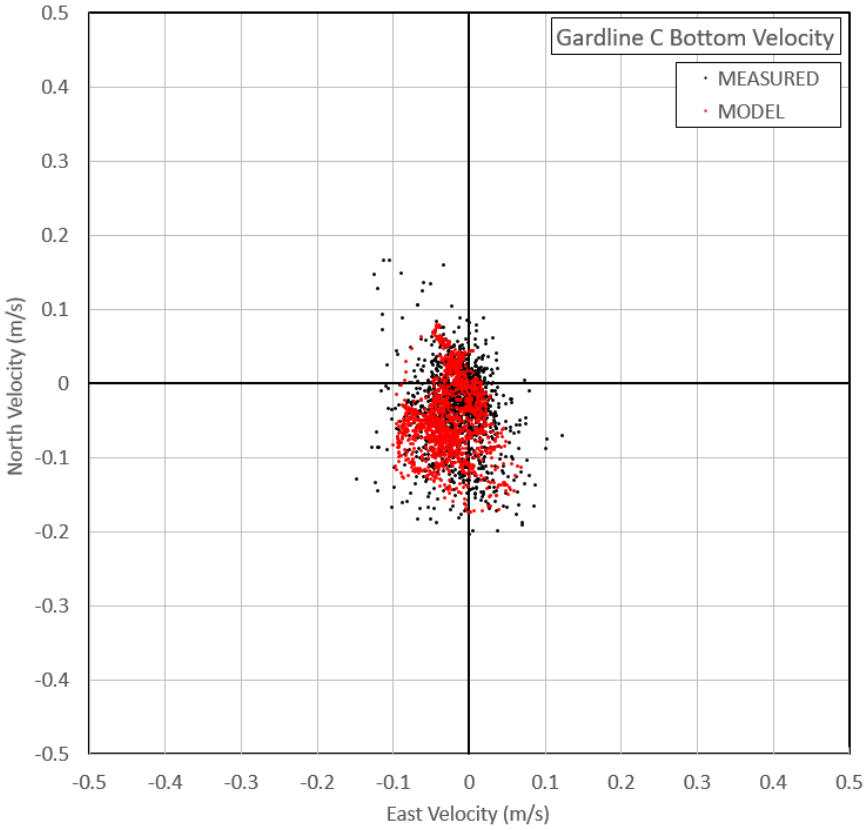

Figure B3-3c Scatter plot of modelled vs. measured current speeds at Gardline C. Bottom, Winter 2017.

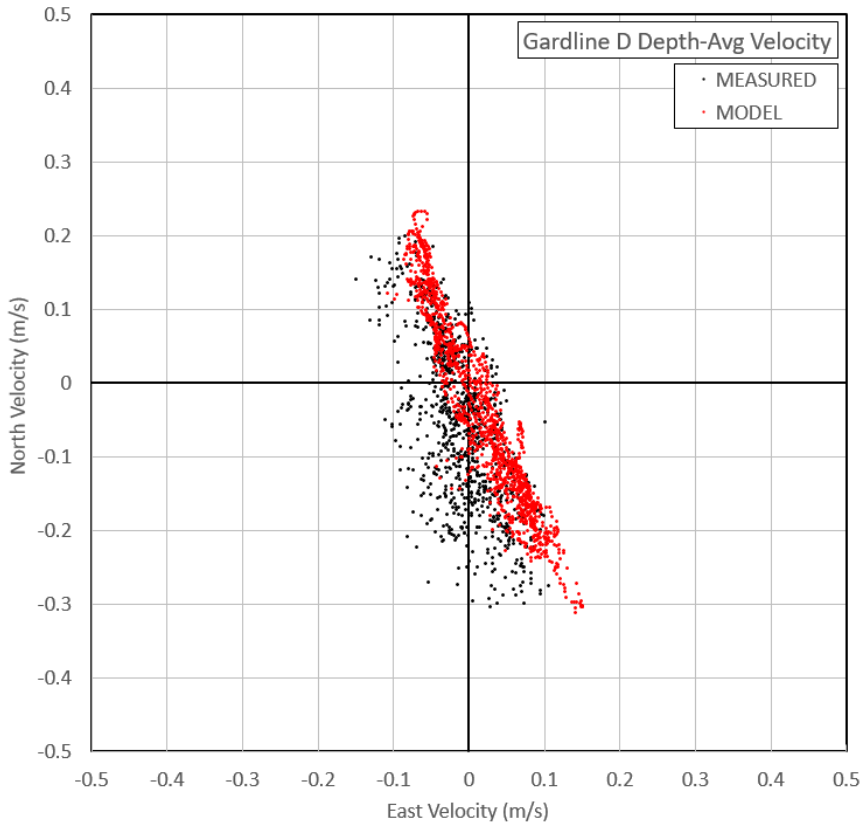

Figure B3-4a Scatter plot of modelled vs. measured current speeds at Gardline D. Depth-integrated, Winter 2017.

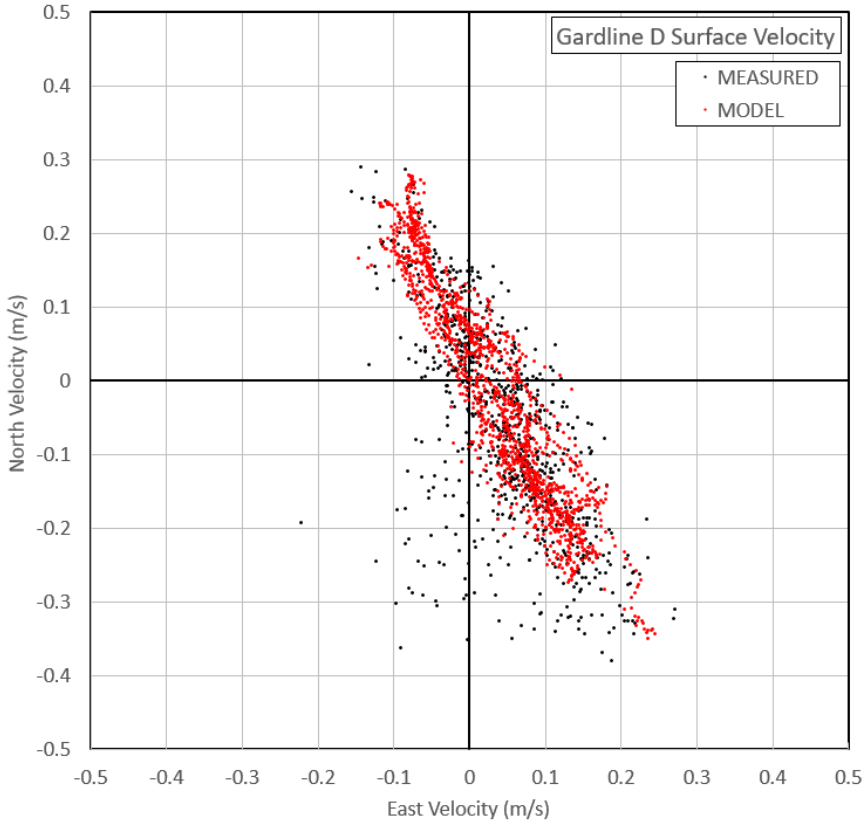

Figure B3-4b Scatter plot of modelled vs. measured current speeds at Gardline D. Surface, Winter 2017.

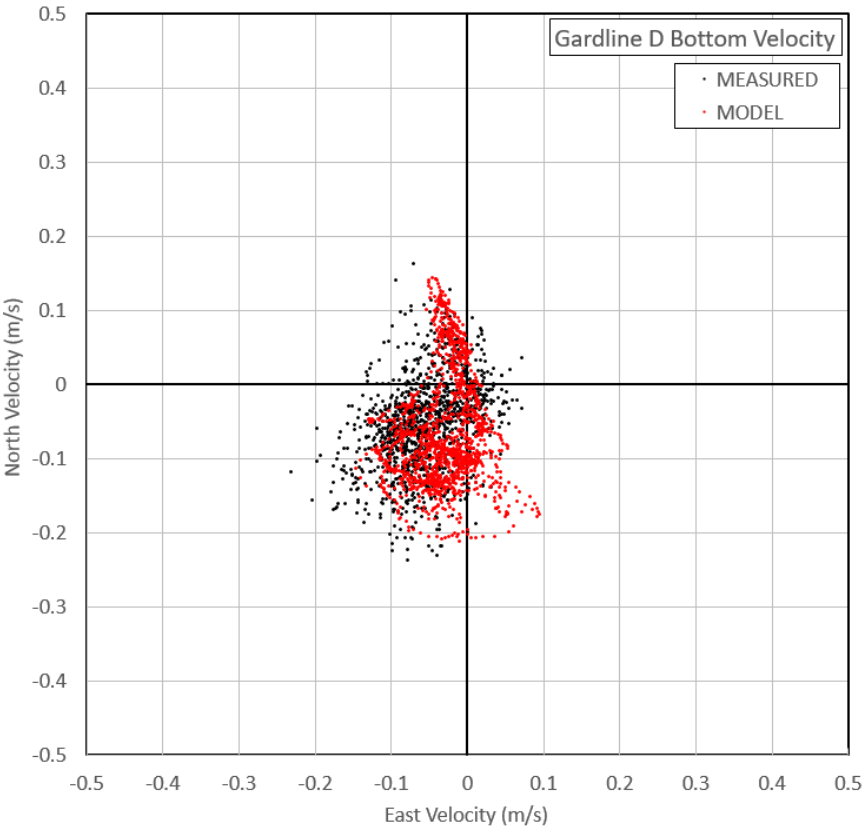

Figure B3-4c Scatter plot of modelled vs. measured current speeds at Gardline D. Bottom, Winter 2017.

APPENDIX B4

Local 3D Model Summer 2017 Calibration

Current Speed Scatter Plots

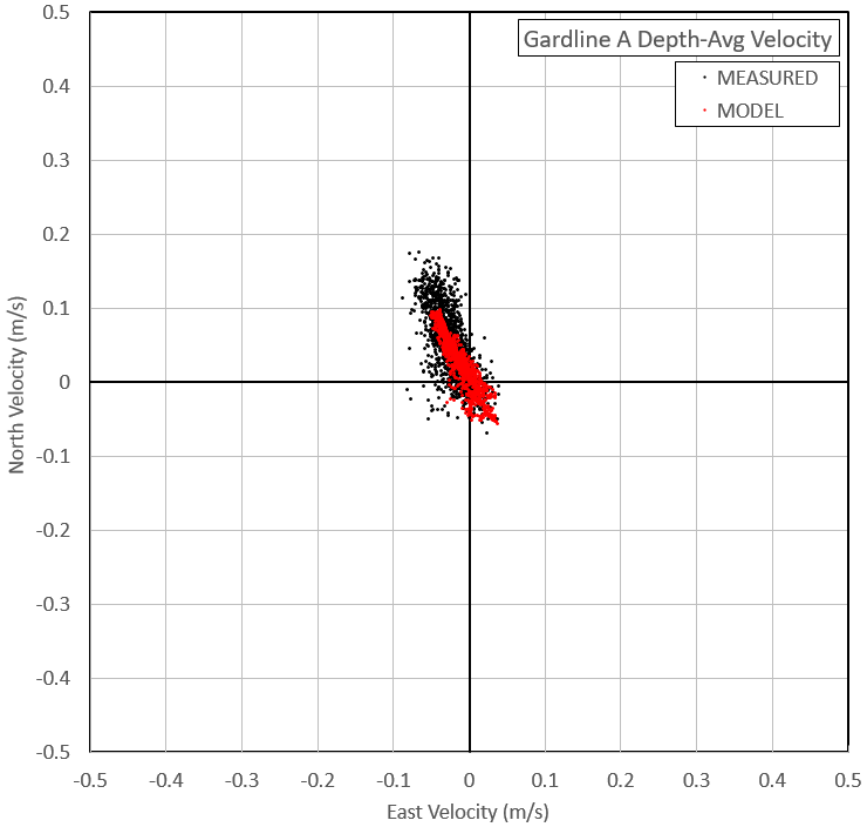

Figure B4-1a Scatter plot of modelled vs. measured current speeds at Gardline A. Depth-integrated, Summer 2017.

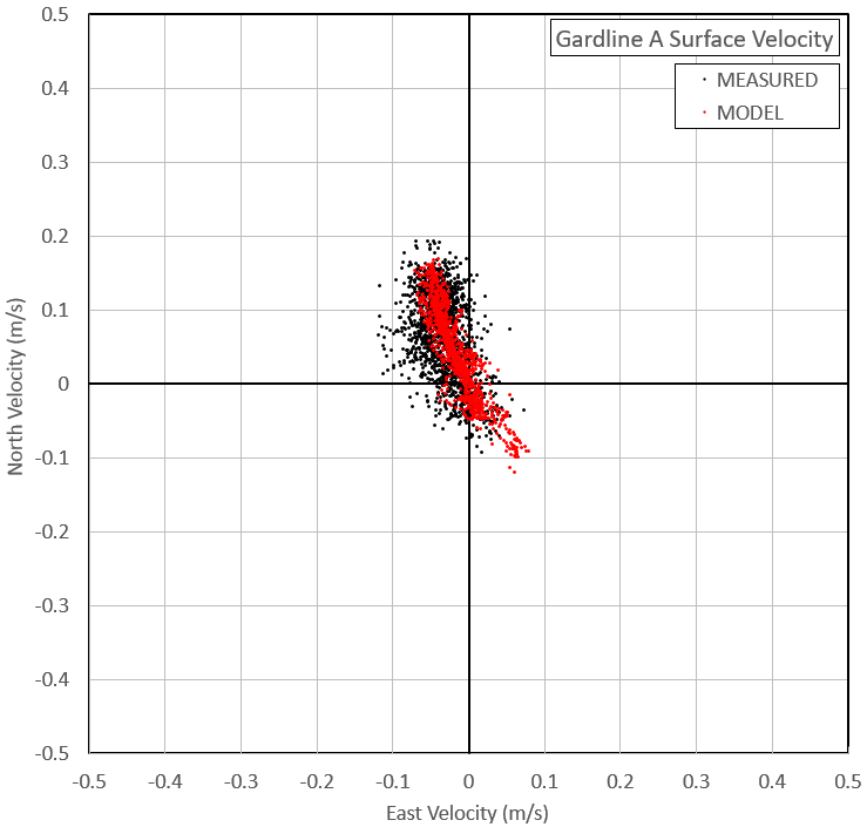

Figure B4-1b Scatter plot of modelled vs. measured current speeds at Gardline A. Surface, Summer 2017.

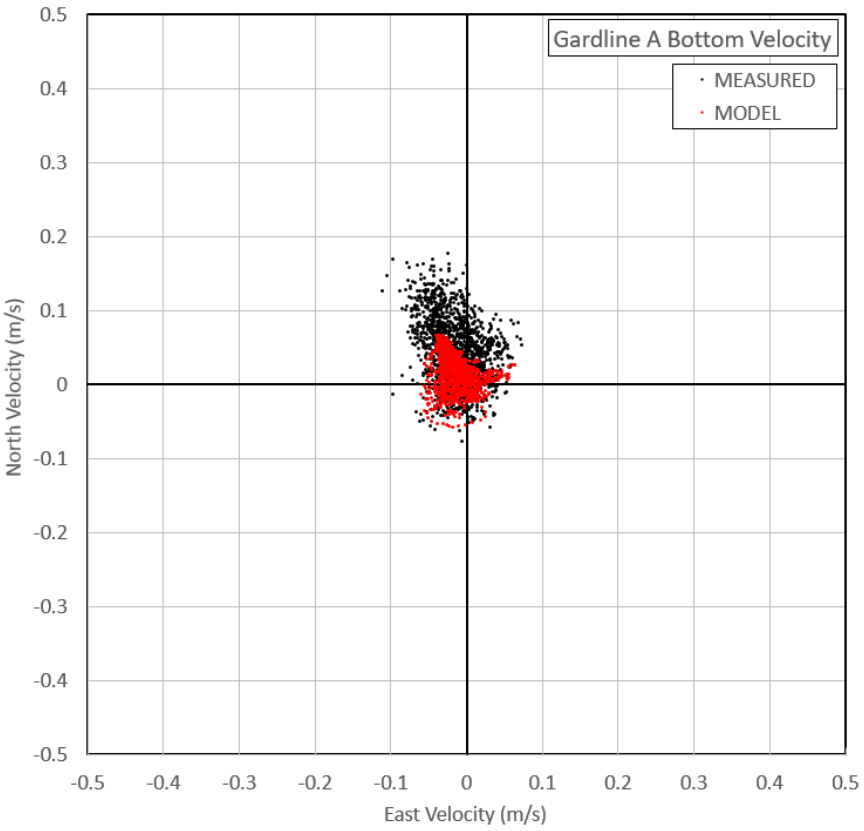

Figure B4-1c Scatter plot of modelled vs. measured current speeds at Gardline A. Bottom, Summer 2017.

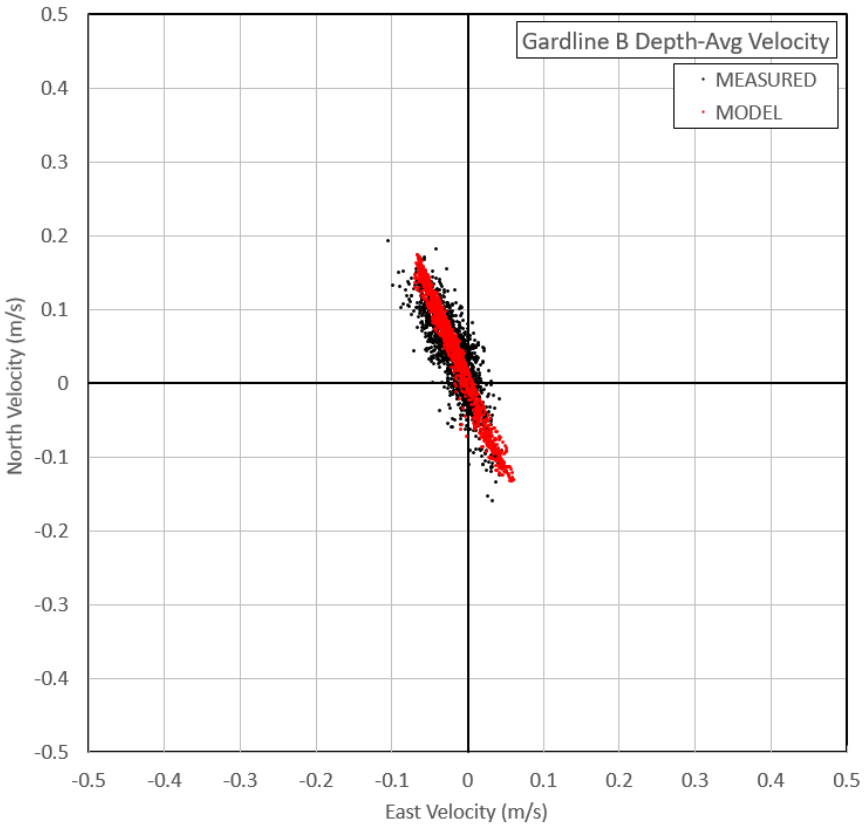

Figure B4-2a Scatter plot of modelled vs. measured current speeds at Gardline B. Depth-integrated, Summer 2017.

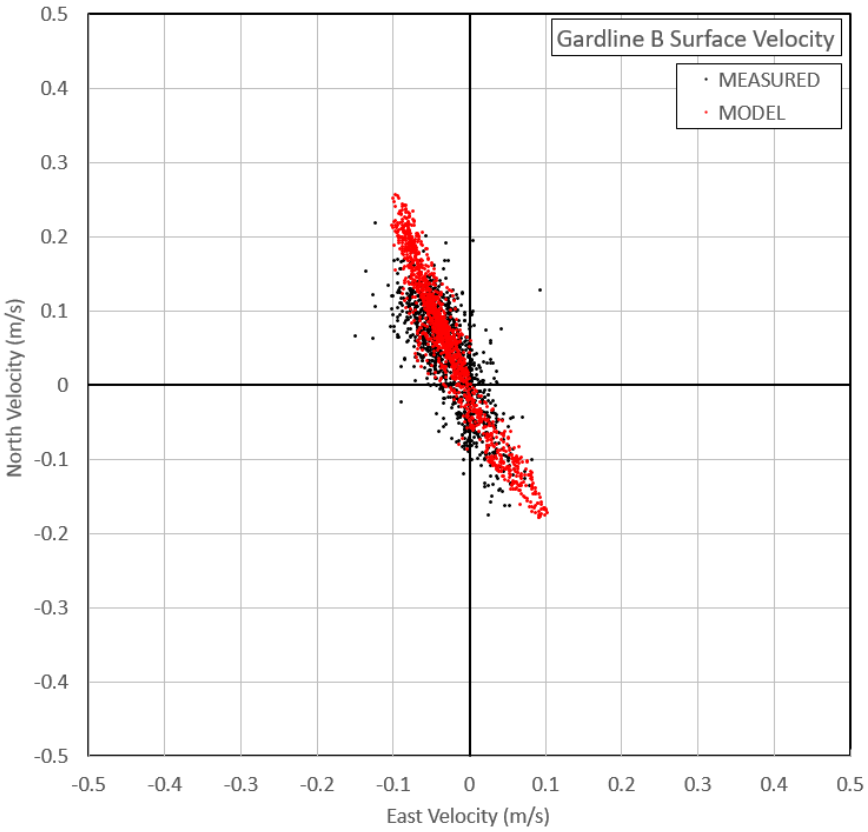

Figure B4-2b Scatter plot of modelled vs. measured current speeds at Gardline B. Surface, Summer 2017.

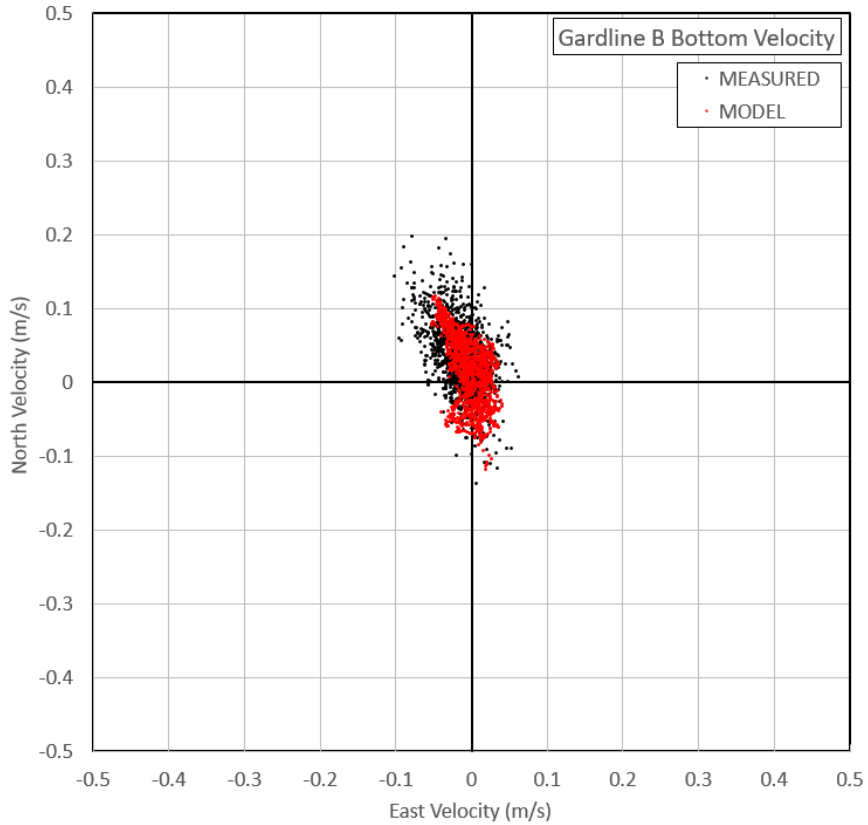

Figure B4-2c Scatter plot of modelled vs. measured current speeds at Gardline B. Bottom, Summer 2017.

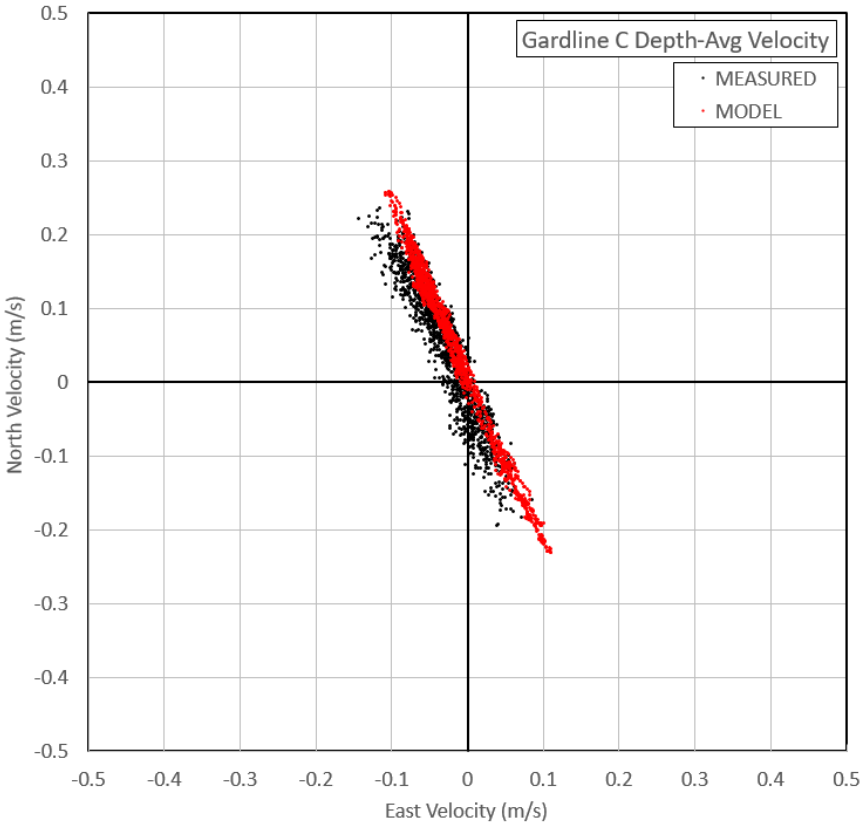

Figure B4-3a Scatter plot of modelled vs. measured current speeds at Gardline C. Depth-integrated, Summer 2017.

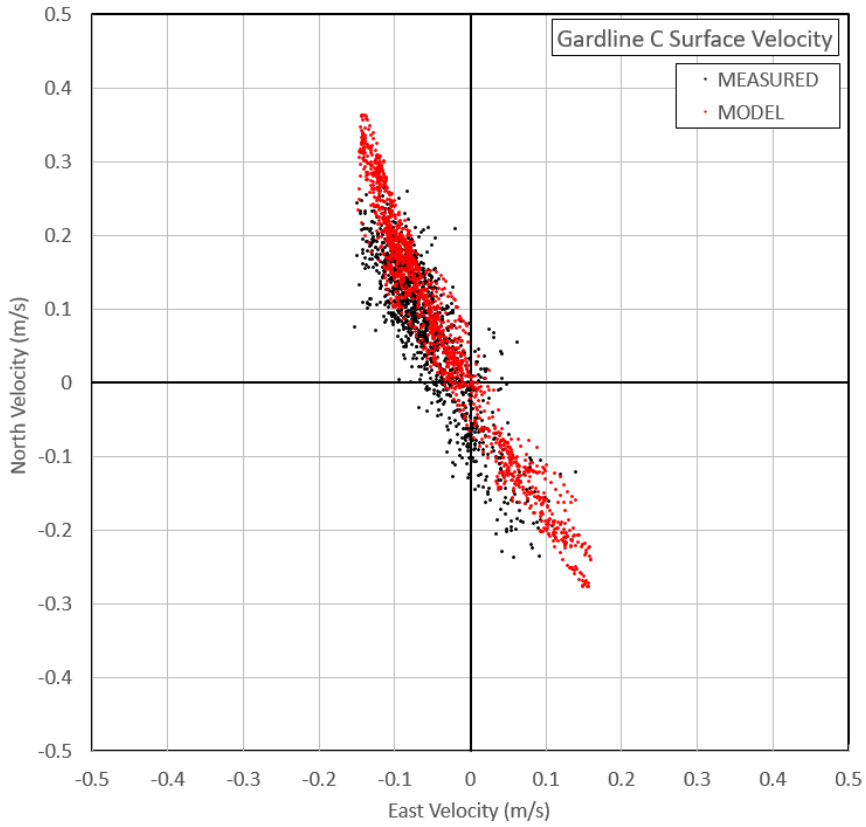

Figure B4-3b Scatter plot of modelled vs. measured current speeds at Gardline C. Surface, Summer 2017.

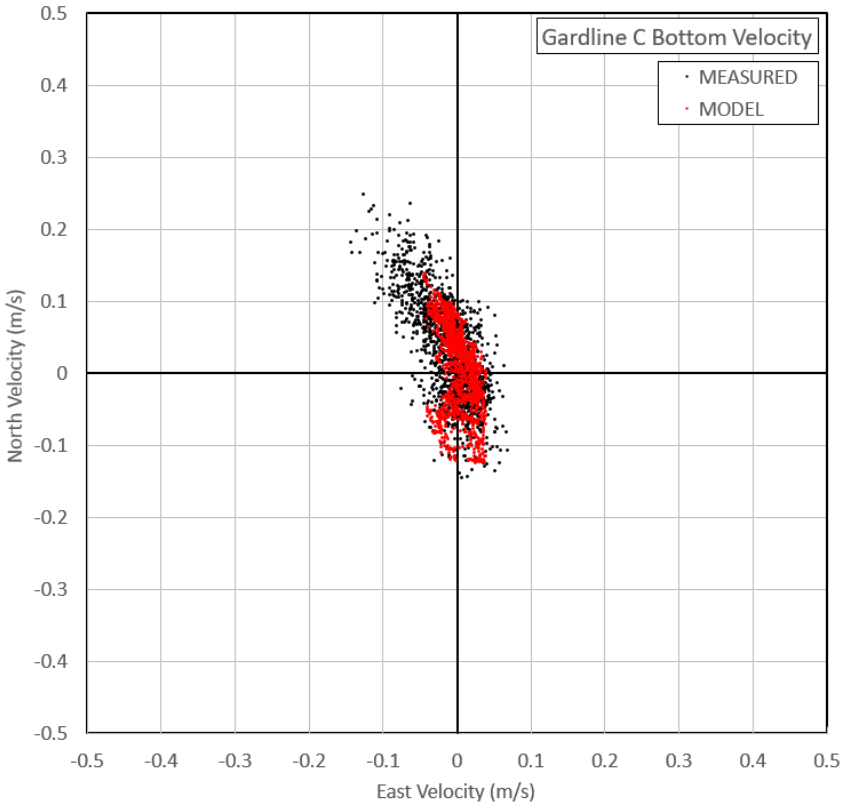

Figure B4-3c Scatter plot of modelled vs. measured current speeds at Gardline C. Bottom, Summer 2017.

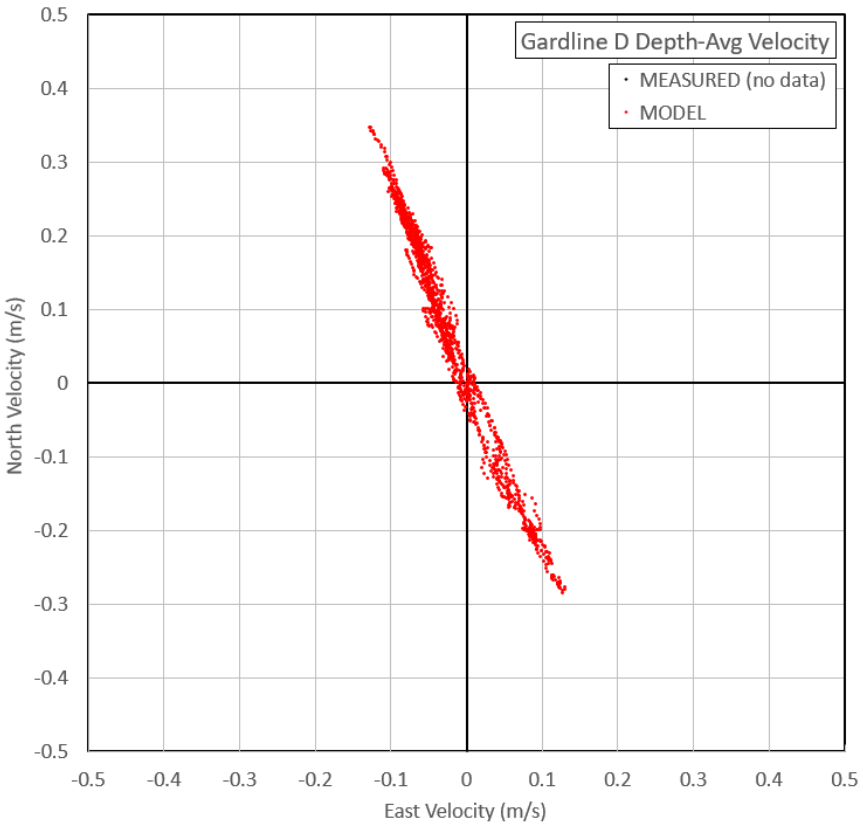

Figure B4-4a Scatter plot of modelled vs. measured current speeds at Gardline D. Depth-integrated, Summer 2017.

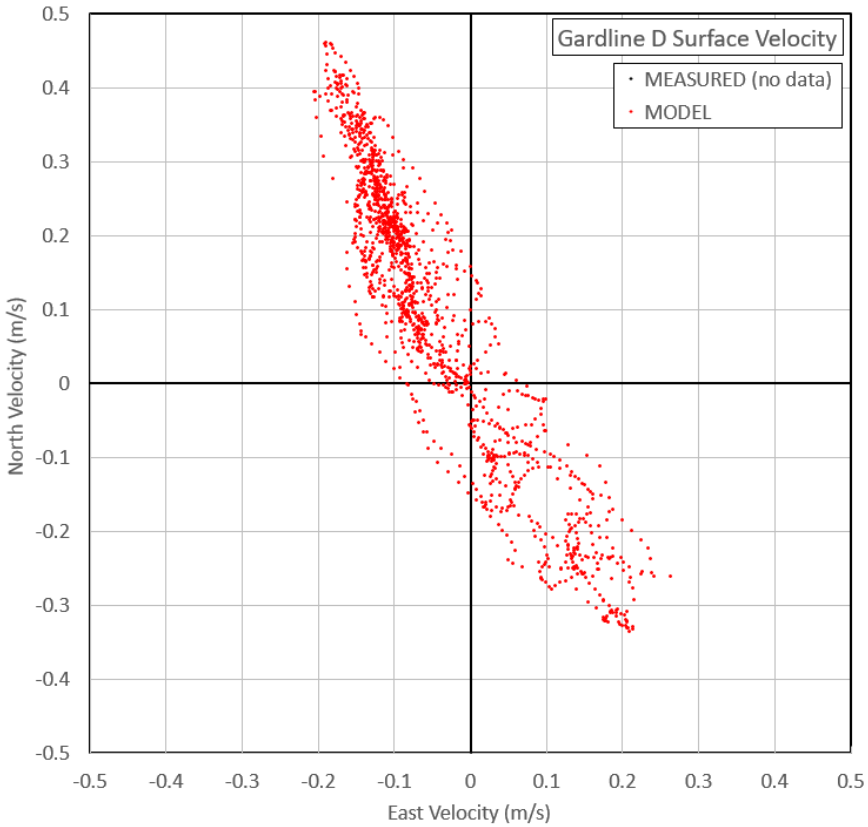

Figure B4-4b Scatter plot of modelled vs. measured current speeds at Gardline D. Surface, Summer 2017.

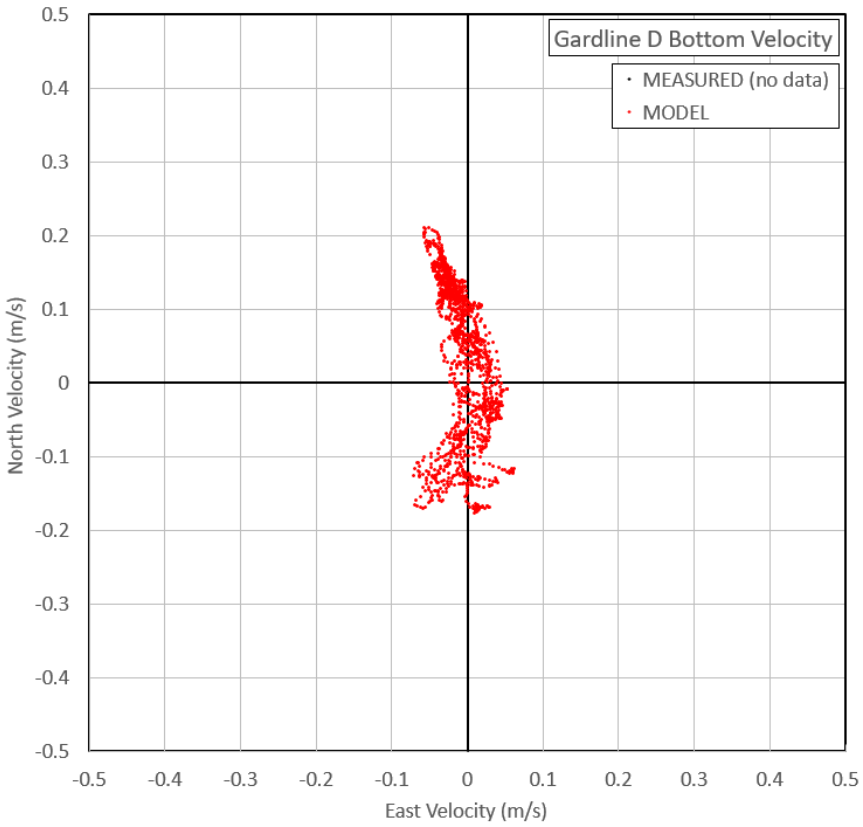

Figure B4-4c Scatter plot of modelled vs. measured current speeds at Gardline D. Bottom, Summer 2017.

APPENDIX C1

Local 3D Model Autumn 2017 Calibration

Current Speed Q-Q Plots

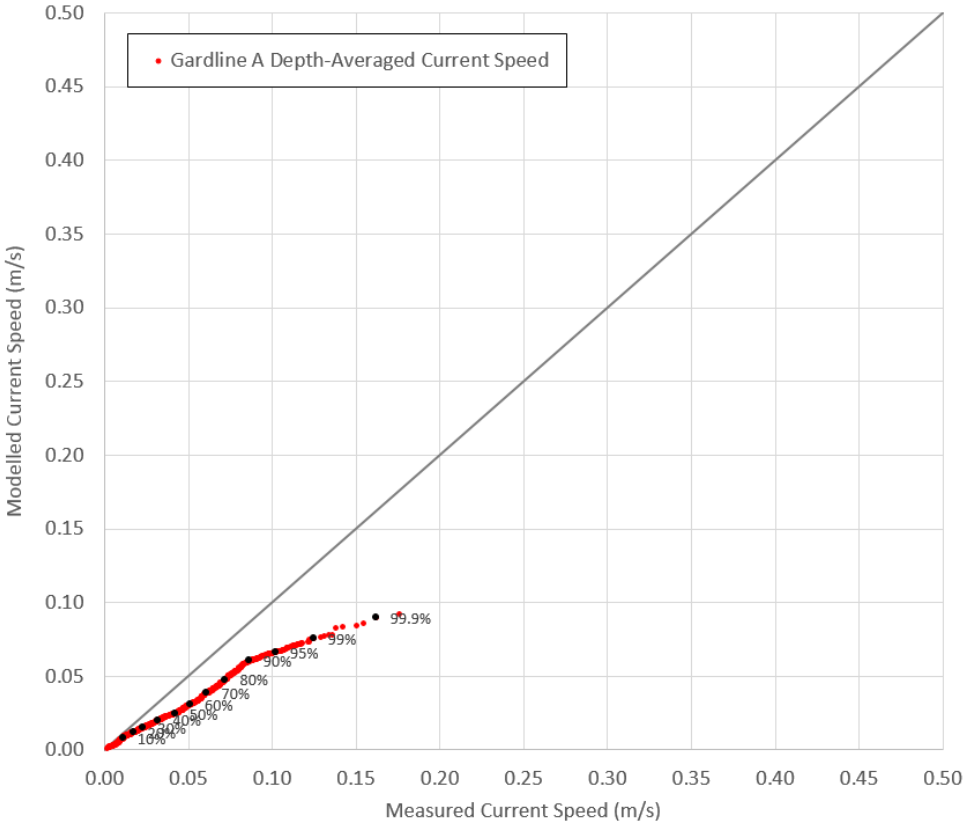

Figure C1-1a Q-Q plot of modelled vs. measured current speeds at Gardline A. Depth-integrated, Autumn 2017.

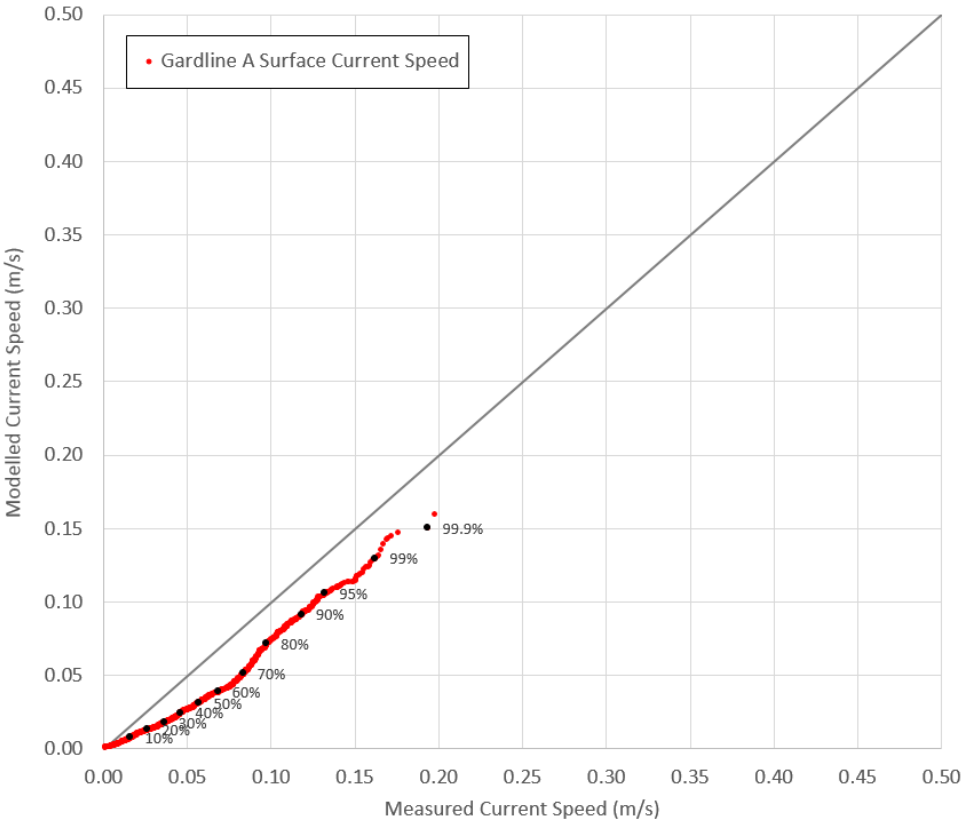

Figure C1-1b Q-Q plot of modelled vs. measured current speeds at Gardline A. Surface, Autumn 2017.

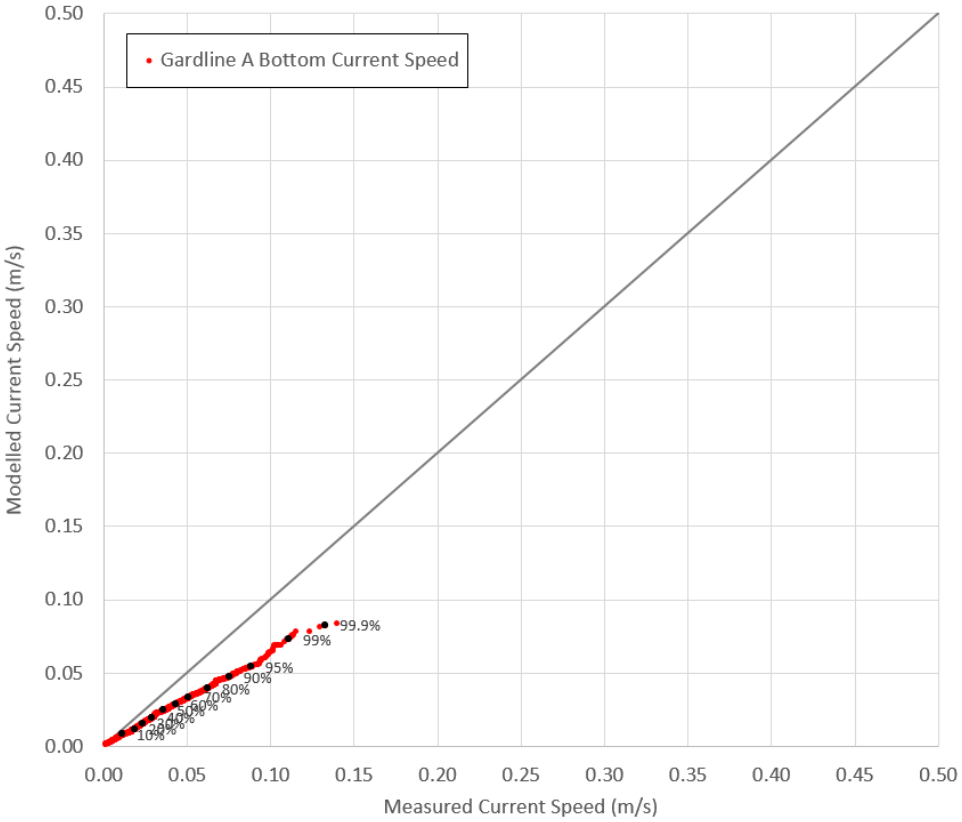

Figure C1-1c Q-Q plot of modelled vs. measured current speeds at Gardline A. Bottom, Autumn 2017.

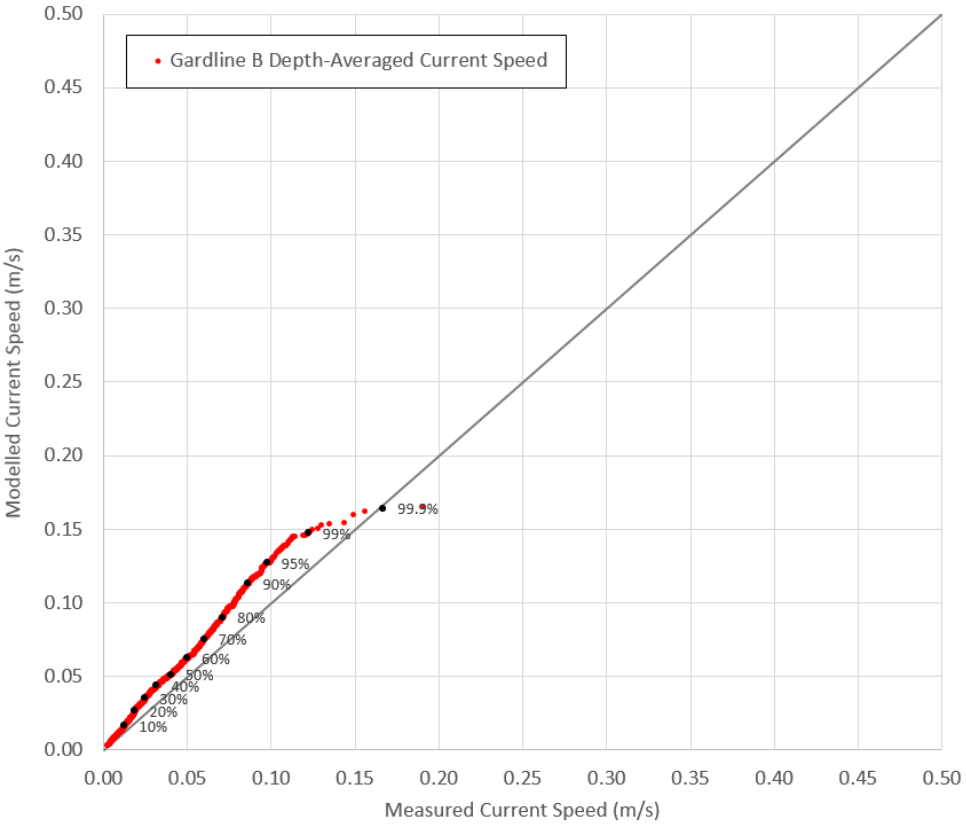

Figure C1-2a Q-Q plot of modelled vs. measured current speeds at Gardline B. Depth-integrated, Autumn 2017.

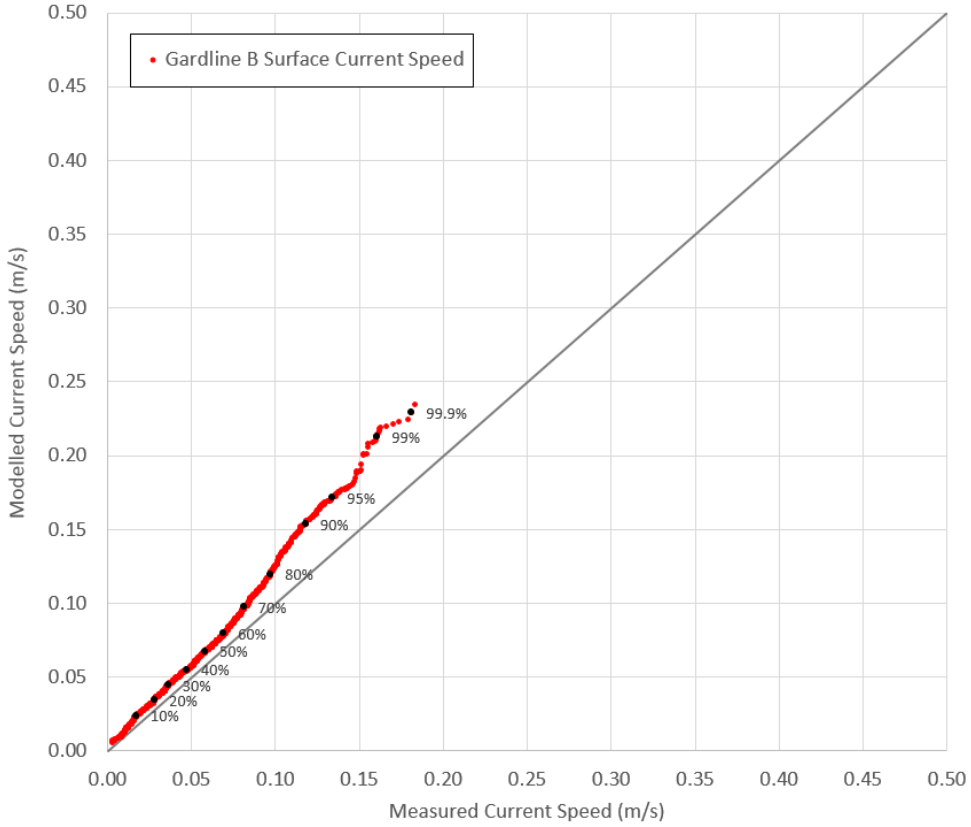

Figure C1-2b Q-Q plot of modelled vs. measured current speeds at Gardline B. Surface, Autumn 2017.

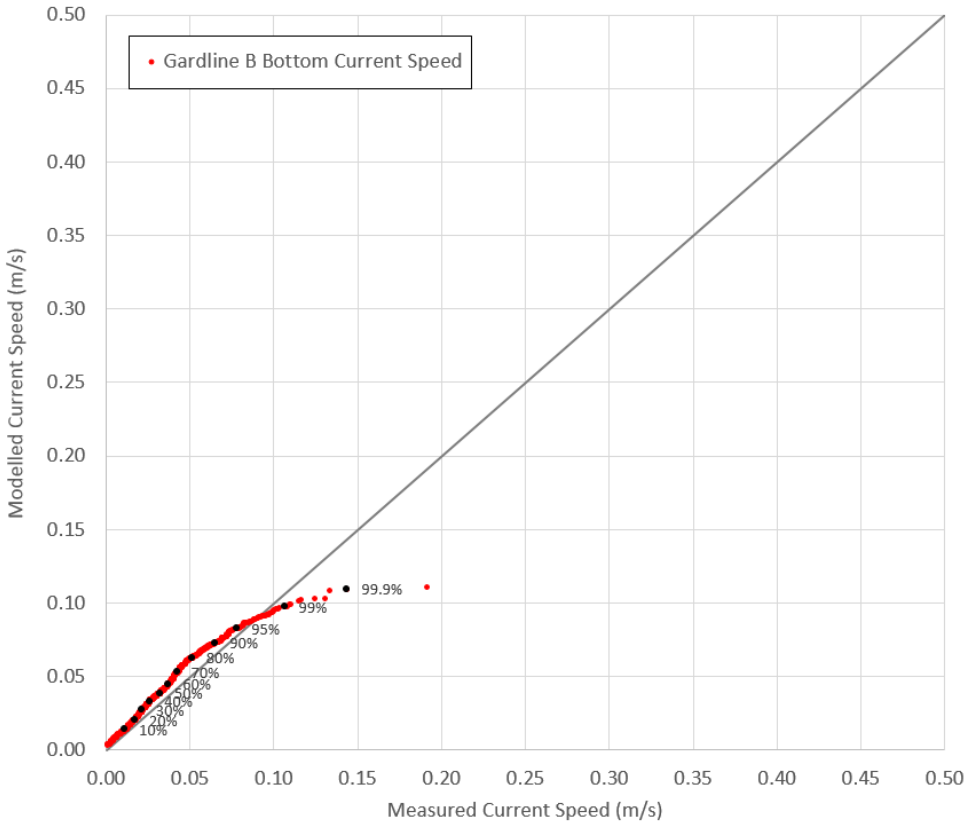

Figure C1-2c Q-Q plot of modelled vs. measured current speeds at Gardline B. Bottom, Autumn 2017.

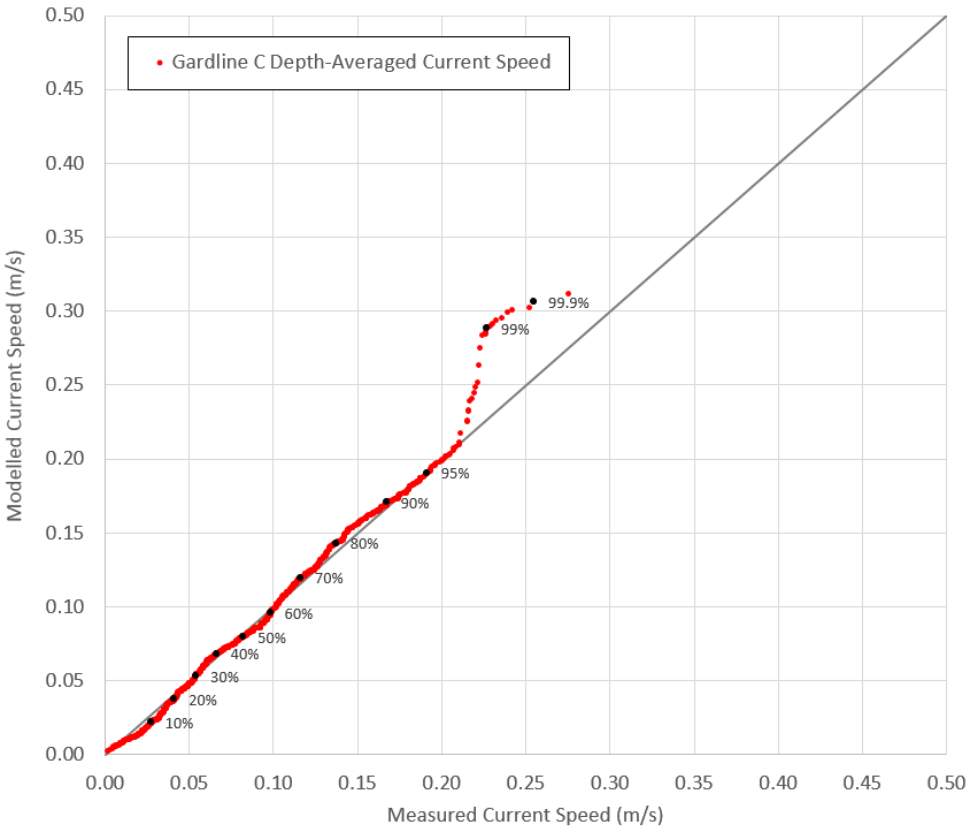

Figure C1-3a Q-Q plot of modelled vs. measured current speeds at Gardline C. Depth-integrated, Autumn 2017.

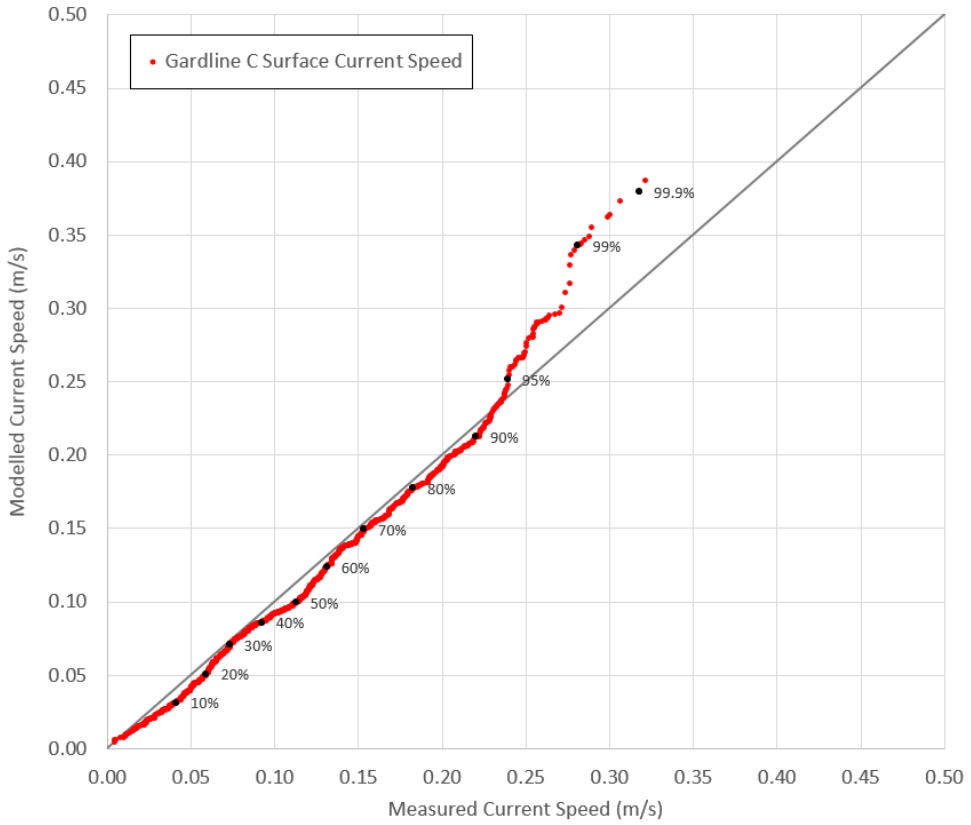

Figure C1-3b Q-Q plot of modelled vs. measured current speeds at Gardline C. Surface, Autumn 2017.

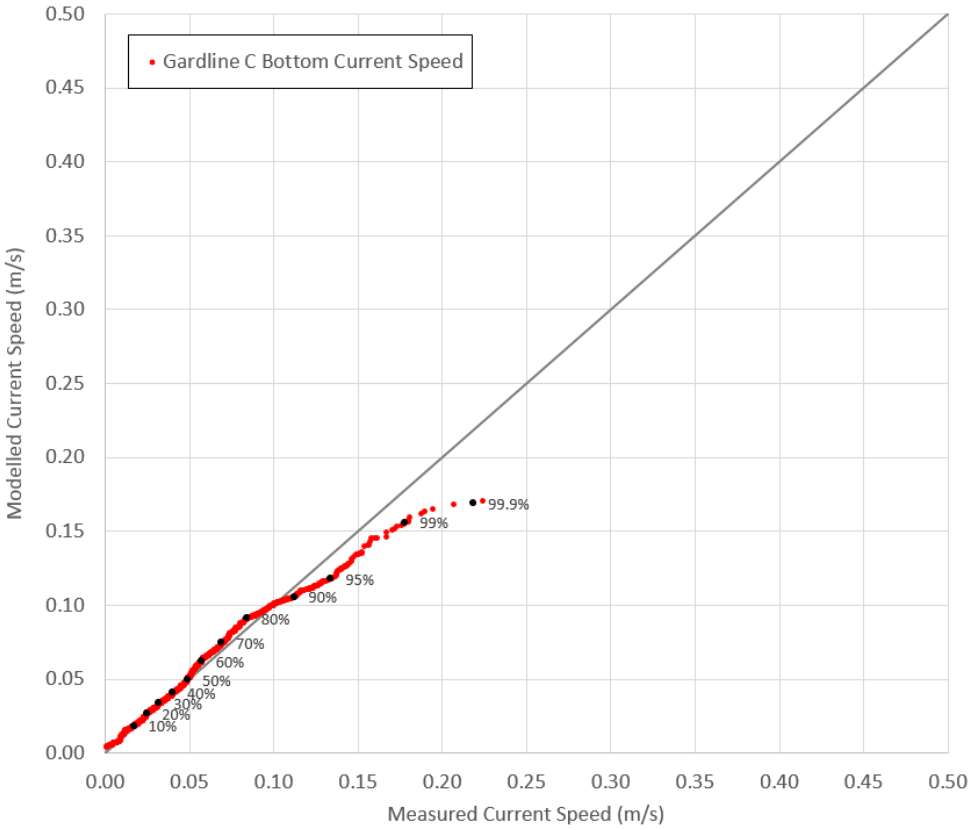

Figure C1-3c Q-Q plot of modelled vs. measured current speeds at Gardline C. Bottom, Autumn 2017.

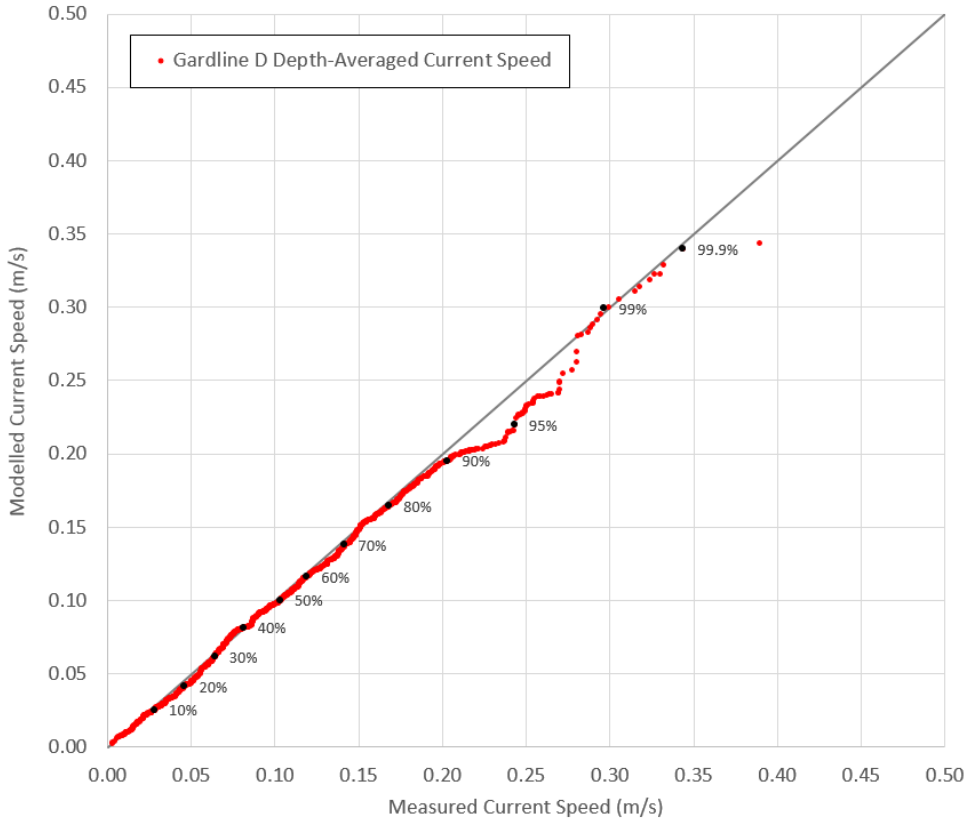

Figure C1-4a Q-Q plot of modelled vs. measured current speeds at Gardline D. Depth-integrated, Autumn 2017.

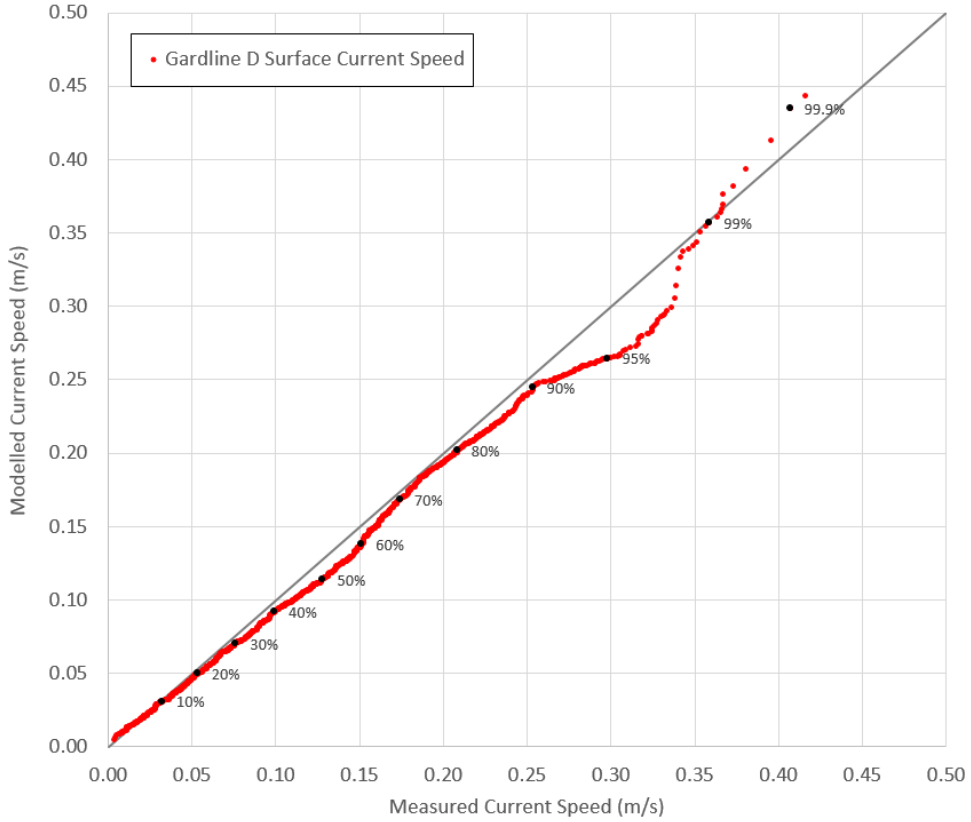

Figure C1-4b Q-Q plot of modelled vs. measured current speeds at Gardline D. Surface, Autumn 2017.

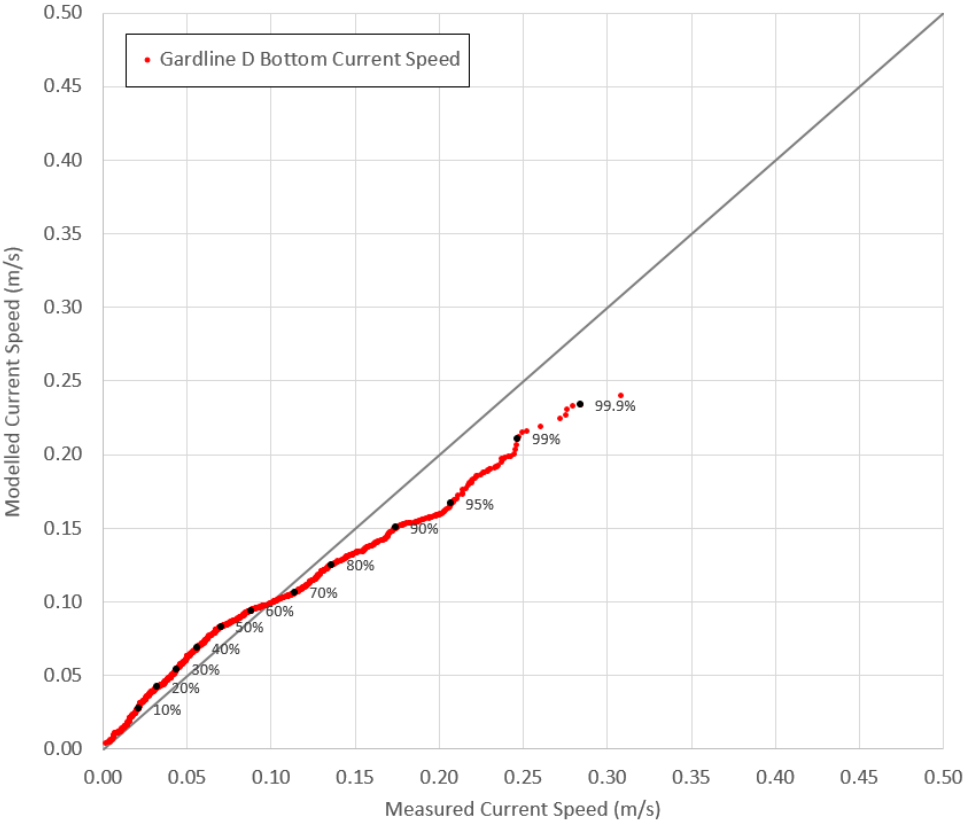

Figure C1-4c Q-Q plot of modelled vs. measured current speeds at Gardline D. Bottom, Autumn 2017.

APPENDIX C2

Local 3D Model Autumn 2005 Validation

Current Speed Q-Q Plots

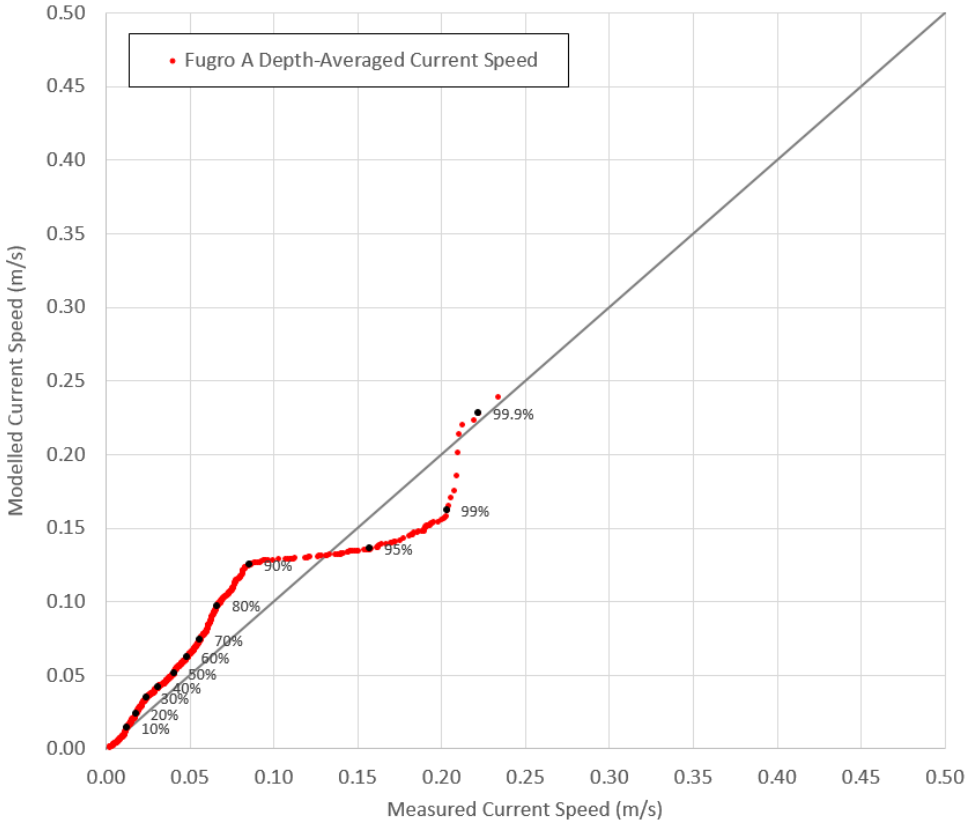

Figure C2-1a Q-Q plot of modelled vs. measured current speeds at Fugro A. Depth-integrated, Autumn 2017.

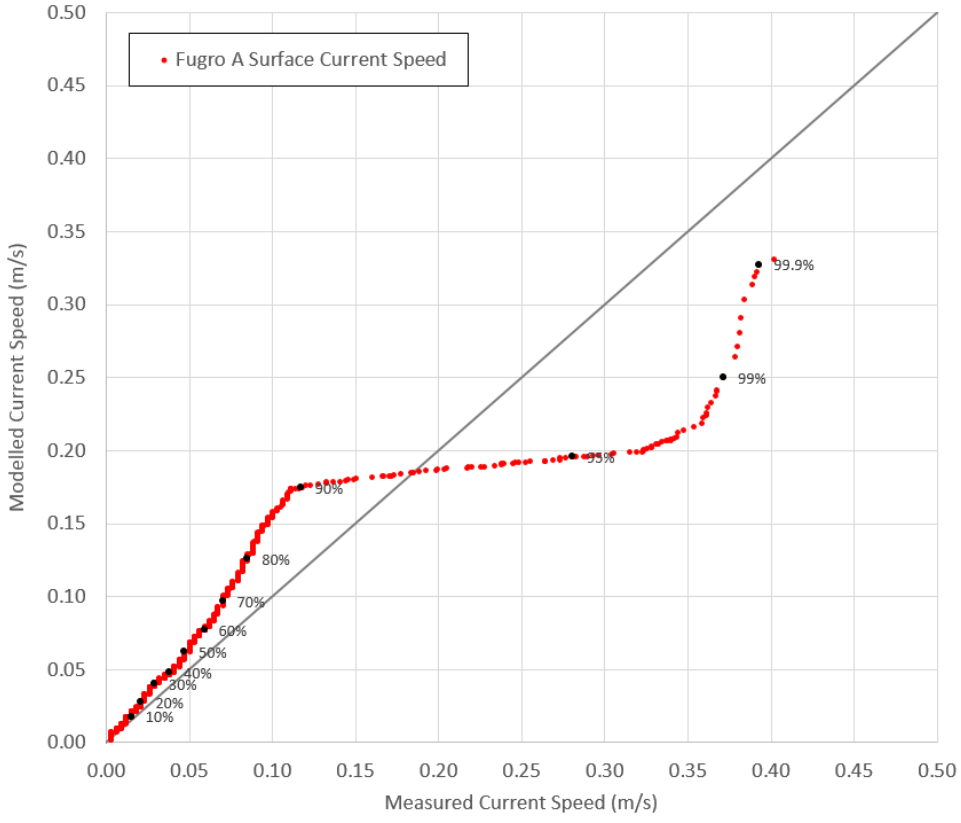

Figure C2-1b Q-Q plot of modelled vs. measured current speeds at Fugro A. Surface, Autumn 2017.

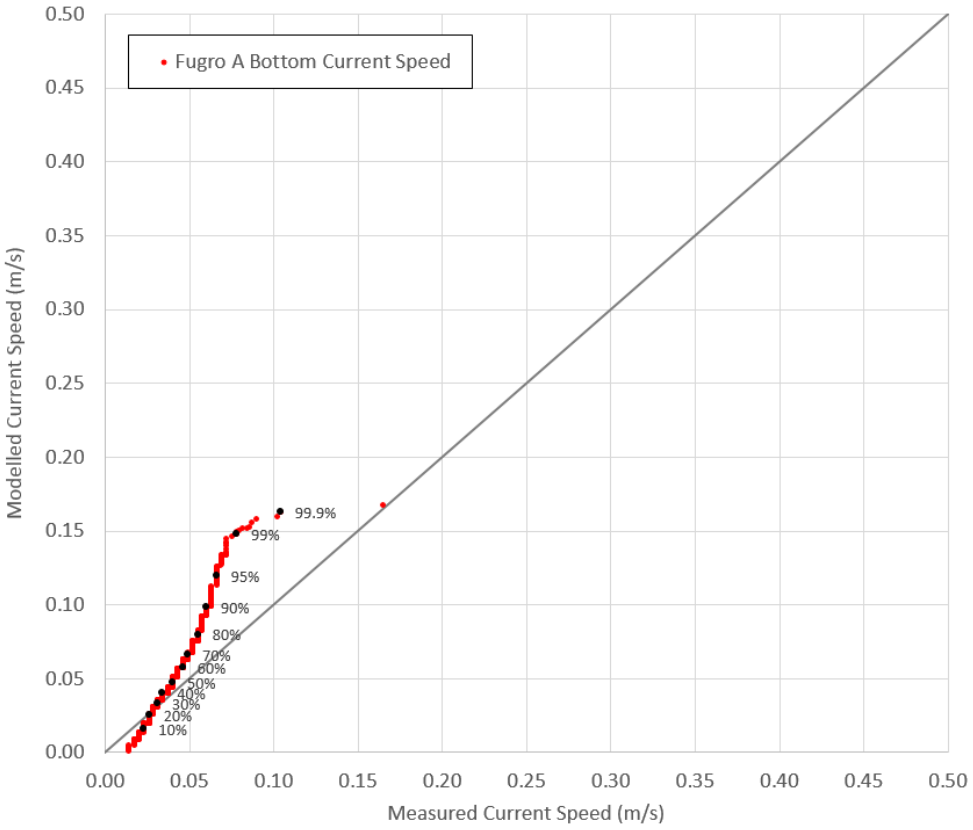

Figure C2-1c Q-Q plot of modelled vs. measured current speeds at Fugro A. Bottom, Autumn 2017.

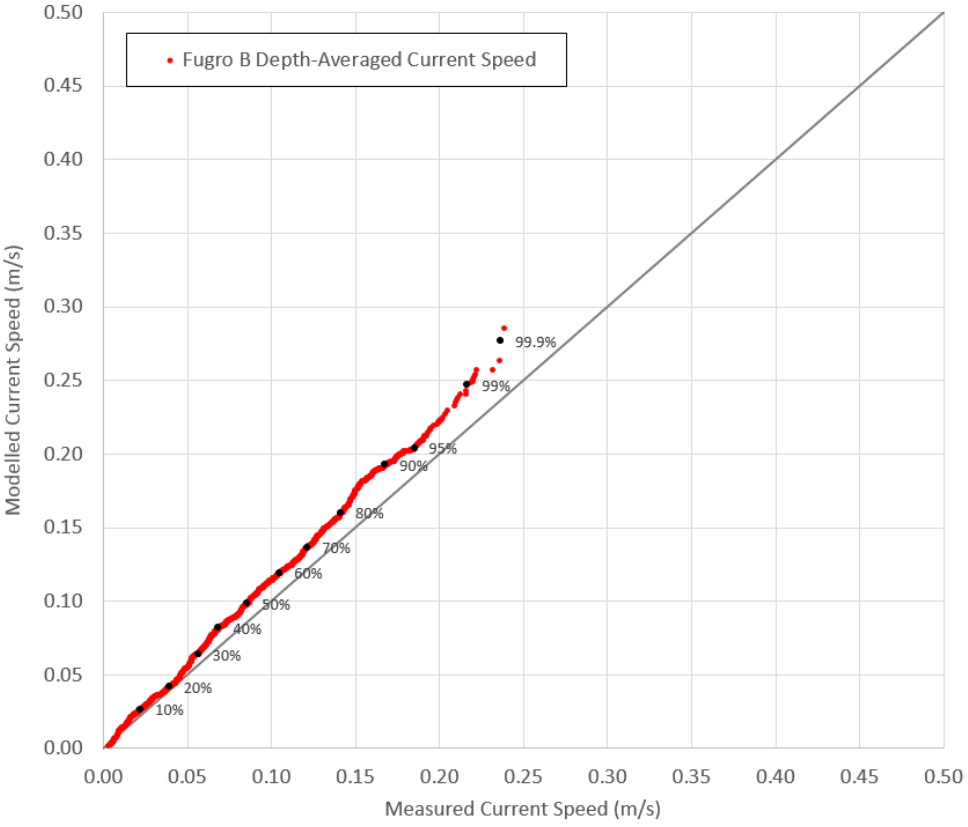

Figure C2-2a Q-Q plot of modelled vs. measured current speeds at Fugro B. Depth-integrated, Autumn 2017.

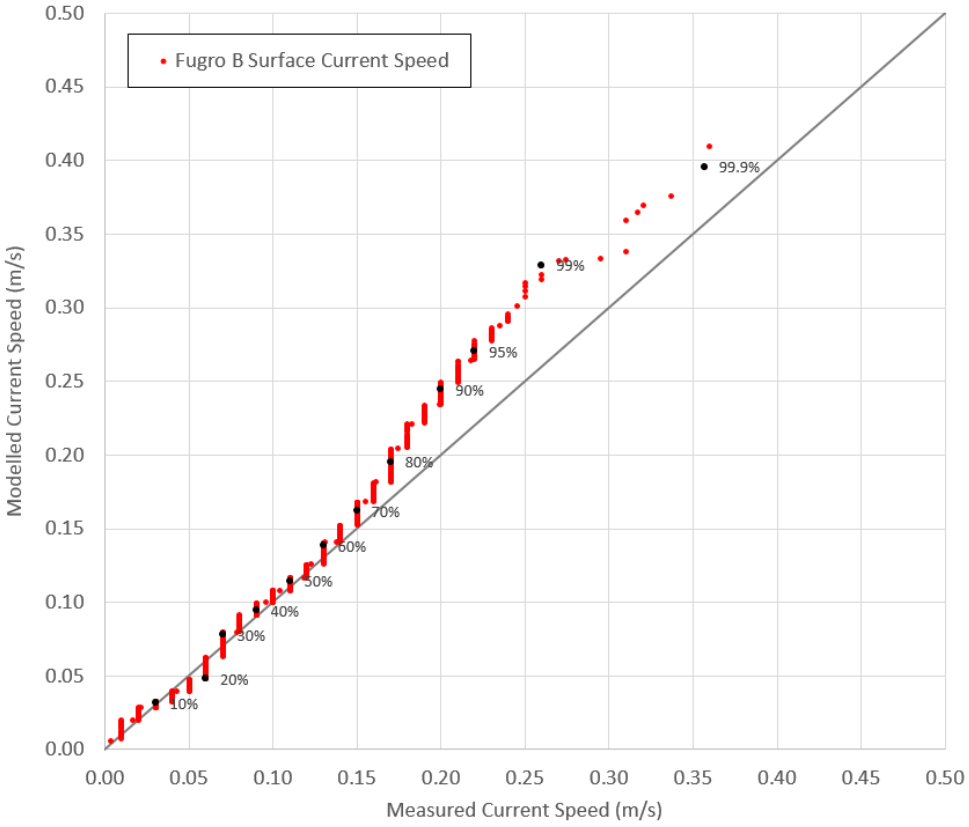

Figure C2-2b Q-Q plot of modelled vs. measured current speeds at Fugro B. Surface, Autumn 2017.

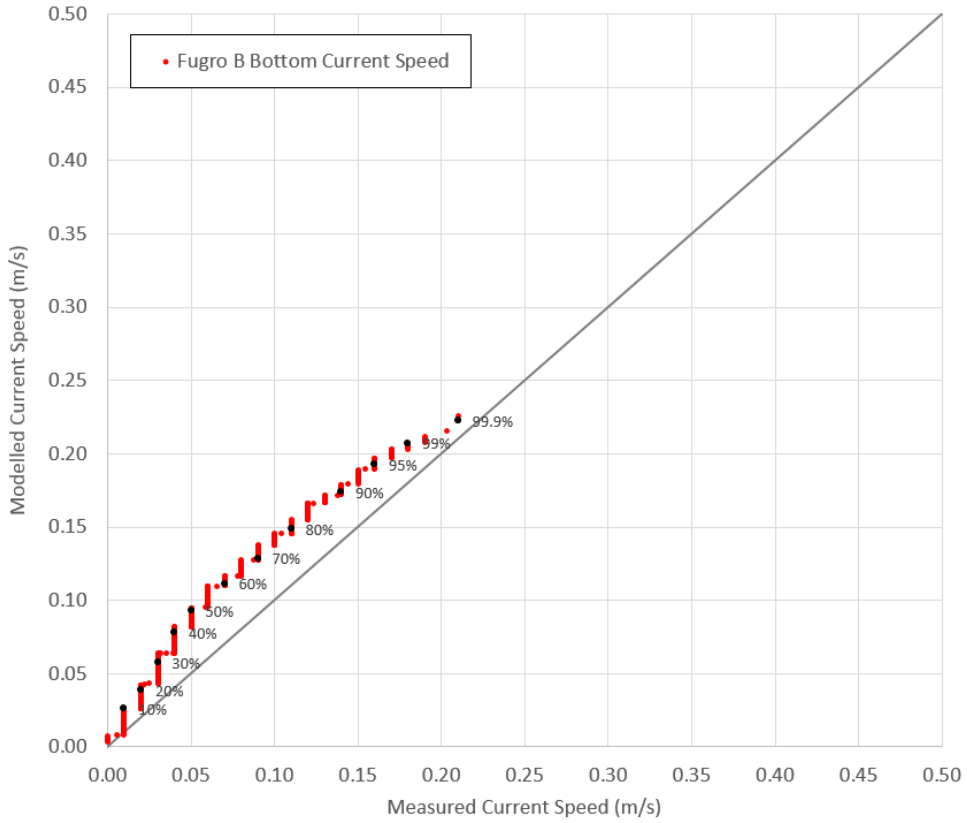

Figure C2-2c Q-Q plot of modelled vs. measured current speeds at Fugro B. Bottom, Autumn 2017.

APPENDIX C3

Local 3D Model Winter 2017 Validation

Current Speed Q-Q Plots

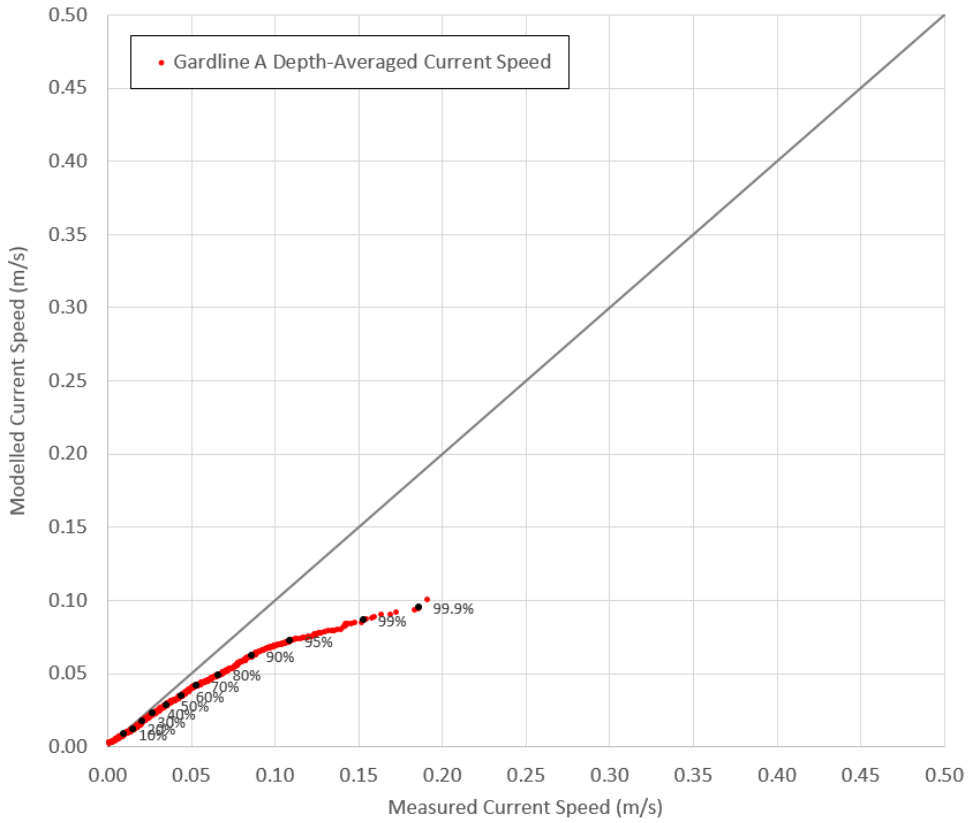

Figure C3-1a Q-Q plot of modelled vs. measured current speeds at Gardline A. Depth-integrated, Winter 2017.

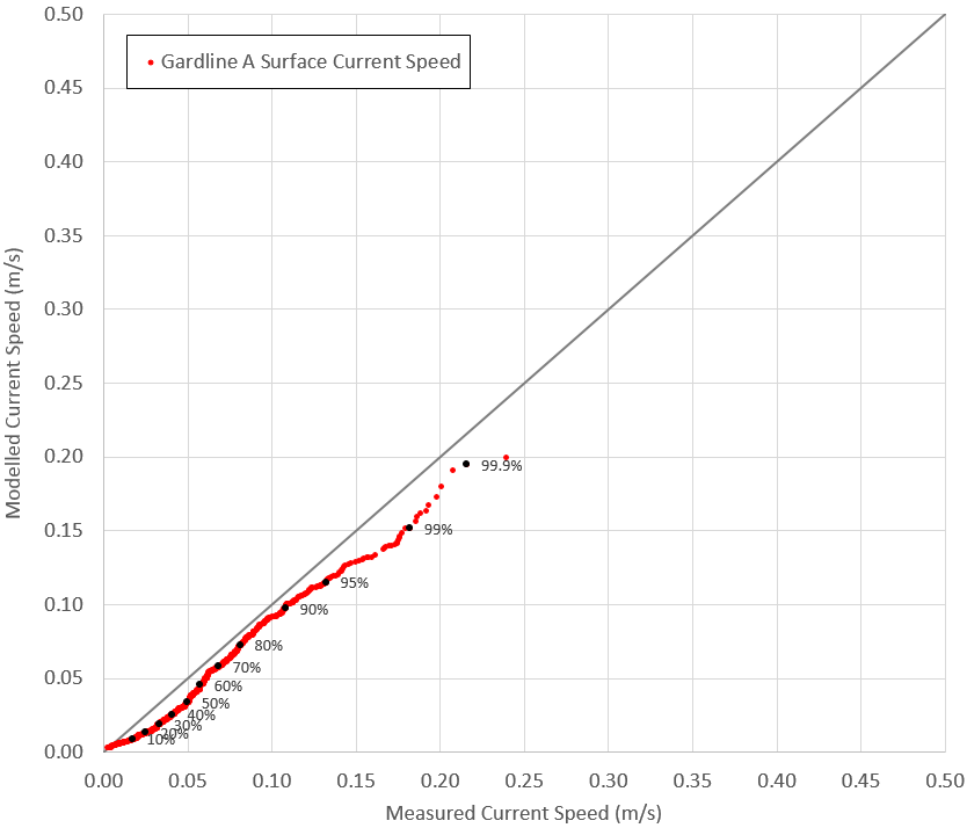

Figure C3-1b Q-Q plot of modelled vs. measured current speeds at Gardline A. Surface, Winter 2017.

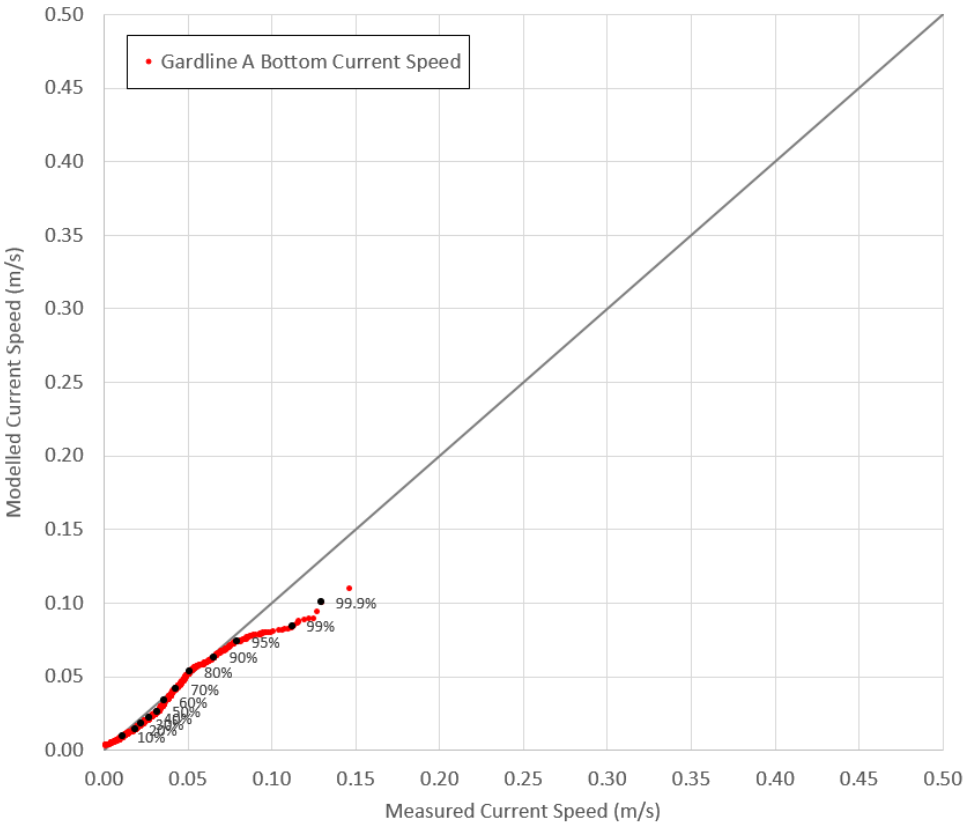

Figure C3-1c Q-Q plot of modelled vs. measured current speeds at Gardline A. Bottom, Winter 2017.

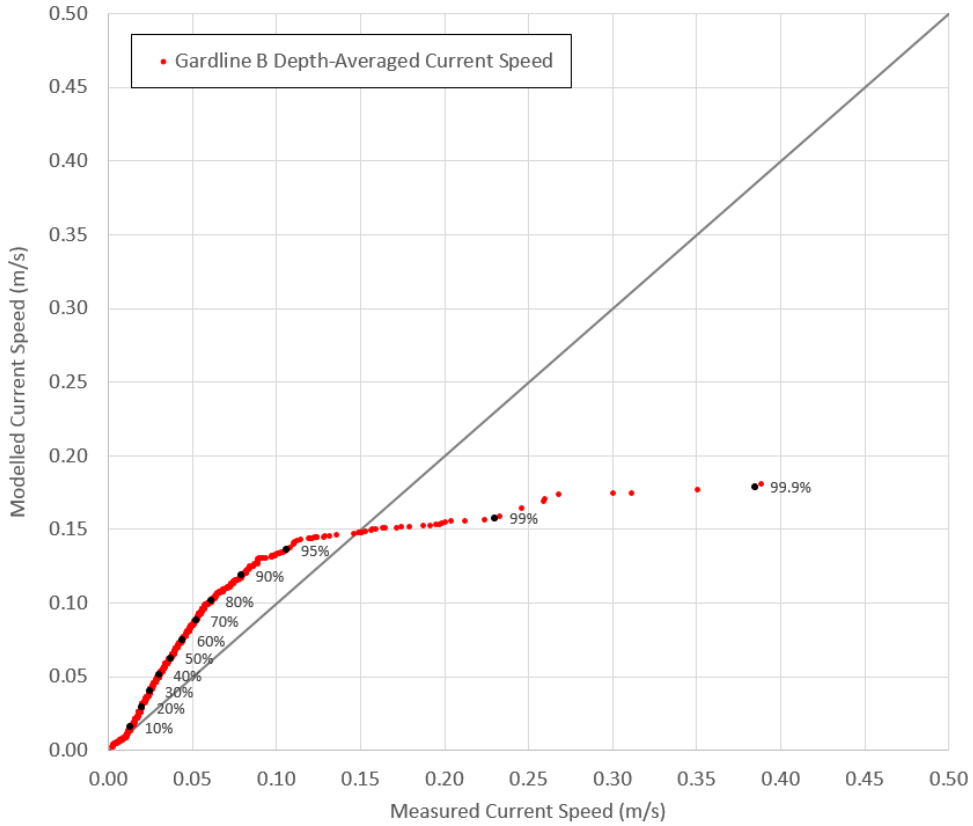

Figure C3-2a Q-Q plot of modelled vs. measured current speeds at Gardline B. Depth-integrated, Winter 2017.

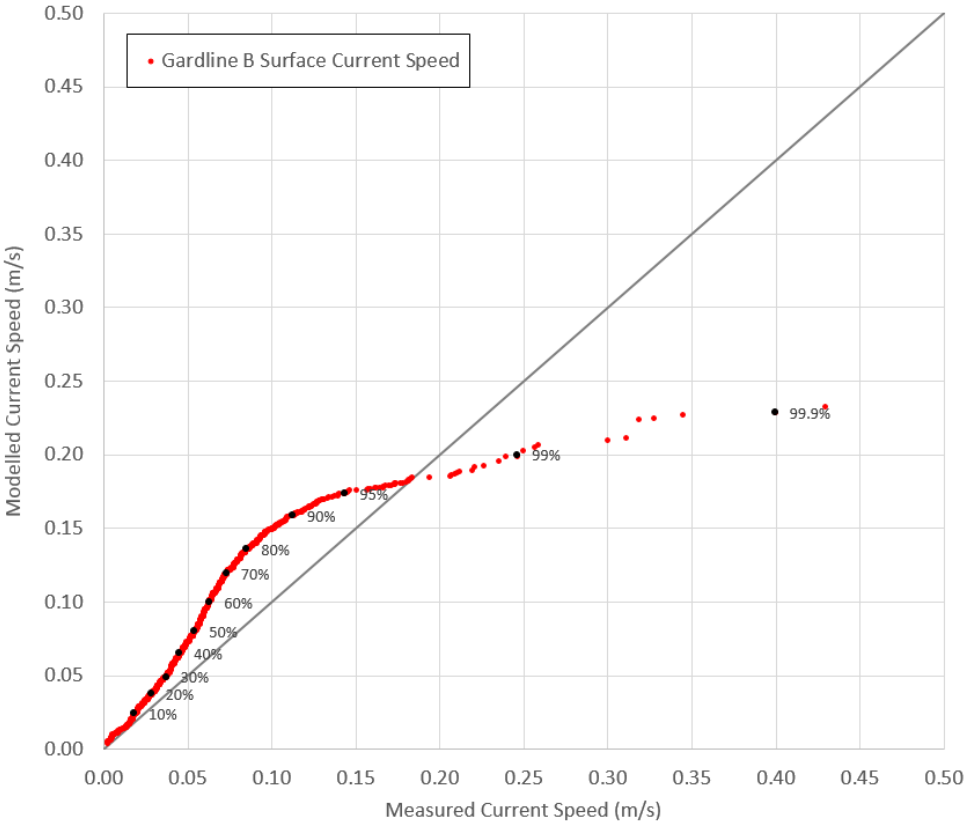

Figure C3-2b Q-Q plot of modelled vs. measured current speeds at Gardline B. Surface, Winter 2017.

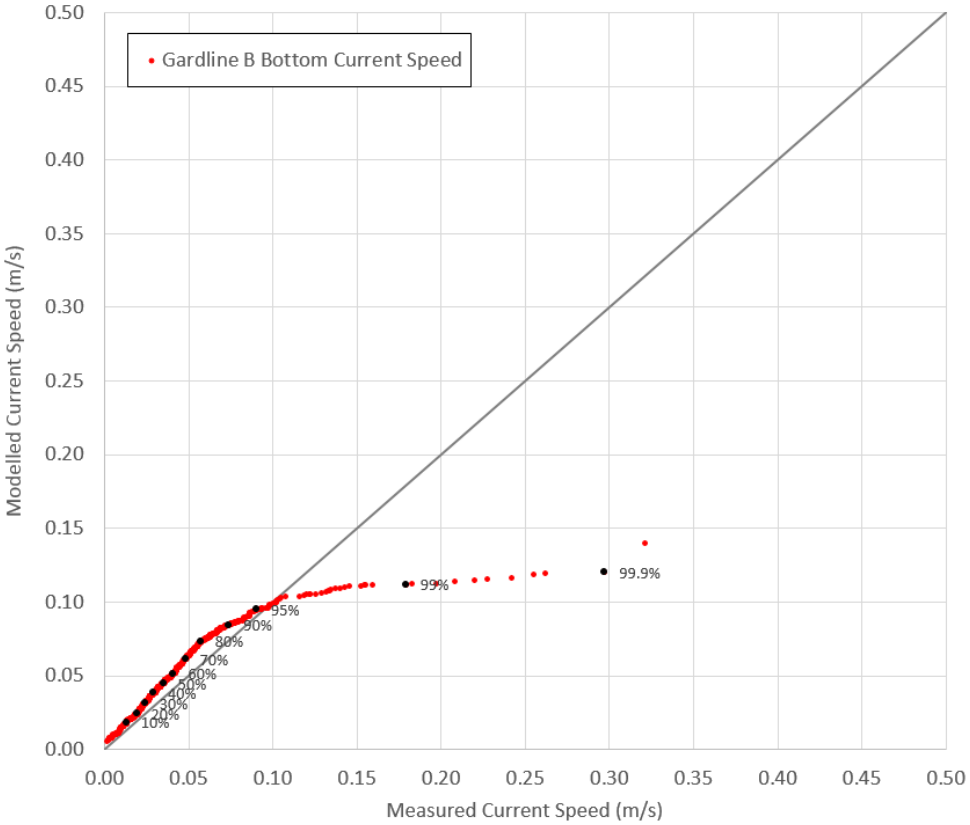

Figure C3-2c Q-Q plot of modelled vs. measured current speeds at Gardline B. Bottom, Winter 2017.

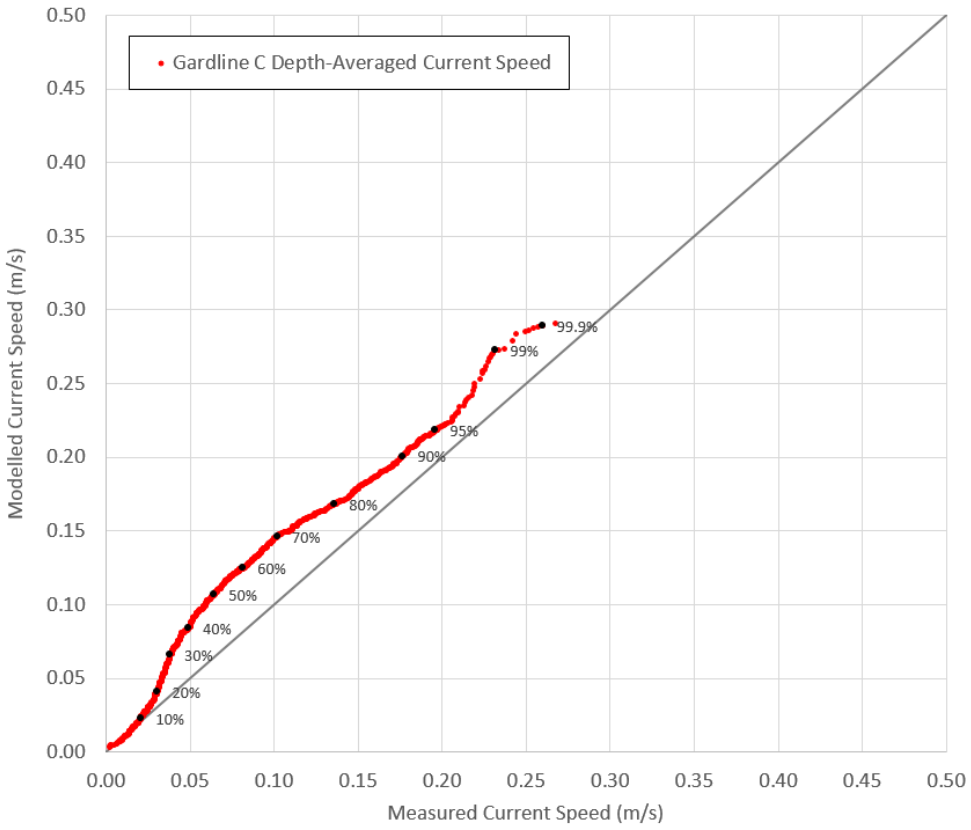

Figure C3-3a Q-Q plot of modelled vs. measured current speeds at Gardline C. Depth-integrated, Winter 2017.

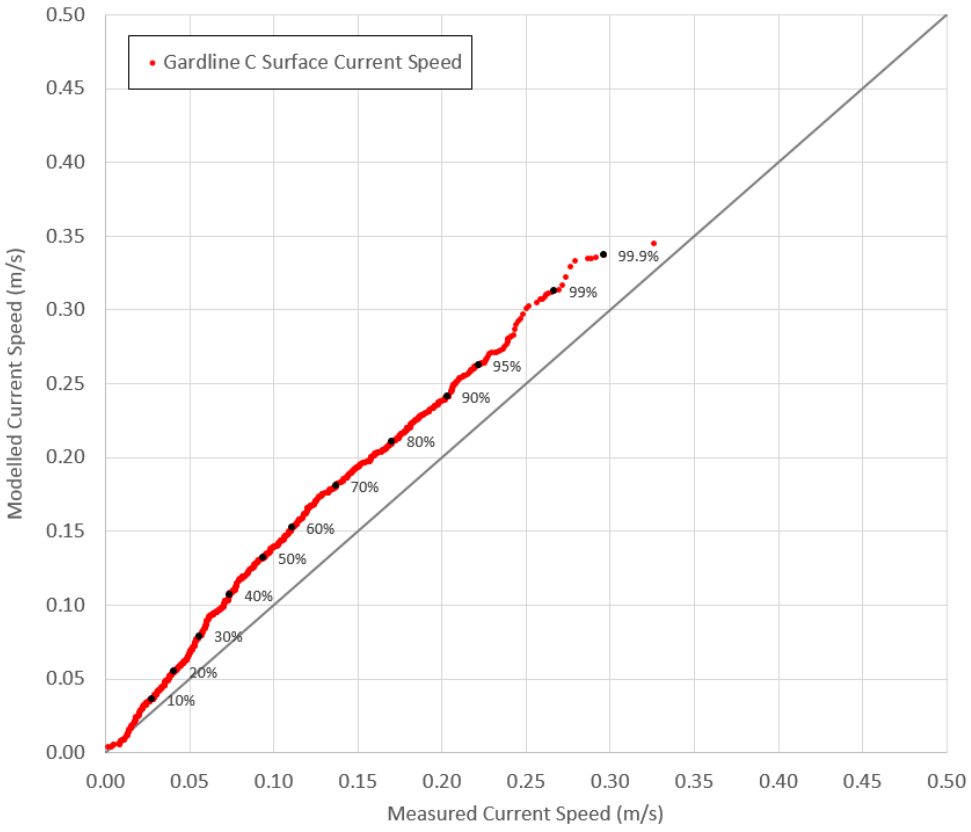

Figure C3-3b Q-Q plot of modelled vs. measured current speeds at Gardline C. Surface, Winter 2017.

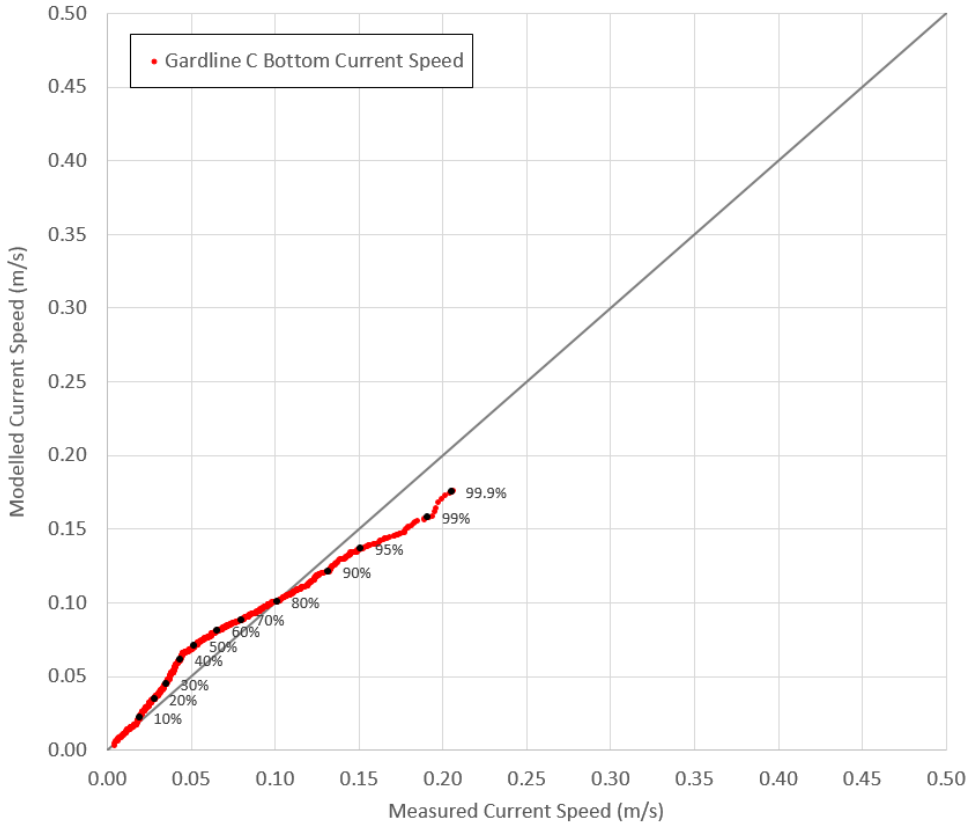

Figure C3-3c Q-Q plot of modelled vs. measured current speeds at Gardline C. Bottom, Winter 2017.

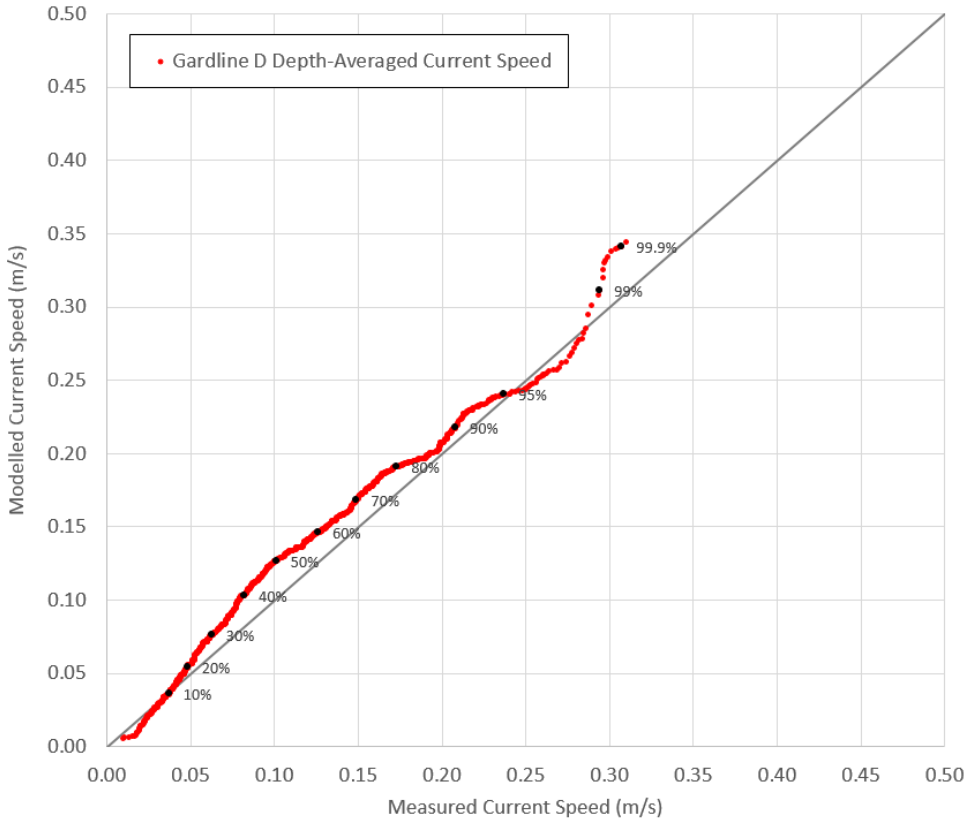

Figure C3-4a Q-Q plot of modelled vs. measured current speeds at Gardline D. Depth-integrated, Winter 2017.

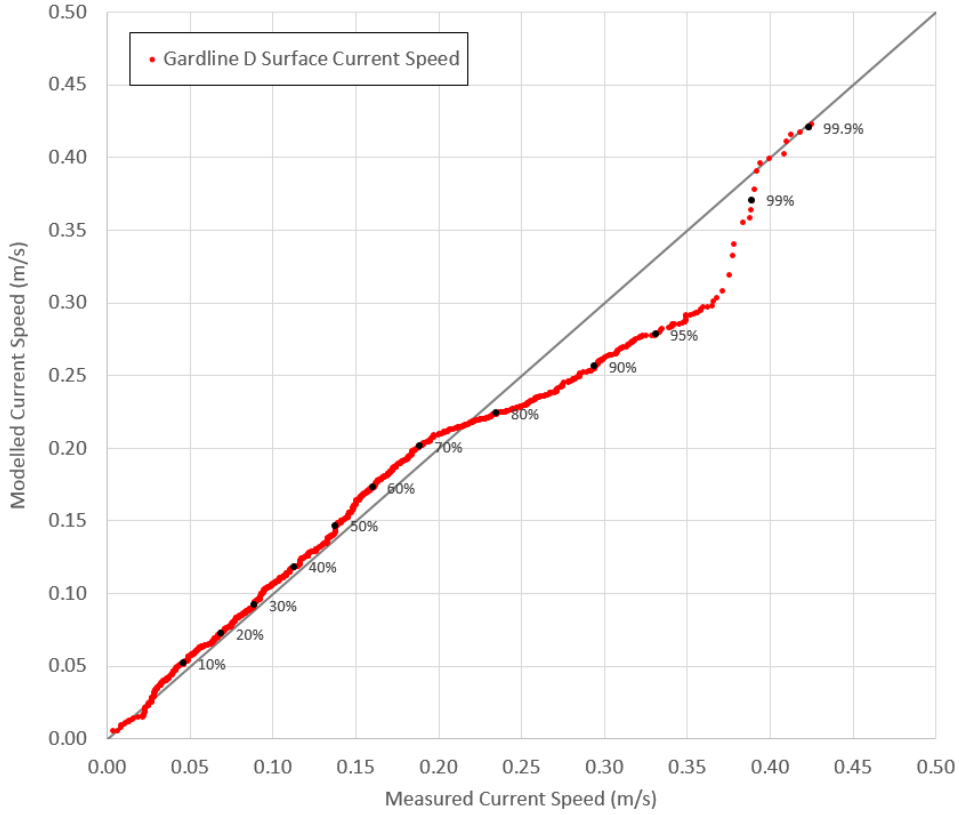

Figure C3-4b Q-Q plot of modelled vs. measured current speeds at Gardline D. Surface, Winter 2017.

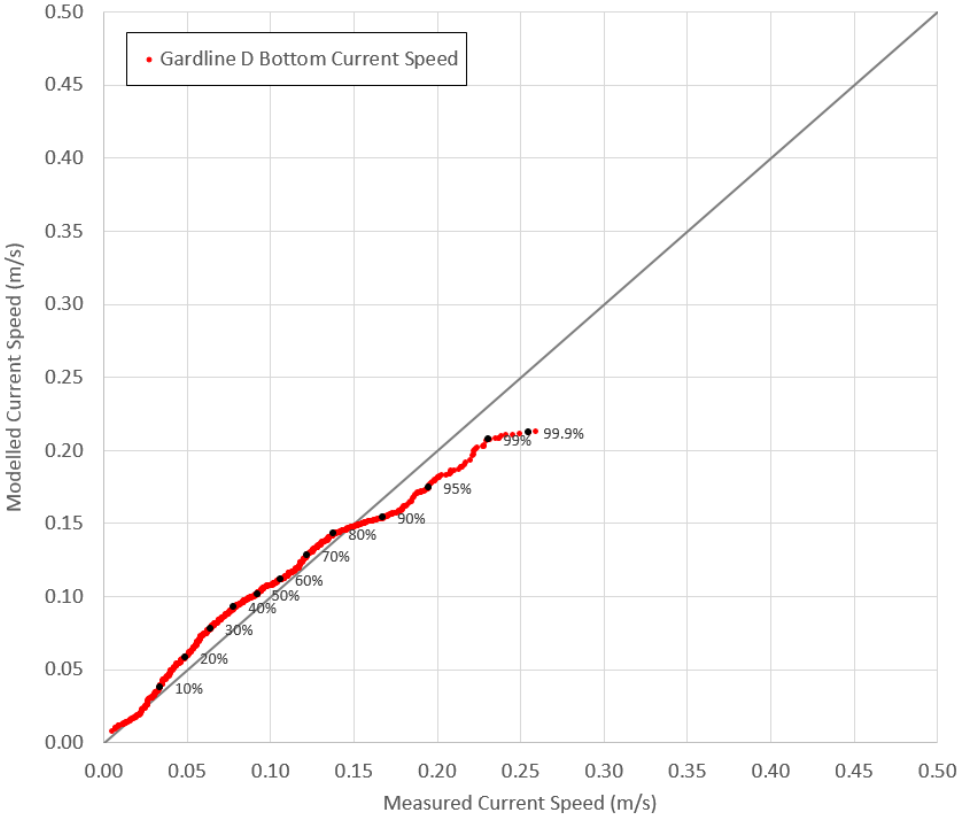

Figure C3-4c Q-Q plot of modelled vs. measured current speeds at Gardline D. Bottom, Winter 2017.

APPENDIX C4

Local 3D Model Summer 2017 Validation

Current Speed Q-Q Plots

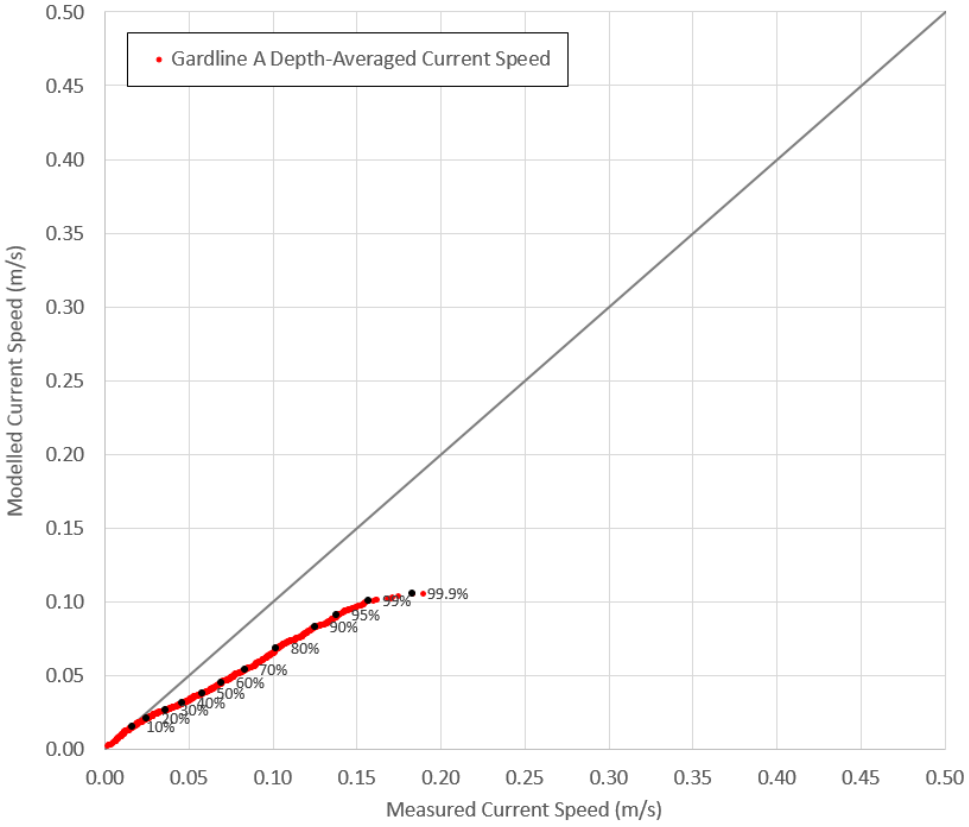

Figure C4-1a Q-Q plot of modelled vs. measured current speeds at Gardline A. Depth-integrated, Summer 2017.

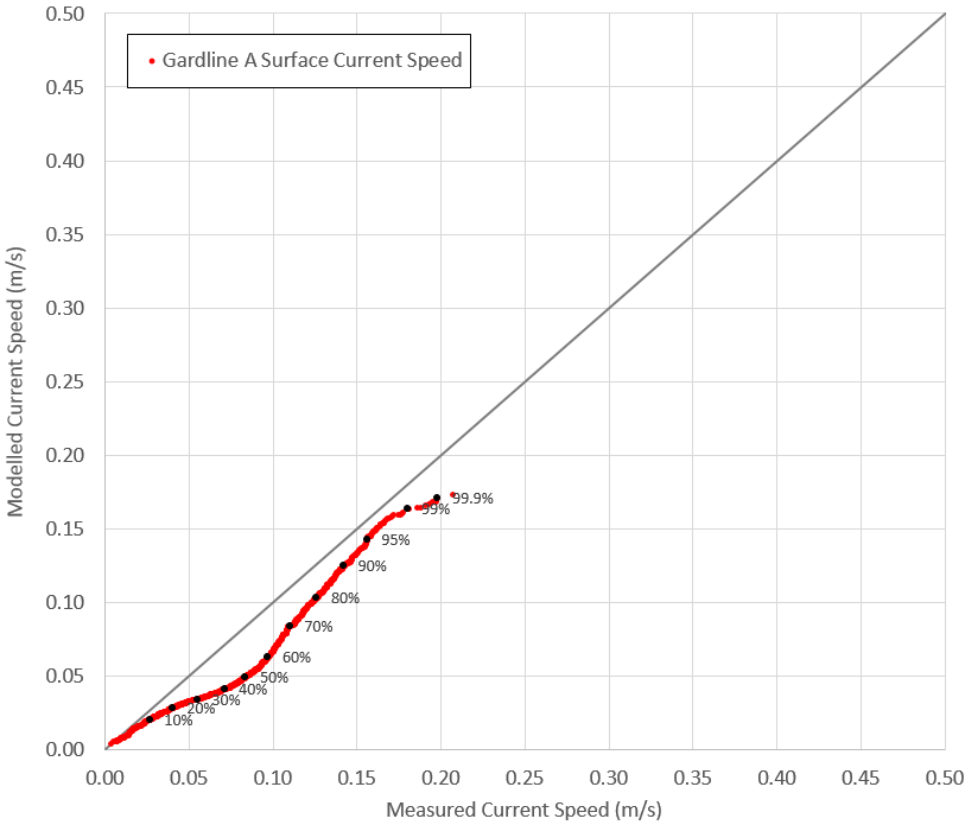

Figure C4-1b Q-Q plot of modelled vs. measured current speeds at Gardline A. Surface, Summer 2017.

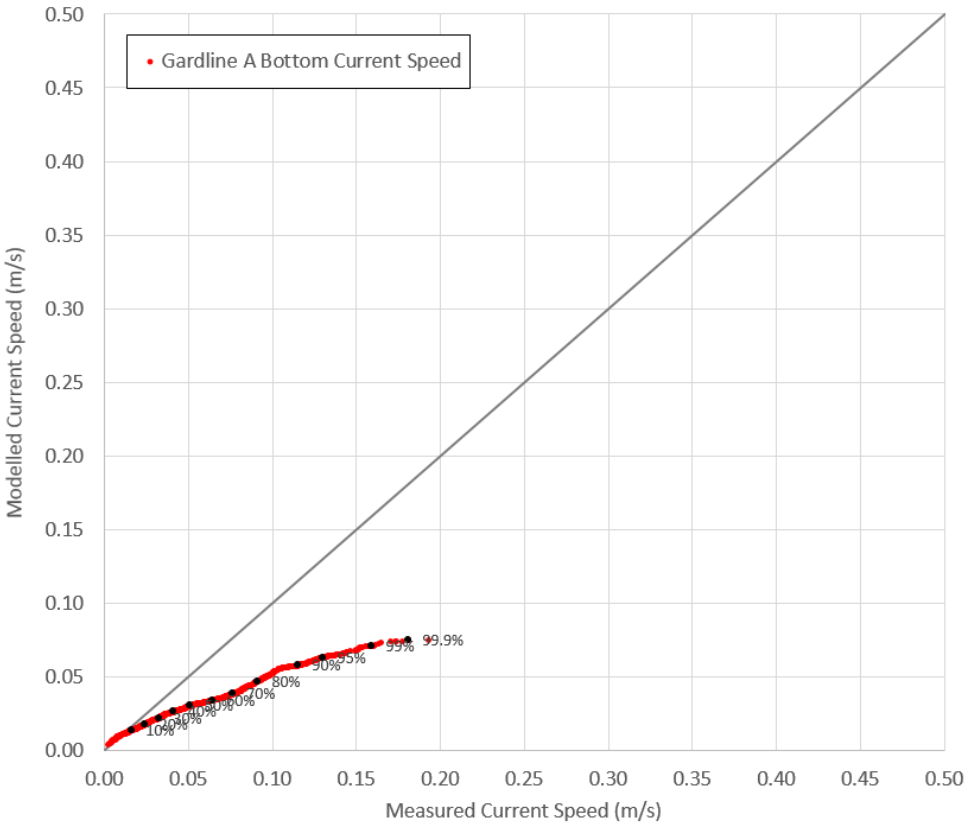

Figure C4-1c Q-Q plot of modelled vs. measured current speeds at Gardline A. Bottom, Summer 2017.

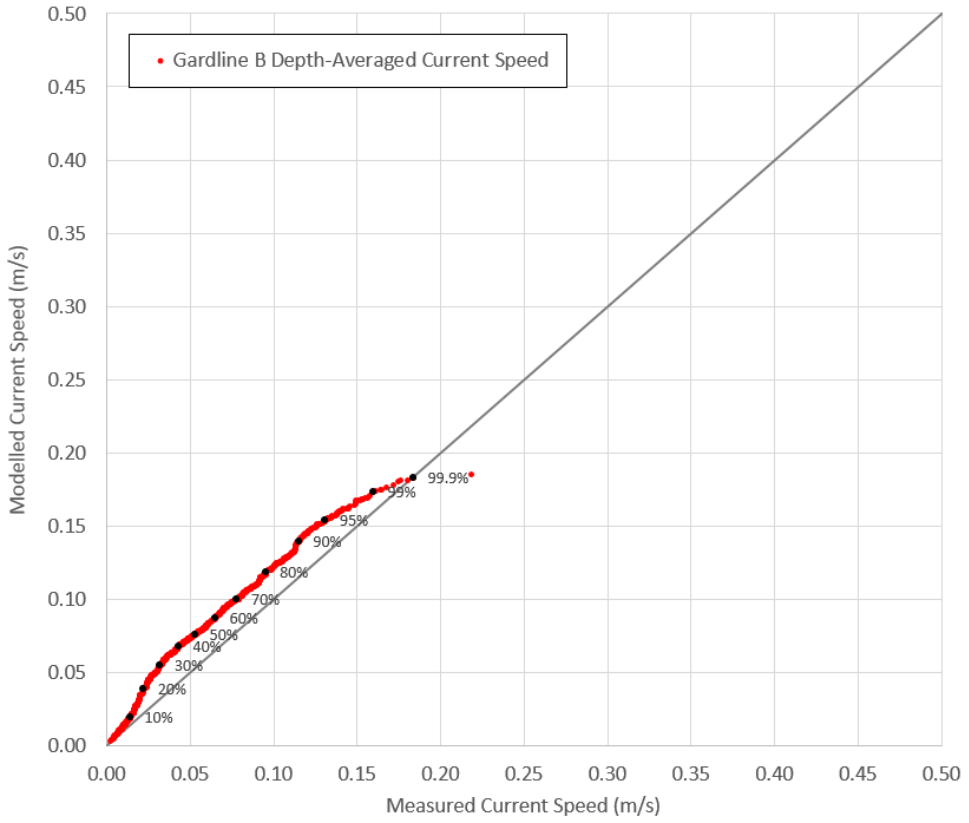

Figure C4-2a Q-Q plot of modelled vs. measured current speeds at Gardline B. Depth-integrated, Summer 2017.

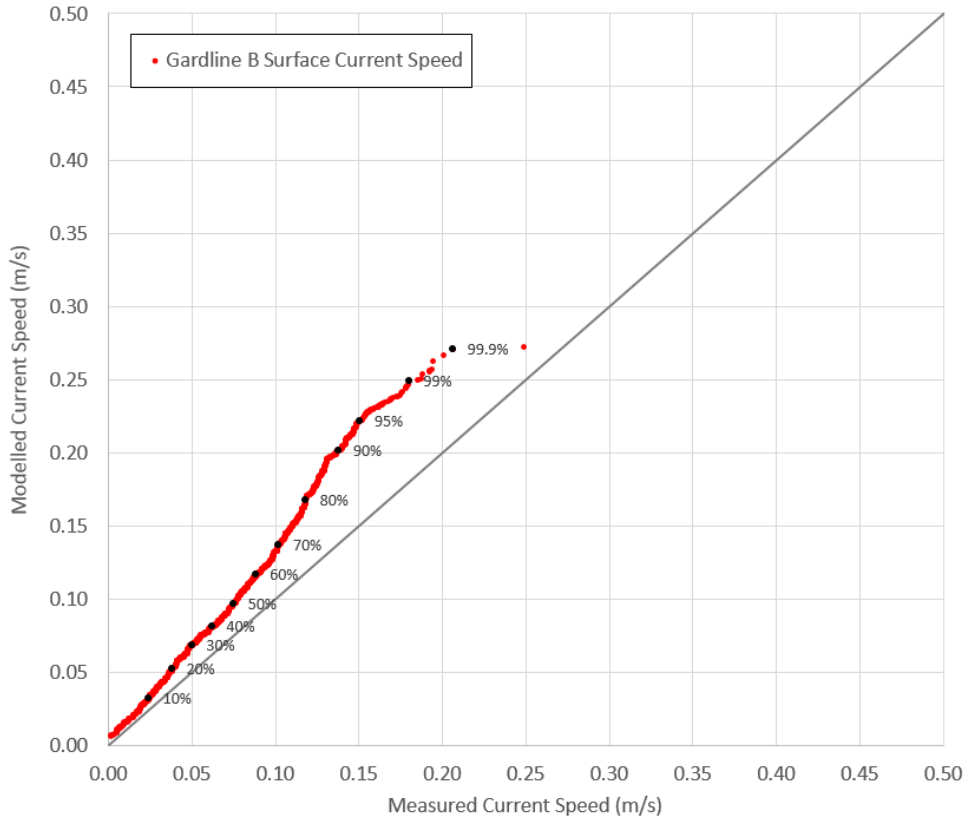

Figure C4-2b Q-Q plot of modelled vs. measured current speeds at Gardline B. Surface, Summer 2017.

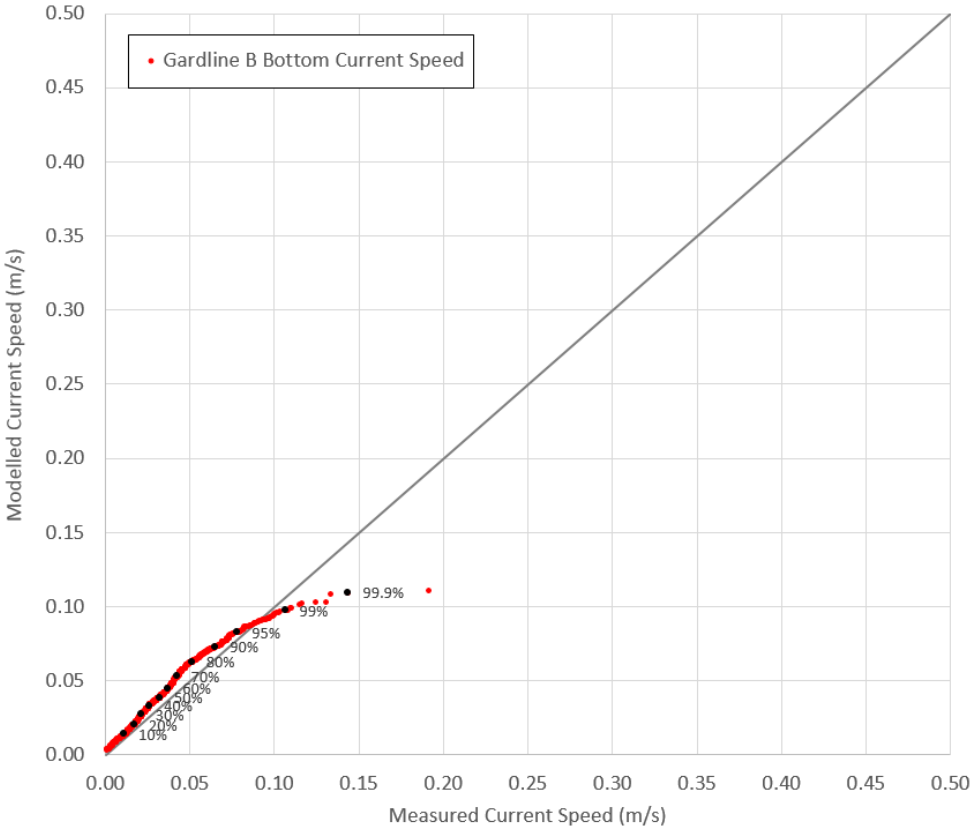

Figure C4-2c Q-Q plot of modelled vs. measured current speeds at Gardline B. Bottom, Summer 2017.

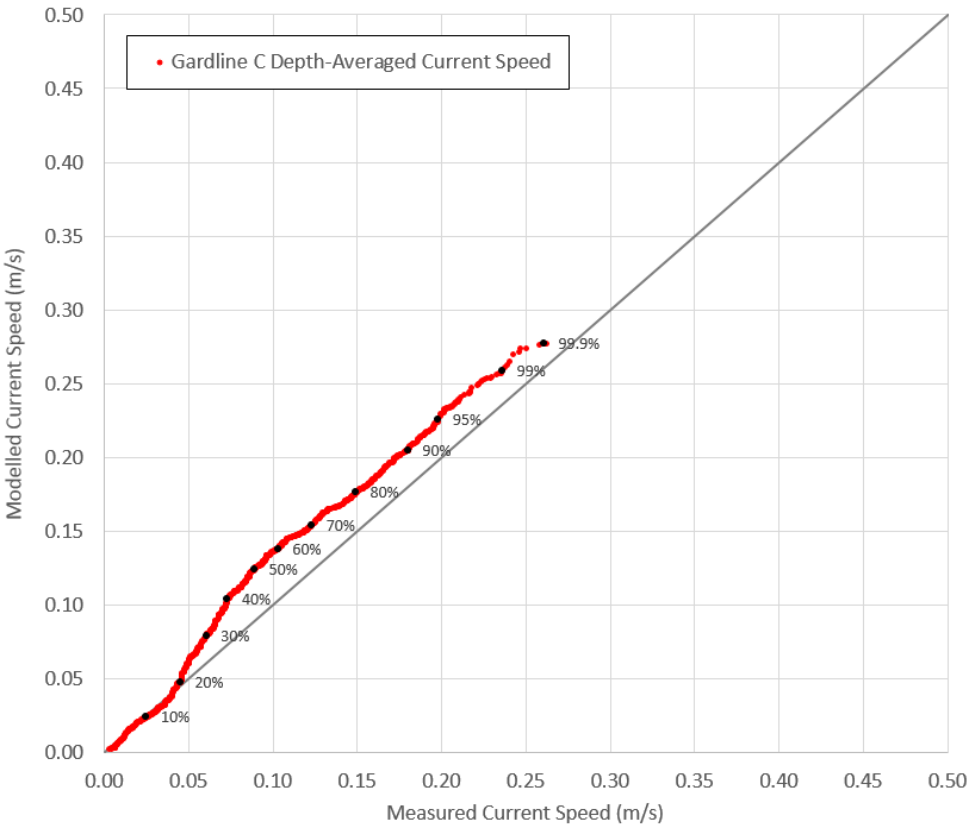

Figure C4-3a Q-Q plot of modelled vs. measured current speeds at Gardline C. Depth-integrated, Summer 2017.

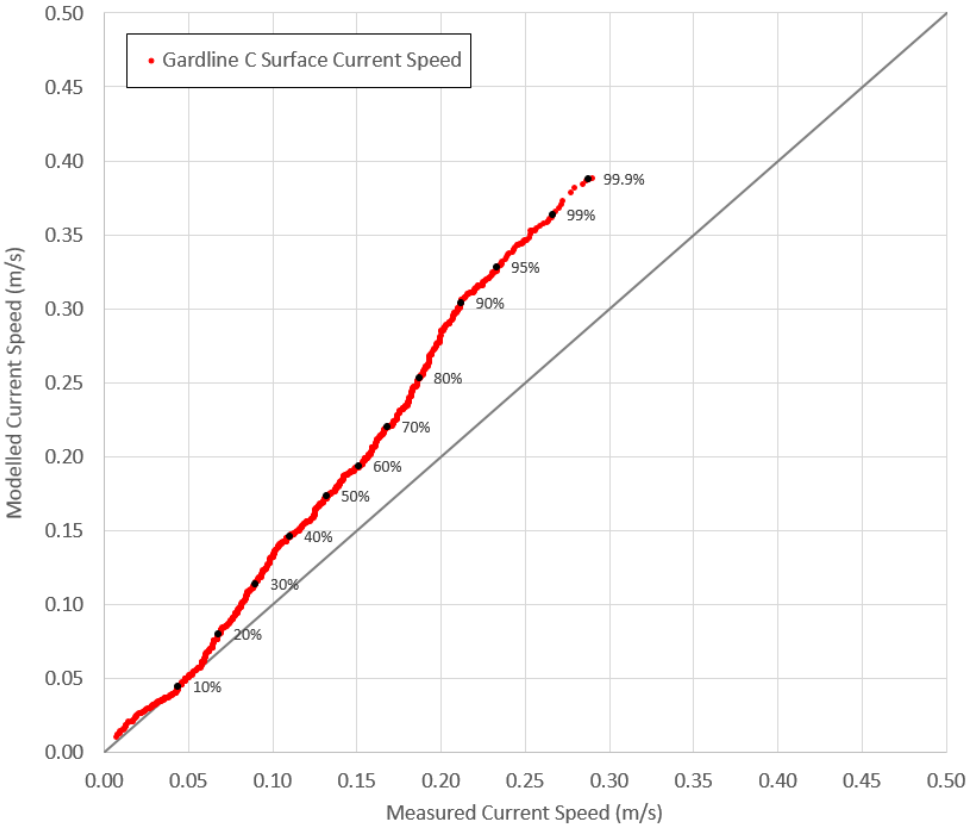

Figure C4-3b Q-Q plot of modelled vs. measured current speeds at Gardline C. Surface, Summer 2017.

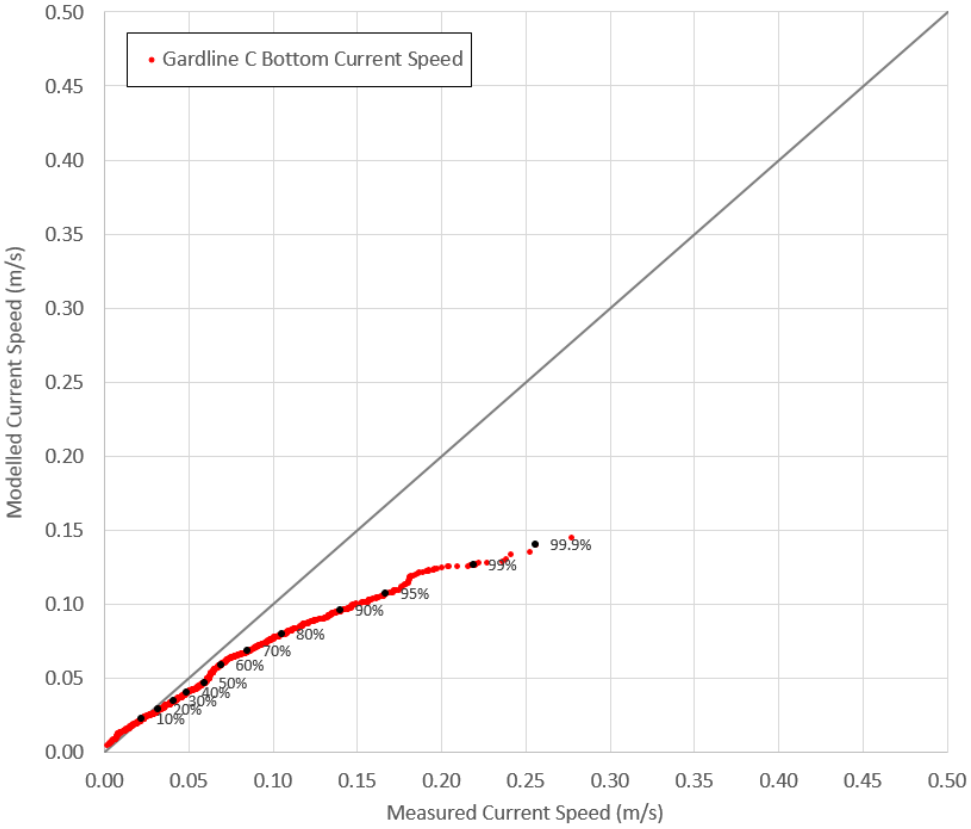

Figure C4-3c Q-Q plot of modelled vs. measured current speeds at Gardline C. Bottom, Summer 2017.

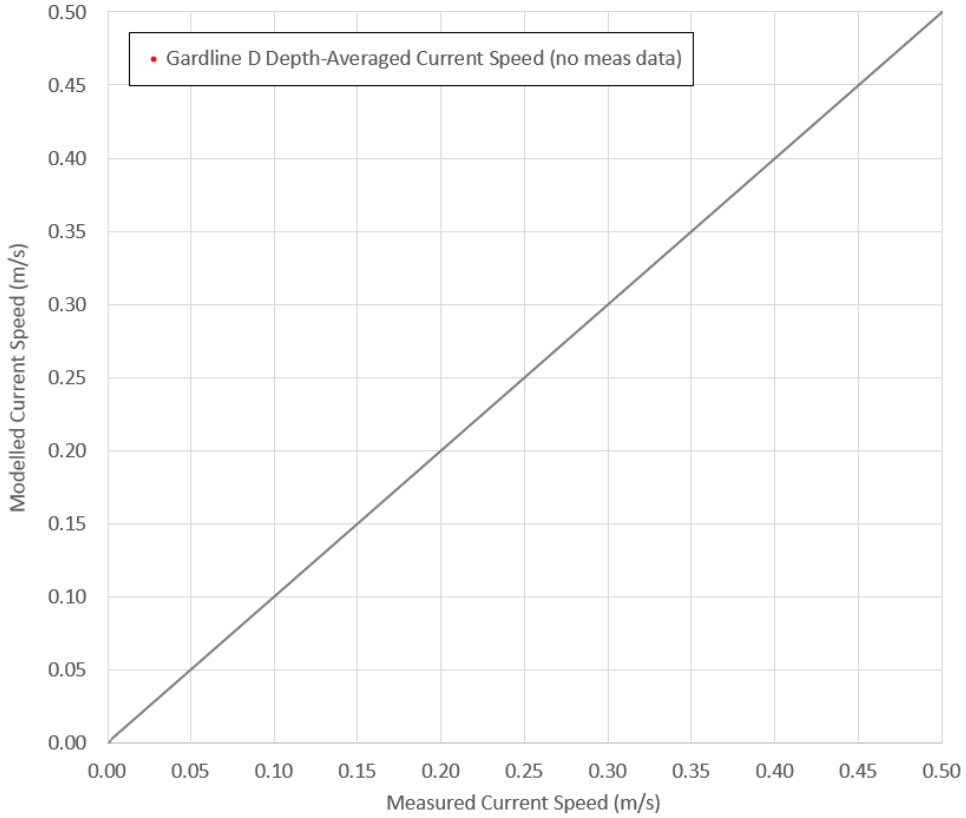

Figure C4-4a Q-Q plot of modelled vs. measured current speeds at Gardline D. Depth-integrated, Summer 2017.

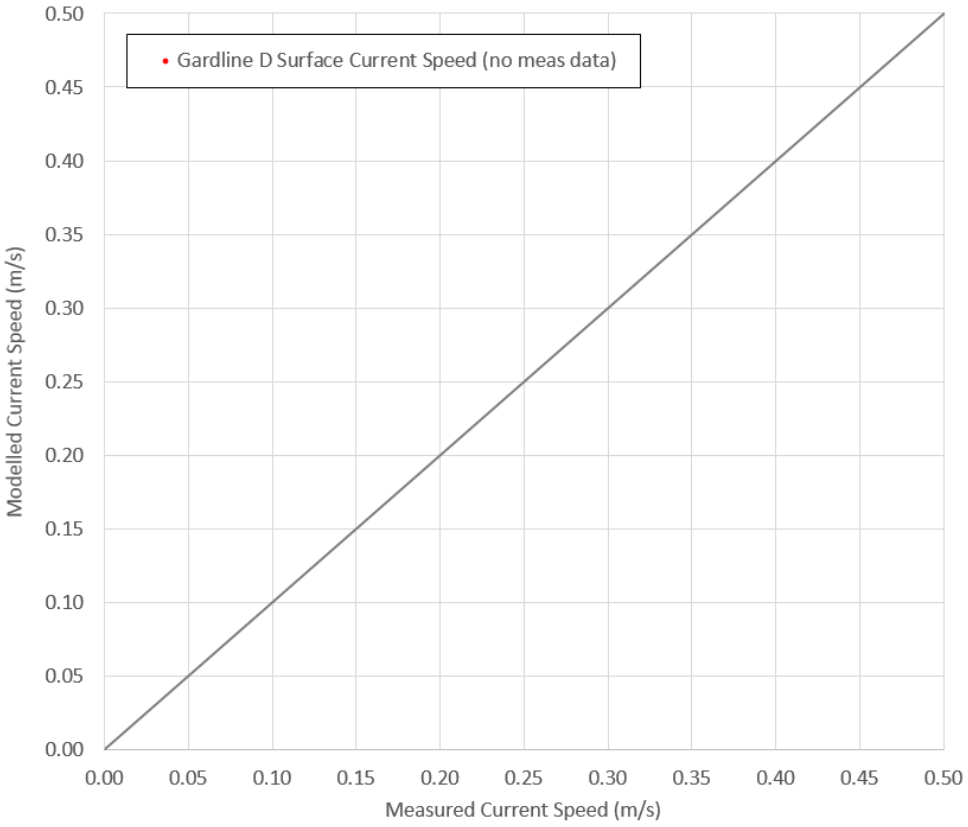

Figure C4-4b Q-Q plot of modelled vs. measured current speeds at Gardline D. Surface, Summer 2017.

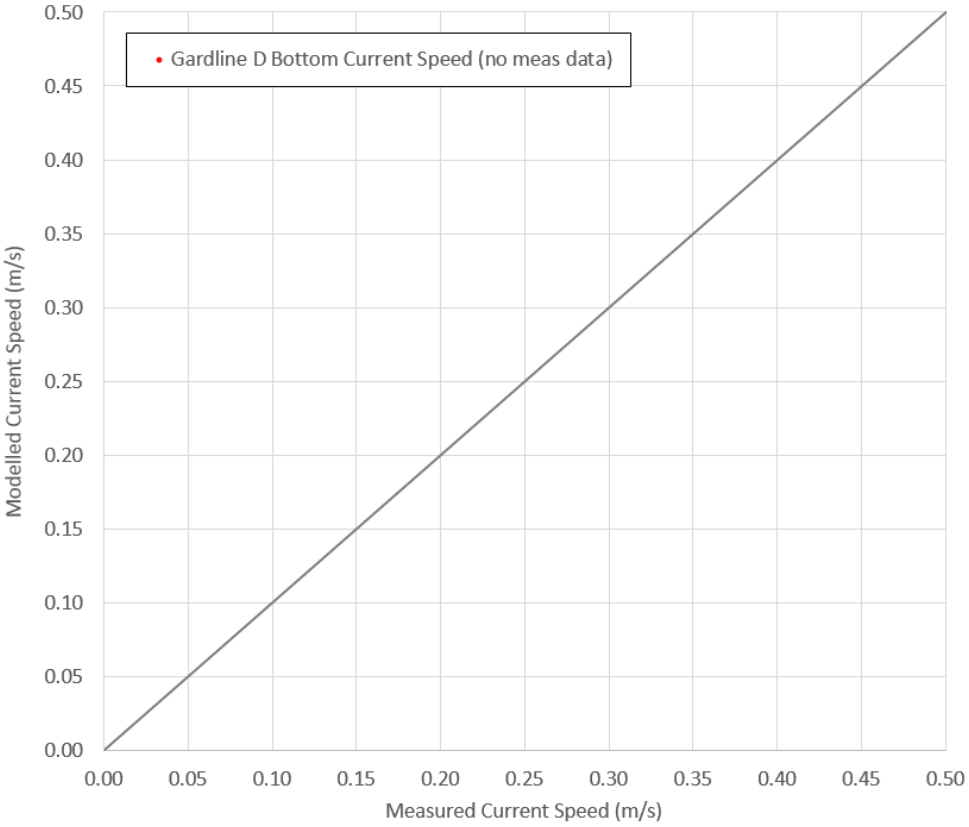

Figure C4-4c Q-Q plot of modelled vs. measured current speeds at Gardline D. Bottom, Summer 2017.

APPENDIX D

Local 3D Model 2017 Calibration/Validation

Near-Bottom Water Temperature Time Series Plots

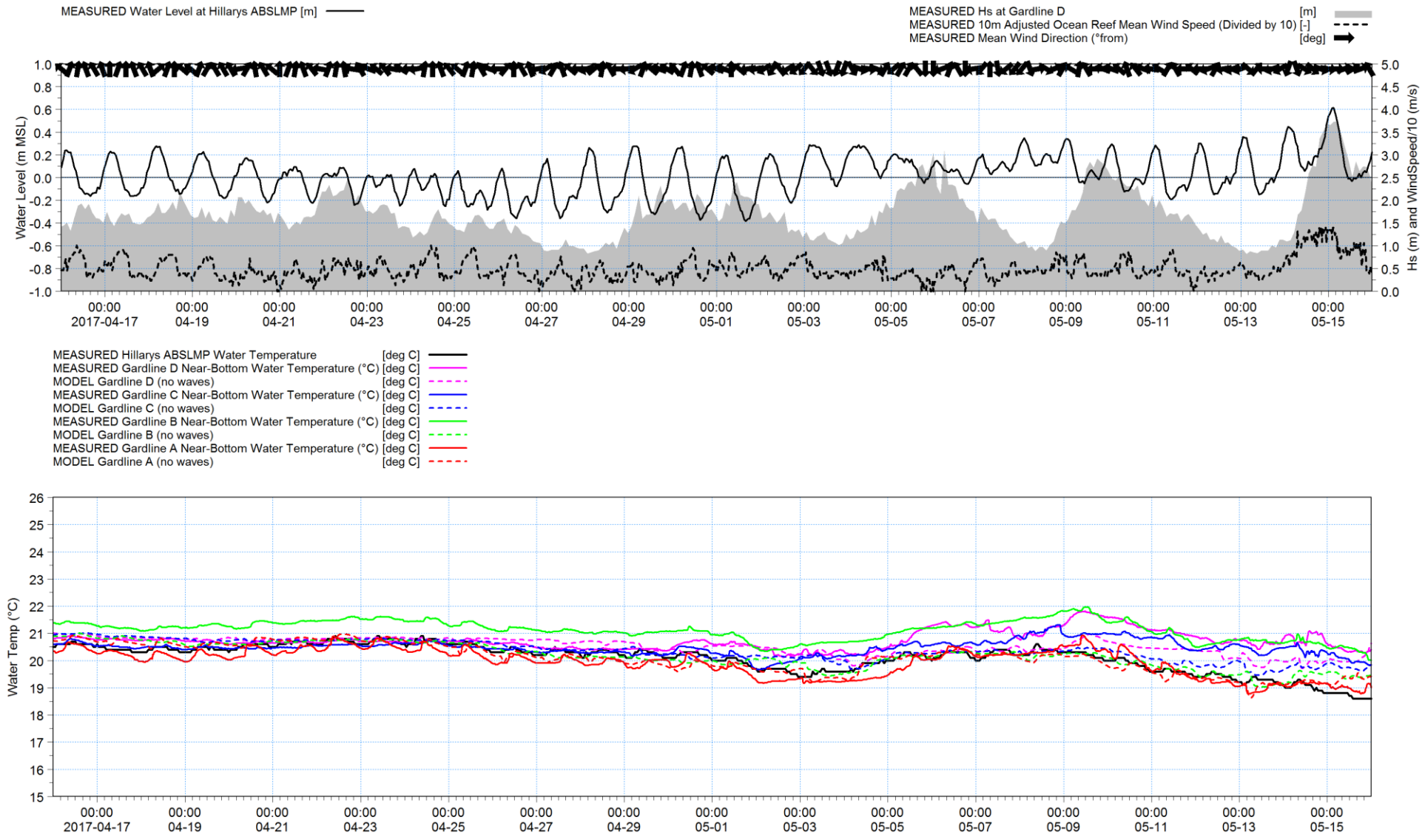

Figure D-1 Time series plot of modelled vs. measured near-bottom water temperature at the four Gardline stations. Autumn 2017 calibration period.

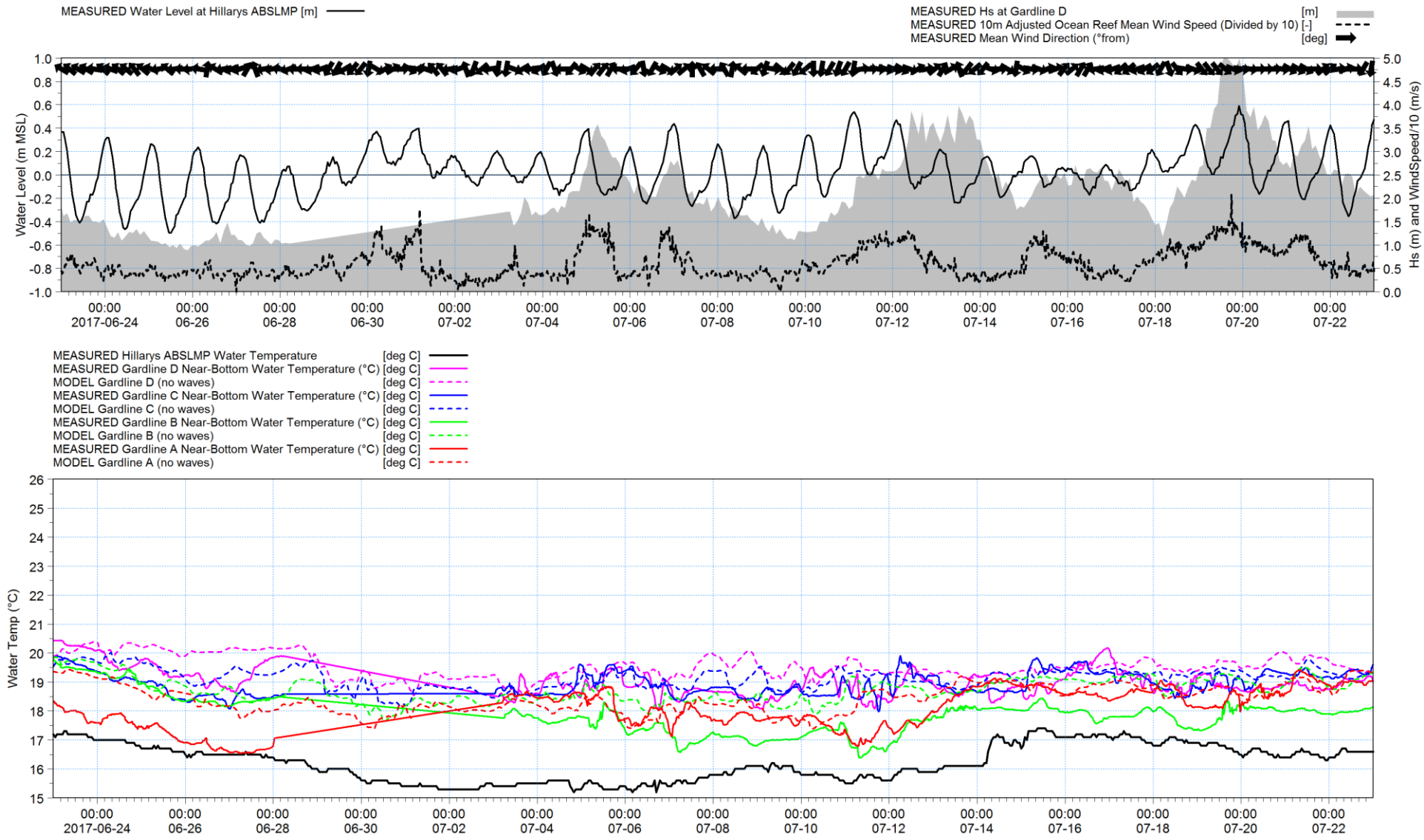

Figure D-2 Time series plot of modelled vs. measured near-bottom water temperature at the four Gardline stations. Winter 2017 validation period. Note that the period of 28 June to 03 July lies between Gardline Deployments 1 and 2, and no measurements are present.

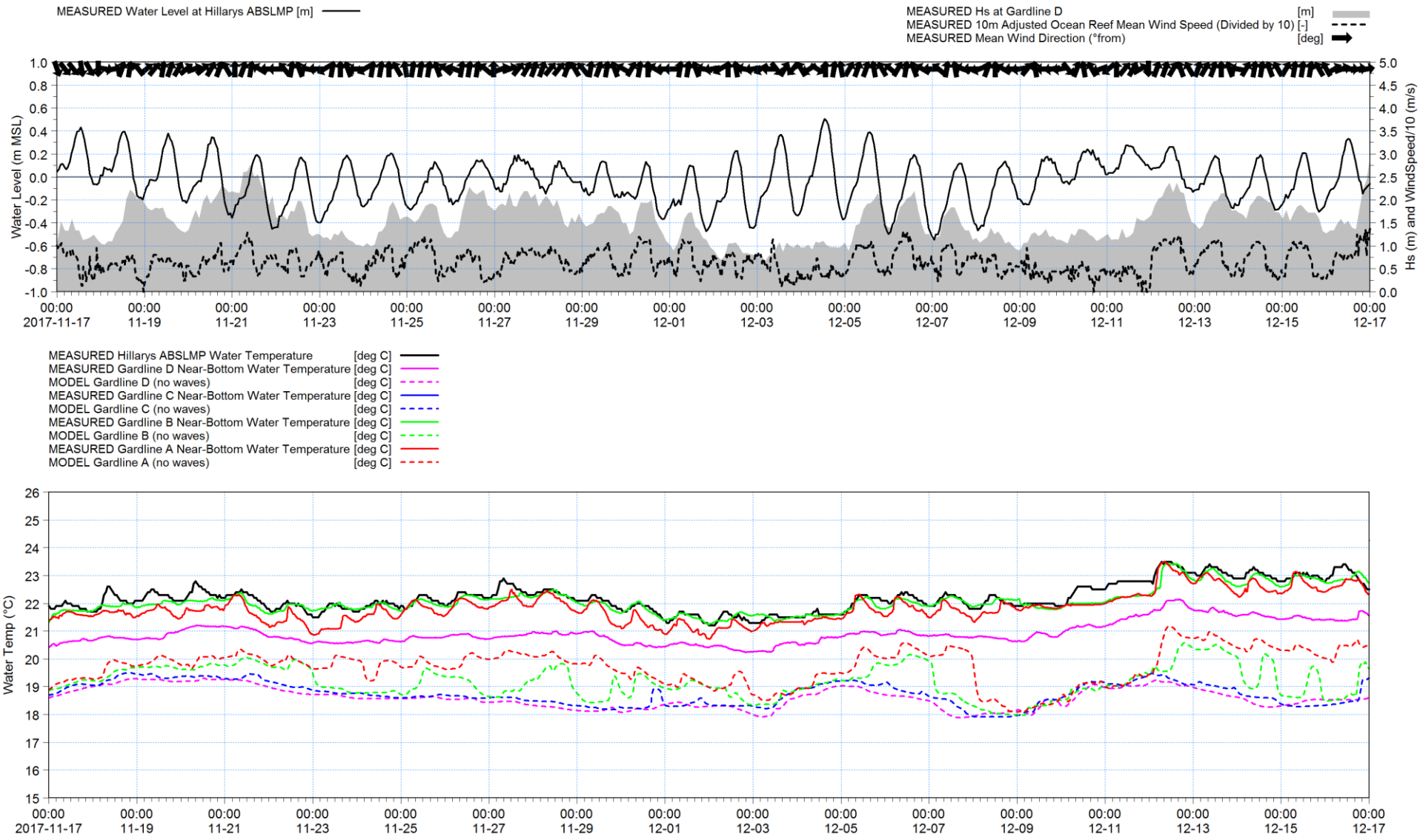

Figure D-3 Time series plot of modelled vs. measured near-bottom water temperature at the four Gardline stations. Summer 2017 validation period.

APPENDIX E

Mesh Resolution Tests

E Mesh Resolution Tests

E.1 Introduction

A key aspect of the model construction and calibration is the choice of horizontal resolution. While this is an inherently more amorphous issue in an unstructured model domain that in a structured one, the nominal resolution achieved in an unstructured mesh is nonetheless a critical input parameter.

As with any numerical model study, the choice here is driven by seeking a manageable balance between the spatial resolution which would ideally be applied and that which is practicable from the perspectives of runtime and cost. Fundamental to this decision is the question of the dominant spatial scales which must be resolved to describe both ambient processes and those most important with respect to the assessment of ASDP plume behaviour. Ambient processes are particularly challenging in the Alkimos application given the spectrum of spatial scales present in the existing reef system.

A range of nominal mesh resolutions have been evaluated as part of the setup and testing phase of the Local Hydrodynamic Model. Ultimately the vast majority of calibration was performed using a nominal mesh resolution of 50m within the area of interest, coarsening to roughly 400m at the open boundaries.

Fundamentally, the ASDP facility would be expected to generate a dense plume which will flow downslope under gravity, and be prone to flowpath constraints by the complex reef geometry. Initial testing with the ASDP discharge present in the Local 3D Hydrodynamic Model confirms this expectation. Results have shown that the ASDP plume retains sufficient excess density at the end of the near field to establish a coherent near-bottom layer in the far-field, and that the footprint of this layer spreads by gravity within the reef system to form a kilometre-scale feature. The shape and extent of this feature at any instant is a dynamic balance between the incoming diluted ASDP effluent, the vertical mixing of the near-bottom footprint of the wastefield, and limited advection due to the dynamics of the overlying water column.

It is a key requirement of the project that the mesh resolution of the model faithfully represents the flowpaths of the ASDP discharge, as well as the temporary storage which occurs while local basins of the reef fill and effluent subsequently cascades in an offshore direction.

In order to confirm that this choice of 50m nominal resolution is viable in terms of an assessment tool for the behaviour of the ASDP plume, a series of tests has been performed in order to compare the storage and transport of a bottom-hugging dense plume which is released within the reef system. In order to support the testing of a very high resolution mesh without incurring an excessive computational burden, these tests have been performed within a 2D analogue to the fully 3D system. While the fully 3D system describes the transport of a dense effluent into an ambient water column, the analogous 2D system applied here describes the flow and storage of water into air – effectively water being discharged onto an initially dry seabed, in a manner similar to a terrestrial floodwater routing study.

A 2D model is applied here which evaluates the spreading of a simplified bottom-hugging flow represented by water being introduced into an initially dry bathymetry, as opposed to a dense discharge being introduced into a less dense ambient. While some fundamental differences exist in the application of this 2D analogue, the 2D air/water parameterisation of the problem is in many respects more challenging with respect to mesh resolution than

the full 3D problem as water in air will form a thinner layer for which the gravity-driven flowpath is more sensitive to geometry than the thicker dense layer within the 3D model.

E.2 Model Setup

A MIKE21 FMHD model has been established which covers the same total domain as the Local 3D Hydrodynamic Model applied in the main report. The model is established as a “bathtub” arrangement with no open boundaries, and is initially fully dry. A discharge is released at the location of the inshore “Outfall A” candidate ASDP location. Water is discharged with a magnitude corresponding to the rate at which diluted ASDP discharge enters the far-field, assuming an achieved near-field dilution of 1:30. Given the ASDP discharge rate of the Water Corporation (2018) of 337 ML/day = 3.90 m^3/s, this gives a far-field source magnitude of 3.90 x 30 = 117 m^3/s.

A single discharge scenario (ASDP Outfall A) has been applied, as the flowpath for this scenario involves a) initial infilling of the inner reef basin, b) cascading into the outer reef basin/channel, c) infilling of the outer reef basin/channel and d) cascading through the outer reef break to the coastal shelf. These features are visualized below in Figure E-1. ASDP Outfall B discharges directly to the outer reef basin/channel, and as such its flowpath is a subset of that followed by ASDP Outfall A. As such, a simulation assessing discharge at ASDP Outfall A also encompasses the flowpath of Outfall B.

Three variants of model mesh were simulated:

- A nominal 50m resolution mesh in the area of interest, including limited edits to tailor the arrangement of elements at key local features/choke points. This is the mesh as applied for the calibration process as described in the main report.
- A nominal 50m resolution mesh in the area of interest as above, which is unregulated with no manual adjustments to the element arrangement.
- A significantly higher (nominally 15m) unregulated mesh with no manual adjustments to the mesh arrangement.

The latter 15m mesh is applied as a reference against which to assess any potential resolution effects for the coarser meshes.

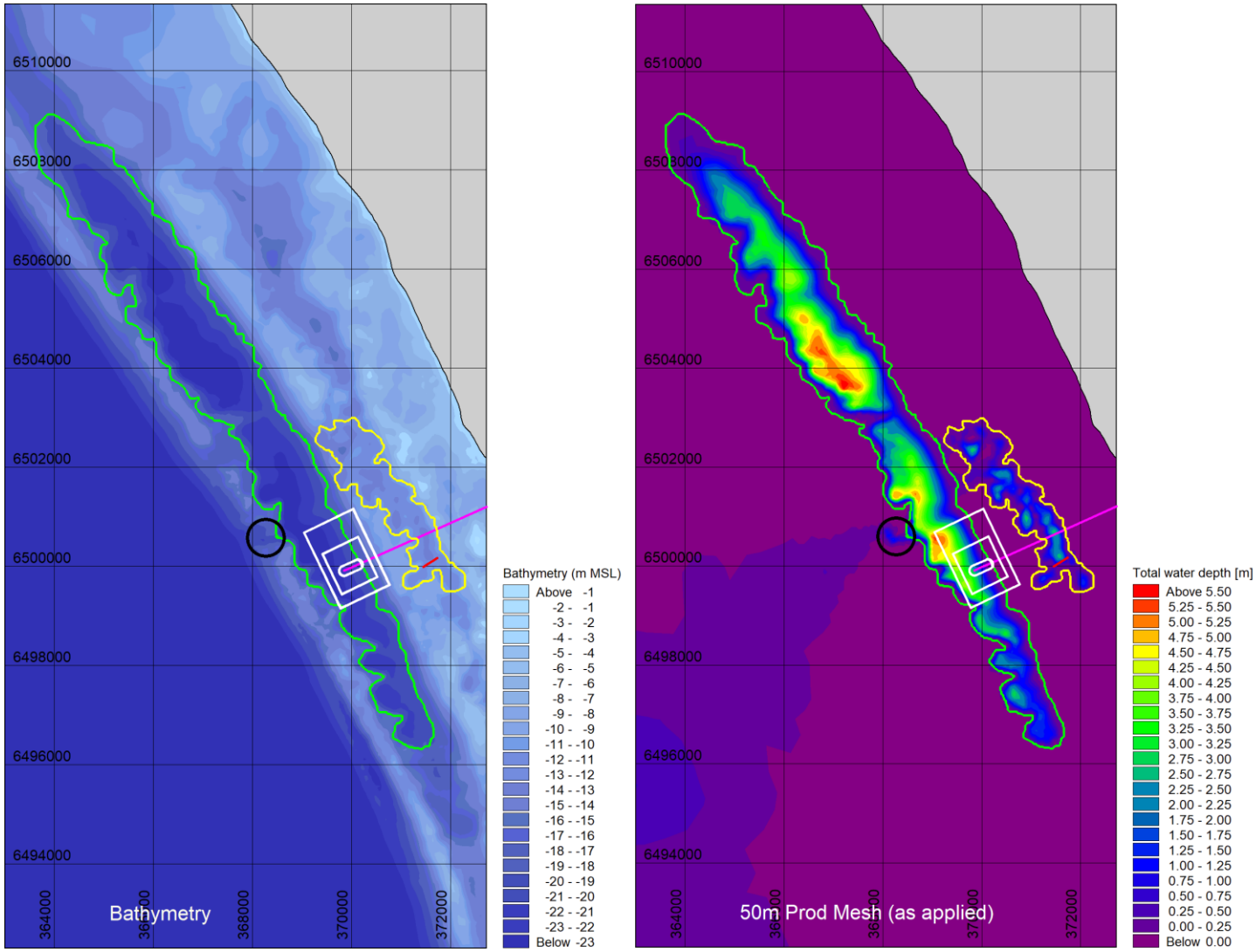

Figure E-1 Bathymetry (left pane) and sample effluent depth field (right) showing flowpath and geometrical constraint due to reef. Coloured outline added to indicate key reef features as described in text: the inner reef basin (yellow polygon), the outer reef basin (green polygon) and the location of the venting passage through the outer reef (black circle).

E.3 Results

Figure E-2 through Figure E-7 show 2D imagery of incremental brine accumulation at times of 3, 6, 12, 24, 48 and 72 hrs after the start of the simulation. In each graphic, three panes are shown, each of which shows the corresponding depth field from each of the three meshes described in the previous section. The magenta line indicates the existing WWTP feeder pipe, the white boxes indicate the regulatory zoning around the existing WWTP, and the red line indicates the location of the ASDP Outfall A linear diffuser supplying the water to these simulations. The contours plotted indicate the instantaneous depth field which has accumulated from the diluted brine discharge.

A brief narrative of the individual results follows:

- Start +3hrs: The inner reef basin, which lies almost entirely north of the ASDP Option A outfall, has largely filled.
- Start +6hrs: The inner reef basin has filled to a level at which two cascades of brine have begun to flow downslope and begun to fill the outer reef basin. Aside from some differences in the depth of the flowpaths at the cascade locations, the three models respond similarly.
- Start +12hrs: The depth field within the inner reef basin has become effectively static, while the outer reef basin continues to fill.
- Start +24hrs: The outer reef basin continues to fill, but the water level has reached a point which is sufficient to begin overflowing through the “venting channel” in the outer reef into the ocean. This occurs in the 15m mesh and in the 50m production mesh, but not in the unregulated 50m mesh.
- Start +48hrs: The outer reef basin continues to fill, with increased outflow through the venting channel in the outer reef into the ocean. This occurs in the 15m mesh and in the 50m production mesh, but not in the unregulated 50m mesh.
- Start +72hrs: The outer reef basin continues to fill, with increased outflow through the venting channel in the outer reef into the ocean. This occurs in the 15m mesh and in the 50m production mesh, but not in the unregulated 50m mesh.
- Start +84hrs: The outer reef basin continues to fill, with increased outflow through the “enting channel in the outer reef into the ocean. This occurs in the 15m mesh and in the 50m production mesh, with venting just initiating in the unregulated 50m mesh. In the latter mesh, the ponded depths in the outer reef basin are seen to be elevated as a result of inadequate resolution and associated throughflow via the venting channel.

It is clear from visual inspection of these results that resolution (within the context of those tested) has minimal impact on the accumulation of brine in the inner reef basin nor on the flow paths connecting the inner and outer reef basins. The discretisation of the “venting channel” is quite sensitive in terms of limiting the accumulation of brine in the outer reef basin, with an unregulated 50m resolution mesh inhibiting exchange with the ocean. However, the 50m mesh applied in the main report for calibration and production testing performs comparably to the higher resolution 15m mesh.

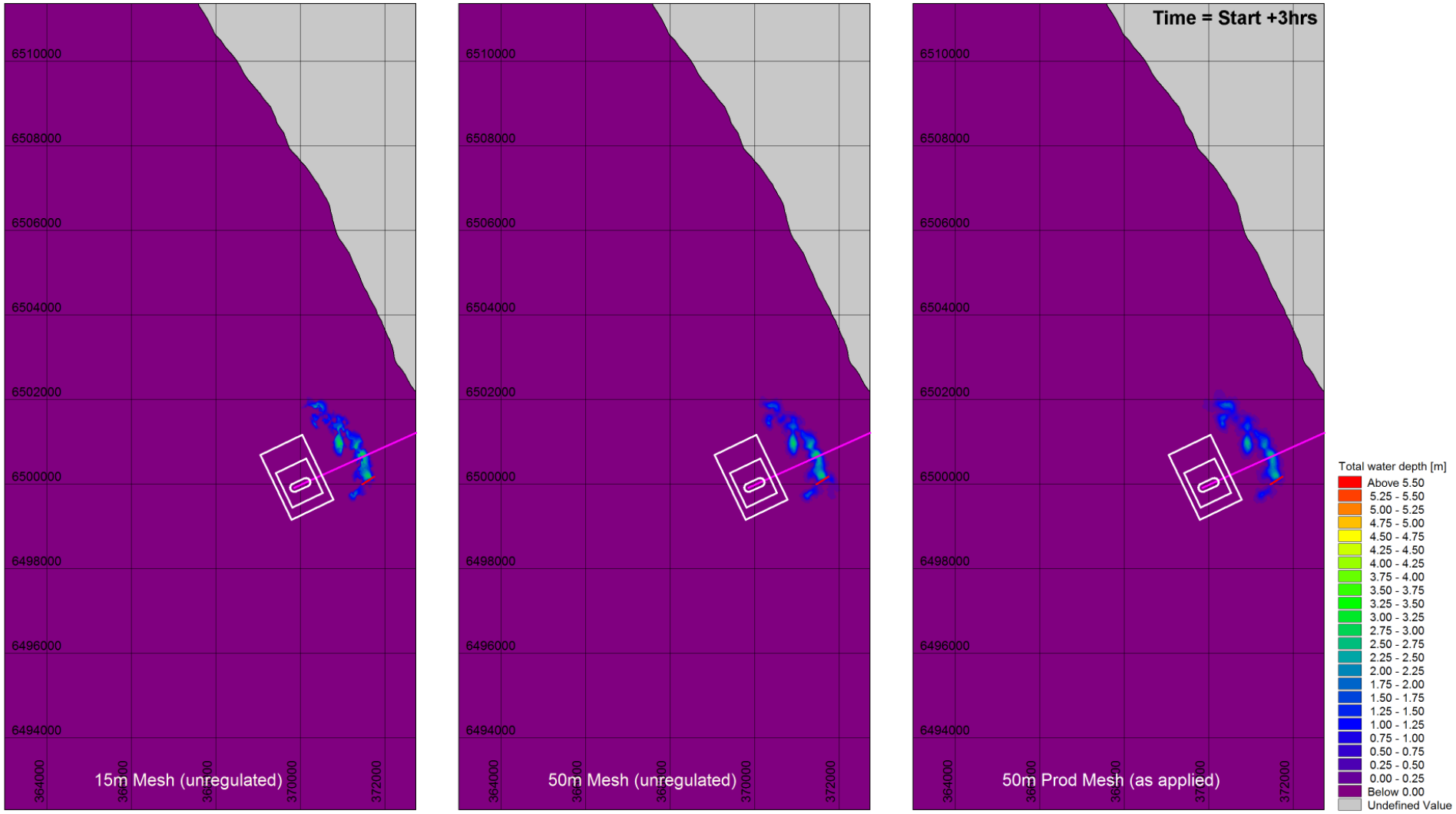

Figure E-2 Comparison of accumulated thickness of indicative ASDP discharge into 2D bare-bed bathymetry after 3 hours of simulation time.

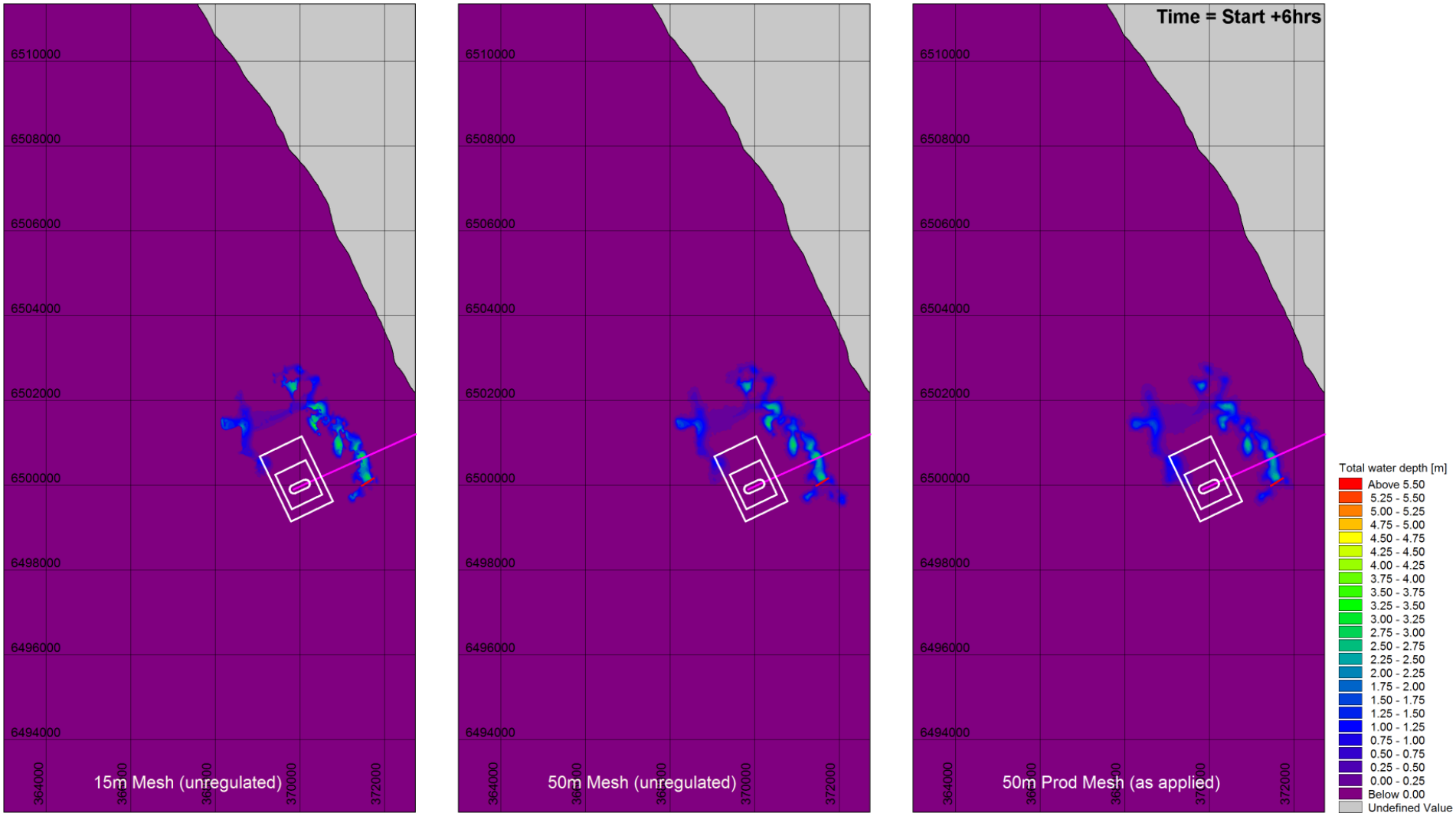

Figure E-3 Comparison of accumulated thickness of indicative ASDP discharge into 2D bare-bed bathymetry after 6 hours of simulation time.

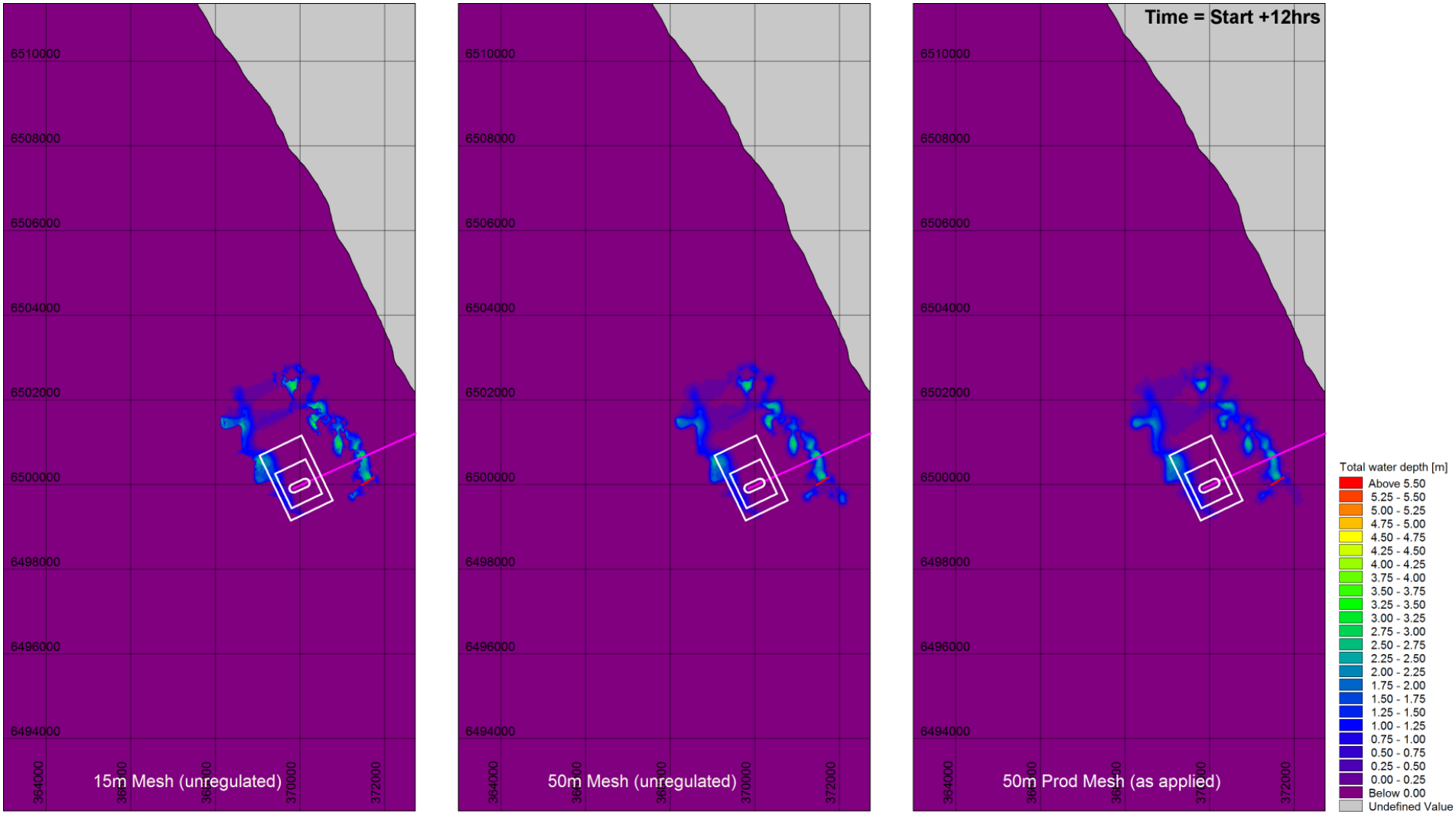

Figure E-4 Comparison of accumulated thickness of indicative ASDP discharge into 2D bare-bed bathymetry after 12 hours of simulation time.

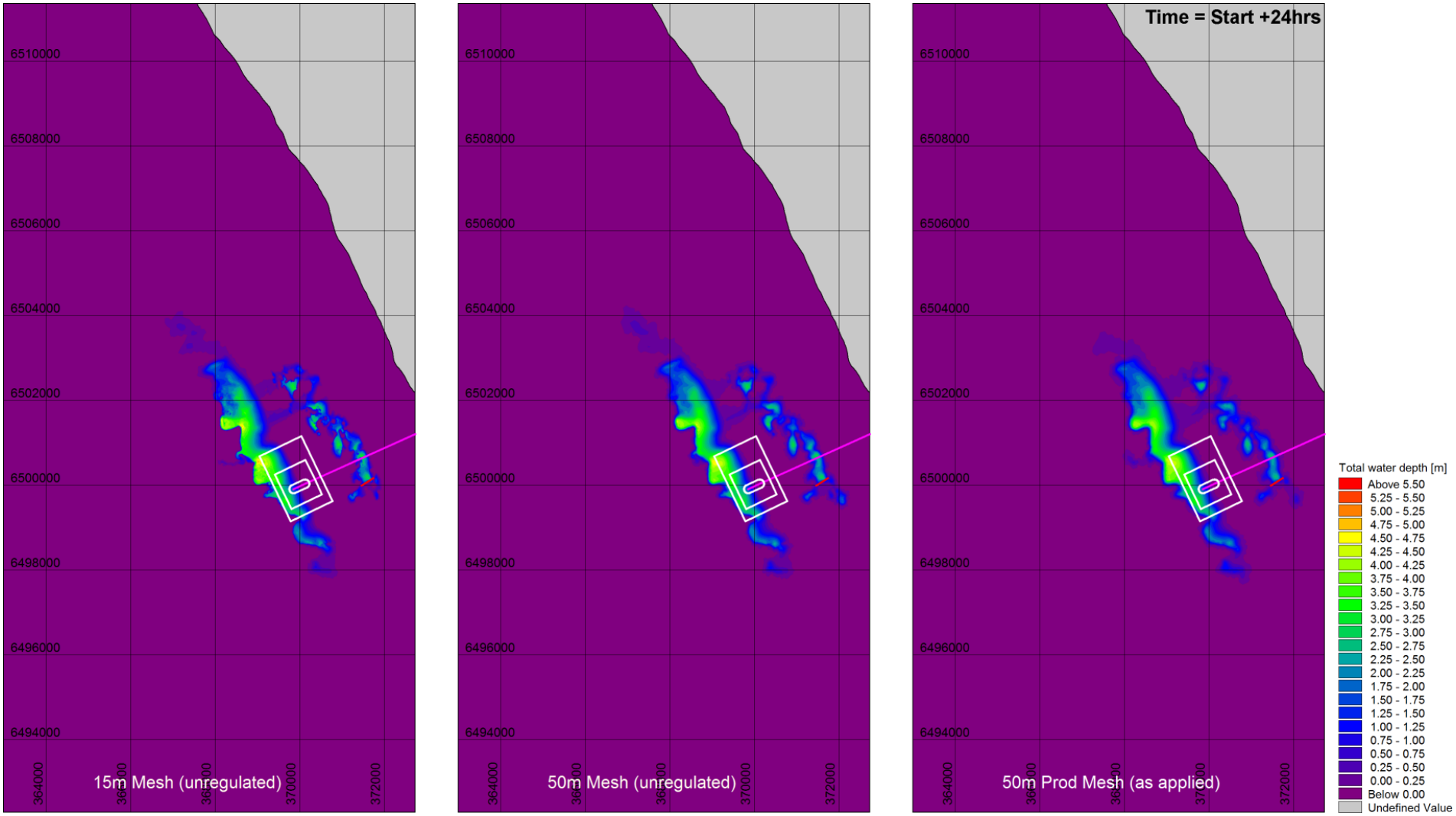

Figure E-5 Comparison of accumulated thickness of indicative ASDP discharge into 2D bare-bed bathymetry after 24 hours of simulation time.

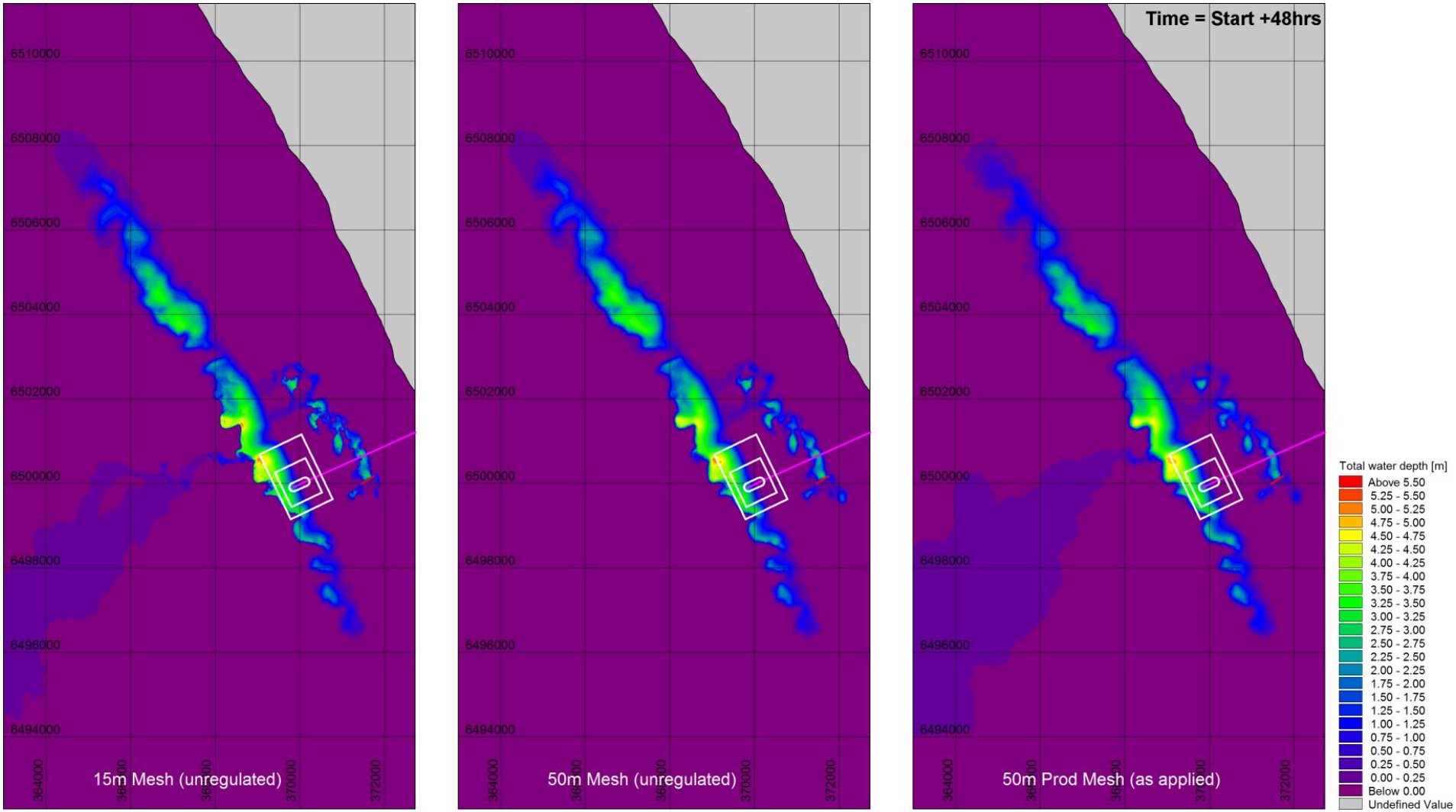

Figure E-6 Comparison of accumulated thickness of indicative ASDP discharge into 2D bare-bed bathymetry after 48 hours of simulation time.

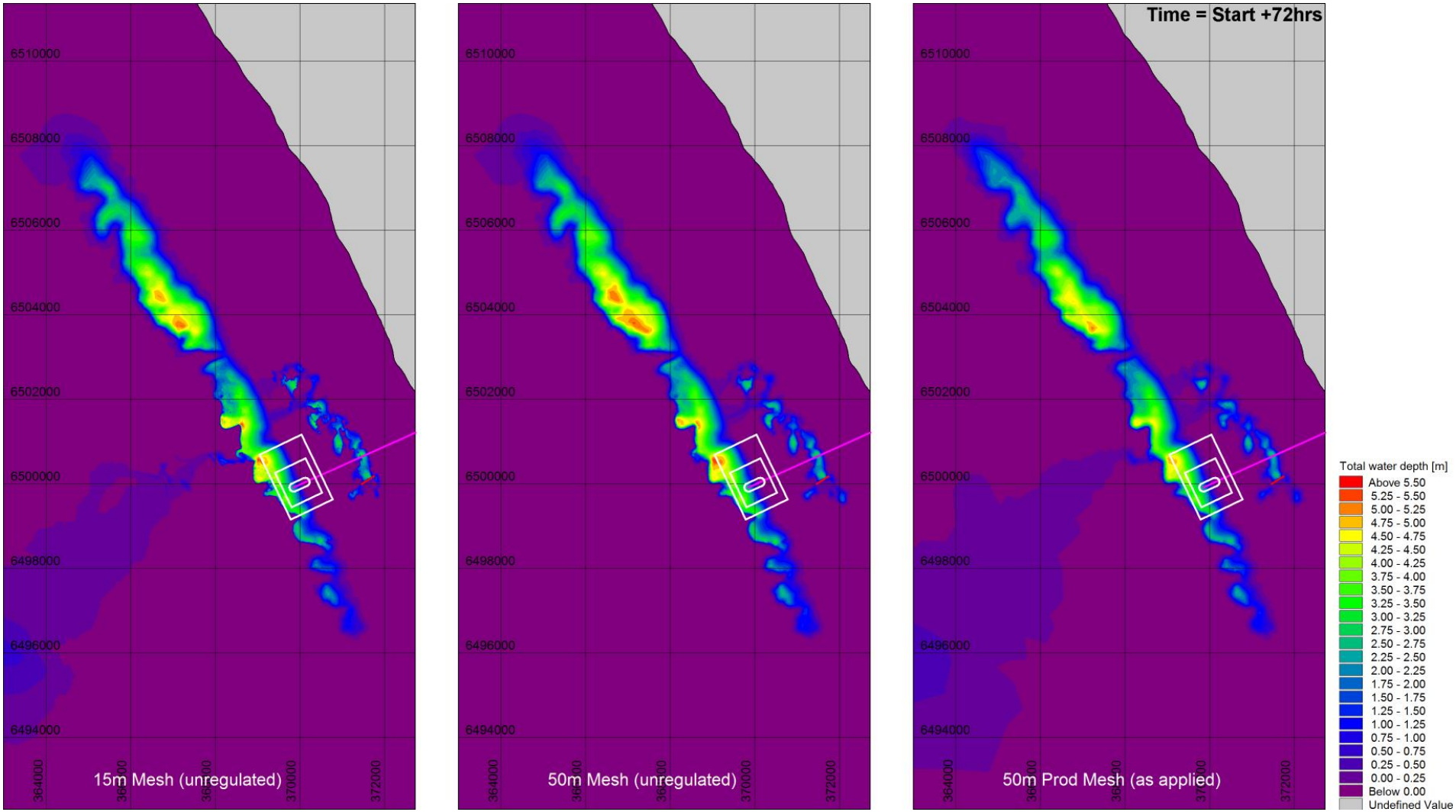

Figure E-7 Comparison of accumulated thickness of indicative ASDP discharge into 2D bare-bed bathymetry after 72 hours of simulation time.

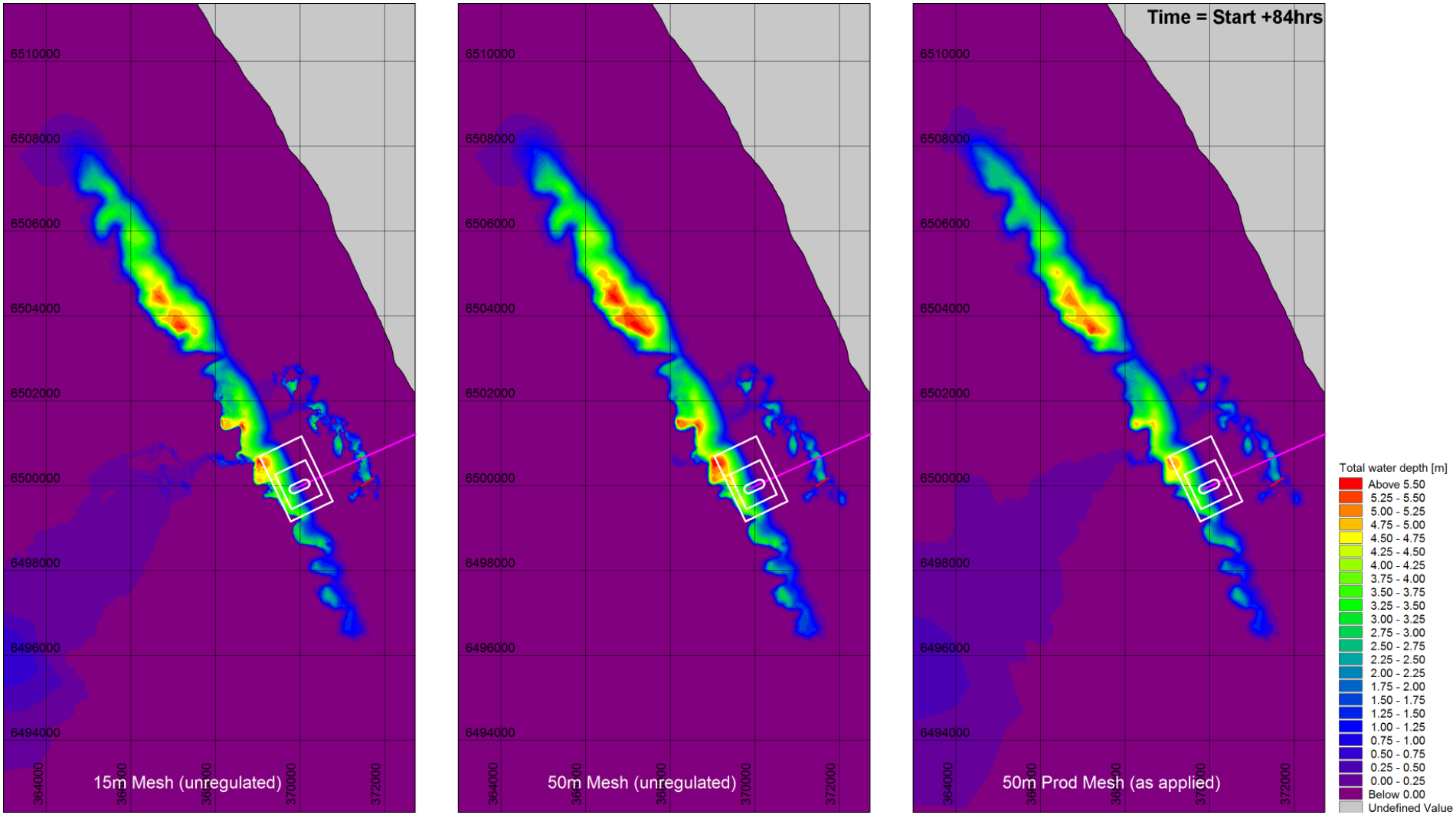

Figure E-8 Comparison of accumulated thickness of indicative ASDP discharge into 2D bare-bed bathymetry after 84 hours of simulation time.